COMILLAS
UNIVERSIDAD PONTIFICIA

ICAI

MÁSTER UNIVERSITARIO EN INGENIERÍA INDUSTRIAL

TRABAJO FIN DE MÁSTER

Optimal tuning of UFLS schemes based on frequency stability margin

Autor: Mónica Vadillo Díaz de Aguilar

Director: Lukas Sigrist

Madrid

Declaro, bajo mi responsabilidad, que el Proyecto presentado con el título

"Optimal tuning of UFLS schemes based on frequency stability margin" en la ETS de Ingeniería - ICAI de la Universidad Pontificia Comillas en el

curso académico 2024/2025 es de mi autoría, original e inédito y

no ha sido presentado con anterioridad a otros efectos.

El Proyecto no es plagio de otro, ni total ni parcialmente y la información que ha sido

tomada de otros documentos está debidamente referenciada.

Fdo.: Mónica Vadillo Díaz de Aguilar Fecha: 14/01/ 2025

Autorizada la entrega del proyecto

EL DIRECTOR DEL PROYECTO

Fdo.: Lukas Sigrist Fecha: 14/ 01/ 2025

MÁSTER UNIVERSITARIO EN INGENIERÍA INDUSTRIAL

TRABAJO FIN DE MÁSTER

Optimal tuning of UFLS schemes based on frequency stability margin

Autor: Mónica Vadillo Díaz de Aguilar

Director: Lukas Sigrist

Madrid

AJUSTE ÓPTIMO DE ESQUEMAS UFLS BASADO EN EL MARGEN DE ESTABILIDAD DE FRECUENCIA

Autor: Vadillo Díaz de Aguilar, Mónica.
Director: Sigrist, Lukas.
Entidad Colaboradora: ICAI – Universidad Pontificia Comillas

RESUMEN DEL PROYECTO

La creciente penetración de las fuentes de energía renovables (FER) afecta a la estabilidad del sistema, en particular a la estabilidad de la frecuencia de pequeños sistemas eléctricos aislados como el de las Islas Canarias. Los deslastres de carga por baja frecuencia (UFLS) se utilizan normalmente como último recurso para proteger los sistemas eléctricos. El objetivo de este proyecto es optimizar los parámetros de un esquema UFLS basado en el margen de estabilidad de frecuencia (FSM) utilizando algoritmos heurísticos, concretamente simulated annealing, y compararlo con el esquema UFLS convencional. El modelo se implementa tanto en el sistema eléctrico de La Palma como en el de Gran Canaria para evaluar su eficacia en caso de perturbación (pérdida grupo generador). Los resultados muestran que la implementación de FSM en el esquema UFLS de La Palma mejora significativamente su rendimiento. Por el contrario, en el caso de Gran Canaria, aunque se reduce el deslastre de carga, el esquema es menos eficaz que los enfoques convencionales a la hora de disminuir las grandes desviaciones de frecuencia en estado estacionario. Además, se presenta un análisis de sensibilidad del esquema UFLS basado en FSM para el sistema eléctrico de La Palma, donde se estudia el efecto de la variación de parámetros clave de diseño como el nivel de penetración de FER, la inclusión de almacenamiento, la formulación de la función objetivo y la inclusión del diseño del tamaño de los escalones de deslastre.

Palabras clave: Metodología de diseño, deslastre de cargas por subfrecuencia, margen de estabilidad de frecuencia, protección del sistema eléctrico insular

1. Introducción

La estabilidad de frecuencia es un aspecto crítico ya que son muy vulnerables a perturbaciones que pueden causar desequilibrios significativos de potencia, afectando su seguridad y confiabilidad. En caso de una contingencia, su reducida inercia puede provocar rápidas caídas de frecuencia, y su falta de interconexión limita el acceso a soporte de sistemas vecinos. Todo ello se acentúa con la creciente penetración de las fuentes de energía renovables (FER), dado que normalmente no aportan inercia y apenas contribuyen al control de frecuencia primario. Además, por su pequeño tamaño y aislamiento, estos sistemas son susceptibles a desequilibrios de potencia activa severos, donde el control primario puede no ser suficientemente rápido para restablecer el equilibrio de potencia y mantener la frecuencia dentro de los límites. Para preservar la integridad del sistema, típicamente se emplean esquemas de deslastre de carga de baja frecuencia (UFLS).

Los esquemas UFLS son una medida de último recurso para evitar la inestabilidad de frecuencia y el colapso del sistema de potencia. La mayoría de los esquemas UFLS actuales son estáticos y semi-adaptativos convencionales [1]. Estos miden continuamente la frecuencia y/o la tasa de cambio de frecuencia (RoCoF) por medio de relés tipo 81 [2] y deslastran una cantidad predefinida de carga en caso de que la frecuencia y/o RoCoF caigan por debajo de un cierto umbral. La efectividad de los esquemas UFLS convencionales depende en gran medida de su diseño, que cumplir dos características clave: robustez y eficiencia. La adecuada selección de las condiciones de operación mejora la robustez del esquema, mientras que la eficiencia se logra ajustando los parámetros del esquema UFLS para minimizar el deslastre de carga y garantizar la estabilidad del sistema [1].

Los esquemas UFLS convencionales, aunque ampliamente utilizados, tienen varios inconvenientes. Carecen de adaptabilidad [1], es decir, se basan en cantidades de deslastre de carga predefinidas y no se ajustan a la gravedad de cada perturbación. Esto puede llevar a desconexiones excesivas o insuficientes de carga. Los esquemas avanzados ofrecen una solución alternativa en este sentido, pero requieren una amplia comunicación y recopilación de datos, lo que los hace complejos y potencialmente caros de implementar. Estos esquemas son principalmente centralizados, mientras que los esquemas UFLS convencionales se distribuyen localmente. Los convencionales pueden mejorarse para distinguir mejor entre perturbaciones críticas que requieren intervención inmediata y aquellas que pueden posponer o incluso evitar el deslastre. Recientemente, [3] ha propuesto un nuevo enfoque adaptativo UFLS que usa el margen de estabilidad de frecuencia (FSM) como criterio de deslastre. A diferencia de los métodos convencionales basados únicamente en mediciones de frecuencia, este enfoque incorpora el FSM. Este criterio depende tanto de la frecuencia como del RoCoF, y permite determinar el tiempo restante antes de alcanzar la frecuencia mínima permitida (p. ej. f_{LIM} = 47,5 Hz). Al comparar la frecuencia y los cálculos de FSM con los umbrales establecidos, el sistema puede iniciar las acciones de deslastre de carga más adecuadas.

Actualmente, no existe un método sistemático para diseñar esquemas UFLS, pero se hna propuesto varios enfoques en la literatura. Existen métodos como el ensayo y error iterativo y los procesos de cribado [4], pero no garantizan un rendimiento eficiente. También se han aplicado algoritmos determinísticos para optimizar parámetros clave en esquemas UFLS convencionales. Sin embargo, dependen de las condiciones iniciales de las variables y pueden enfrentar problemas por discontinuidades en la función objetivo. Los algoritmos heurísticos, como los genéticos o el simulated annealing (SA), son alternativas efectivas para optimizar funciones objetivo con no linealidades [1]. No obstante, enfrentan desafíos en pequeños sistemas de potencia aislados debido al tamaño limitado los escalones de potencia.

Un diseño robusto depende en gran medida de la selección adecuada de contingencias. Hay varios tipos, pero este proyecto solo considera las interrupciones de generación, dado su gran impacto en las desviaciones de frecuencia. Comúnmente, se evalúan las condiciones operativas en varios niveles de carga-demanda y se diseña el esquema UFLS en función de las interrupciones de los generadores más grandes y más pequeños. Un método basado en clutering, propuesto en [5], permite identificar escenarios representativos de operación y contingencia (OC). Este proyecto implementa un esquema UFLS basado en FSM en sistemas eléctricos españoles aislados reales. El método propuesto se basa en [1] donde se presenta un enfoque eficiente y robusto para el diseño de esquemas UFLS, pero se adapta para incluir el criterio FSM propuesto por [3]. Para optimizar los parámetros del esquema UFLS, se utiliza SA, con el objetivo de minimizar la carga deslastrada.

2. Definición del Proyecto

Este proyecto busca mejorar la estabilidad de frecuencia en pequeños sistemas de potencia aislados mediante la optimización de esquemas UFLS. Basándose en investigaciones previas que resaltan la efectividad del umbral FSM, se busca automatizar y mejorar el esquema UFLS propuesto en [6] usando algoritmos avanzados. Los objetivos específicos son:

- Utilizar técnicas de minería de datos para identificar escenarios representativos, identificando contingencias que representen eficazmente posibles perturbaciones.
- Formular el ajuste de los parámetros de un esquema UFLS como problema de optimización, resolviéndolo con algoritmos heurísticos para los sistemas eléctricos de La Palma y de Gran Canaria.

- Comparar el rendimiento del esquema UFLS basado en FSM con los diseños estáticos y semi-adaptativos convencionales.
- Realizar un análisis de sensibilidad para evaluar cómo las modificaciones en variables clave, como la mayor penetración de FER, los cambios en la función objetivo, la implementación de almacenamiento, y el ajuste de los escalones de deslastre, afectan el rendimiento del esquema UFLS.

Asimismo, la metodología contempla una revisión exhaustiva de las prácticas actuales de UFLS, seguida por el desarrollo de un nuevo enfoque de diseño y modelado. Esto integra el criterio FSM con diseños estáticos y semi-adaptativos convencionales. Se utilizará el sistema eléctrico de La Palma como caso base. Además, se usará MATLAB para la optimización de parámetros y Simulink para simular el sistema de potencia.

3. Modelado del sistema de potencia

Esta sección presenta el modelo empleado para representar y simular pequeños sistemas de potencia aislados con esquema UFLS. Este modelo es capaz de capturar la dinámica de frecuencia a corto plazo de pequeños sistemas de potencia aislados.

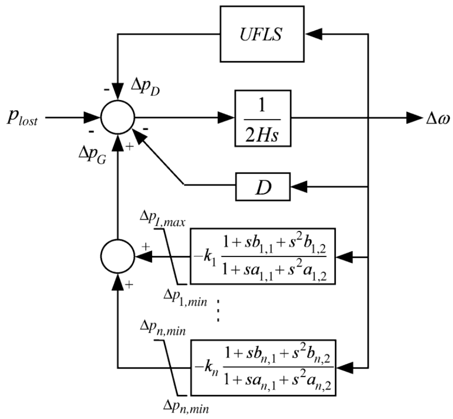

Figura 1. Dinámica de frecuencia del sistema de potencia [1]

El modelo del sistema de potencia comprende *n* unidades generadoras. Cada una se denota por una aproximación de segundo orden de su sistema turbina-gobernador. De hecho, la dinámica de frecuencia está influenciada principalmente por las dinámicas del rotor y del sistema turbina-gobernador. Los transitorios de excitación y del generador se pueden despreciar, ya que operan mucho más rápido que las dinámicas del sistema turbina-gobernador. Las turbinas de vapor suelen modelarse con modelos de primer orden. No obstante, el mix de generación también incluye turbinas de gas y diésel, lo que podría requerir modelos de orden superior [1].

Los parámetros del modelo se detallan en la Figura 1. La frecuencia se puede considerar uniforme [2], lo que permite calcular la inercia equivalente del sistema, H. El factor de amortiguación de carga, D, generalmente tiene un impacto insignificante, pues su influencia en condiciones de estado estacionario es menor en comparación con la ganancia del regulador de la turbina. Para cada generador g, se especifica la ganancia k_g y los parámetros $a_{g,1}$, $a_{g,2}$, $b_{g,1}$ y $b_{g,2}$, los cuales se pueden obtener de modelos adicionales o pruebas de campo. El modelo también incluye límites de salida del generador, $\Delta p_{g,min}$ y $\Delta p_{g,max}$, debido a las restricciones de reserva primaria.

4. Método para el diseño de un esquema UFLS basado en FSM

Esta sección se presenta la metodología para diseñar esquemas UFLS robustos y eficientes basado en FSM. Esto implica dos pasos: i) seleccionar los escenarios de OC adecuados y, ii) optimizar los parámetros (frecuencia, FSM, retardos) utilizando el algoritmo SA.

4.1. Selección de escenarios de operación y contingencia

La selección adecuada de los escenarios OC es crucial para garantizar la robustez del esquema UFLS. Aquí, solo las interrupciones de generación se consideran como contingencia, dado que conducen a las desviaciones de frecuencia más significativas en pequeños sistemas de energía aislados [1]. Para identificar escenarios representativos OC, se aplica el método basado en clústeres descrito en [5]. Este enfoque utiliza la técnica de K-Means para determinar el número óptimo de escenarios y los patrones que mejor representan las respuestas dinámicas de frecuencia de todas las contingencias posibles. Posteriormente, se identifican las respuestas reales que se aproximan con precisión a los patrones calculados.

4.2. Ajuste de los parámetros del esquema UFLS

La eficiencia del esquema UFLS se basa en el ajuste de sus parámetros, que se realiza para los escenarios representativos OC seleccionados. El problema de ajuste de UFLS se expresa como un problema de optimización con la siguiente función objetivo a minimizar:

$$\sum_{i=1}^{M} \alpha_{f,i} \cdot P_{shed,i}(\boldsymbol{x}_d) \tag{1}$$

Donde $\alpha_{f,i}$ es el i-ésimo factor de ponderación, que toma valor 1 como en [1], $P_{shed,i}$ representa la cantidad de carga deslastrada (pu) para la i-ésima contingencia y M denota el número total de escenarios representativos. Las variables de decisión, $\boldsymbol{x}_d$, incluye FSM, la frecuencia (ω), y los retardos intencionales asociados a la frecuencia y FSM, respectivamente ($t_{\omega,int}$ y $t_{FSM,int}$). Por lo tanto:

$$\boldsymbol{x}_d = [\omega \quad FSM \quad t_{int,\omega} \quad t_{int,FSM}]^T \tag{2}$$

El tamaño de los escalones de deslastre no se incluye como variable de decisión, ya que en pequeños sistemas de potencia aislados suele ser determinado define la compañía eléctrica y depende del alimentador conectado a los relés [1]. t_{open} tampoco se ha incluido, dado que representa el retardo de la señal de apertura, y normalmente se fija en 200 ms.

Las restricciones del sistema de potencia y el esquema UFLS son similares a las propuestas en [7] e incluyen: i) límites mínimos y ii) máximos de frecuencia. Por lo general, la restricción de frecuencia mínima admisible va acompañada de un retardo de tiempo máximo durante el cual la frecuencia puede estar por debajo de este umbral. Para pequeños sistemas de potencia aislados, un valor común es 47,5 Hz durante un 3 s [8]. Sin embargo, como en [1], este proyecto adopta valores más conservadores de 48Hz – 2 s. La frecuencia máxima permitida se establece en 52 Hz. Estas restricciones se formulan para los M escenarios OC:

$$g_1(\boldsymbol{x}_d) = t_{\omega \leq \omega_{min,allowable},i}(\boldsymbol{x}_d) - t_{\omega_{min,allowable}} \text{ for } i = 1, \dots, M \tag{3}$$

$$g_2(\boldsymbol{x}_d) = \omega_{max,i}(\boldsymbol{x}_d) - \omega_{max,allowable} \tag{4}$$

Las restricciones del esquema UFLS son: iii) el FSM debe permanecer por encima de su valor mínimo permitido (FSM = 0s), iv) el FSM no debe exceder su valor máximo permitido, (FSM = 1,2s), v) el esquema UFLS no actúa una vez que la frecuencia ha alcanzado su valor mínimo, pues la frecuencia se está restableciendo a su valor nominal, vi) la carga deslastrada es menor o igual a la potencia real perdida, y vii) se respeta la prioridad de las cargas.

$$g_3(\boldsymbol{x}_d, t) = FSM_{min,allowable} - FSM_{min,j}(\boldsymbol{x}_d) \tag{5}$$

$$g_4(\boldsymbol{x}_d) = FSM_{max,i}(\boldsymbol{x}_d) - FSM_{max,allowable} \tag{6}$$

$$g_5(\boldsymbol{x}_d) = t_{shed,j}(\boldsymbol{x}_d) - t_{\omega_{min},i}(\boldsymbol{x}_d) \tag{7}$$

$$g_6(\boldsymbol{x}_d) = A \cdot \boldsymbol{x}_d - \boldsymbol{\sigma_\omega} \tag{8}$$

Donde:

$$A = \left[\begin{array}{ccccc|ccccc|ccc|c|c|c|ccc}
-1 & 1 & \cdots & & & 0 & & \cdots & & 0 & 0 & \cdots & 0 & \cdots & \cdots & \cdots & 0 & \cdots & 0 \\
0 & 0 & \vdots & & & 0 & & \vdots & & 0 & & & & & & & & & \\
0 & 0 & 0 & -1 & 1 & 0 & & \cdots & & 0 & & \vdots & & \vdots & \vdots & \vdots & & \vdots & \\
0 & & \cdots & & & -1 & 1 & \cdots & & & & \vdots & & \vdots & \vdots & \vdots & & \vdots & \\
0 & & \vdots & & & 0 & 0 & \vdots & & & & & & & & & & & \\
0 & & \cdots & & & 0 & 0 & 0 & -1 & 1 & 0 & \cdots & 0 & \cdots & \cdots & \cdots & 0 & \cdots & 0
\end{array}\right]$$

$$\boldsymbol{\sigma_\omega} = \begin{bmatrix} \sigma_\omega \\ \vdots \\ \vdots \\ \sigma_\omega \end{bmatrix}$$

$$g_7(\boldsymbol{x}_d) = p_{shed,i}(\boldsymbol{x}_d) - p_{loss,i} \quad (9)$$

El problema de optimización se resuelve con el algoritmo de optimización SA. Las restricciones se tienen en cuenta añadiendo un término de penalización a la función objetivo.

5. Aplicación a sistemas eléctricos españoles aislados

La metodología descrita anteriormente se aplica a los sistemas de potencia aislados de La Palma y Gran Canaria, que cuentan con una demanda máxima de 35 MW (11 generadores) y 530 MW (22 generadores), respectivamente. Las condiciones de operación del sistema y los parámetros de las unidades generadoras se derivan de [1]. Los despachos de generación incluyen la generación de energía desacoplada (DPG) que representa hasta el 12% de la demanda total [1]. El esquema UFLS diseñado para La Palma se denominará caso base y será utilizado para realizar un análisis de sensibilidad sobre las condiciones de diseño.

5.1. Caso base – Sistema de potencia de La Palma

El diseño comienza con la identificación de escenarios representativos OC. Para ello, se aplica de forma iterativa el algoritmo K-Means, hallando que cuatro clústeres son suficientes para cubrir los 164 posibles escenarios de OC. La selección incluye contingencias N-1, ya que la pérdida de un solo generador puede superar el 50% de la demanda total. Note que durante la selección de escenarios OC, el esquema UFLS permanece inactivo. La Tabla 1 se presentan los escenarios representativos OC obtenidos.

Escenario	Generador	P_{dem} (MW)	P_{loss} (MW) (%)
8	11	27.37	2.35 (9.24)
3	17	18.48	9.55 (51.68)
8	15	27.37	6.10 (22.29)
1	17	22.09	10.41 (47.13)

Tabla 1. Escenarios representativos del sistema de potencia de La Palma

Para rediseñar el esquema UFLS semi-adaptativo y estático, se aplica el método propuesto en la Sección 4. Las variables de decisión incluyen los umbrales de frecuencia (ω_{thr}), los umbrales FSM (FSM_{thr}) y los retardos intencionales asociados a cada umbral ($t_{int,\omega thr}$, $t_{int,FSMthr}$). Los parámetros del esquema UFLS están acotados de la siguiente manera: i) 48 Hz $\leq \omega_{thr} \leq$ 49 Hz, ii) 0 s $\leq FSM_{thr} \leq$ 1,2 s, iii) 0 s $\leq t_{int,\omega thr} \leq$ 0.5 s, y iv) 0 s $\leq t_{int,FSMthr} \leq$ 0.5 s. El tamaño de los escalones de deslastre del esquema UFLS no se considera como variable de decisión; por lo que se utilizarán los propuestos en [1]. Además, se considera un tiempo de apertura del relé de 200 ms. Las restricciones de optimización son: v) $\omega <$ 48 Hz for t_{max} = 2 s, vi) 47 Hz$< \omega \leq$ 52 Hz vii) prioridad de deslastre de carga, y viii) deslastre de carga [MW] ≤ pérdida de generación [MW], y ix) el deslastre no debe ocurrir una vez alcanzado f_{min}. Seis escalones de deslastre de carga son suficientes para estabilizar la frecuencia, considerando una pérdida de generación del 51,68% en el peor de los casos. La Tabla 2 muestra el esquema UFLS propuesto (valores ajustados resaltados en negrita) y la Figura 2 c) ilustra su respuesta en frecuencia para todas las contingencias posibles.

Escalón	Subestación	ω_{thr} (Hz)	FSM_{thr} (s)	$t_{thr,F}$ (s)	$t_{thr,FSM}$ (s)	t_{open} (s)	Tamaño escalón (%)
1	2101	**49.00**	**0.80**	**0.03**	**0.20**	0.2	7.1
2	2102	**48.87**	**0.62**	**0.05**	**0.29**	0.2	0.6
3	3101	**48.72**	**0.32**	**0.02**	**0.06**	0.2	14.5
4	3102	**48.61**	**0.19**	**0.08**	**0.11**	0.2	3.6
5	2103	**48.44**	**0.17**	**0.14**	**0.08**	0.2	7.3
6	1101	**48.19**	**0.05**	**0.06**	**0.06**	0.2	13.6

Tabla 2. Esquema UFLS propuesto basado en FSM para el sistema de potencia de La Palma

El esquema propuesto tarda más en activarse en las dos primeras etapas. Si bien la tercera etapa tiene un tiempo de respuesta más corto en comparación con la optimizada convencional [1], pero en términos generales la respuesta se retrasa. En el resto de los casos, el FSM responde más rápido. Esto destaca uno de los principios del esquema basado en FSM: permitir que el sistema se recupere de forma natural en contingencias menores y que responda rápidamente en los casos más graves.

		Esquema UFLS existente		Esquema UFLS optimizado		Esquema UFLS basado en FSM	
Escenario	Generador (MW) (%)	ω_{min} (Hz)	P_{shed} (MW) (# relays)	ω_{min} (Hz)	P_{shed} (MW) (# relays)	ω_{min} (Hz)	P_{shed} (MW) (# relays)
8	2.35 (9.24)	49.13	0 (0)	49.13	0 (0)	49.13	0 (0)
3	9.55 (51.68)	45.74	10.94 (7)	47.01	8.63 (6)	47.12	8.63 (6)
8	6.10 (22.29)	48.01	7.06 (4)	47.79	6.08 (3)	48.30	1.94 (1)
1	10.41 (47.13)	46.59	13.08 (7)	47.21	10.32 (6)	47.37	10.32 (6)

Tabla 3. Respuesta de los diferentes esquemas UFLS aplicados al sistema de La Palma

La Tabla 3 proporciona información adicional sobre el rendimiento de los esquemas UFLS propuesto, existente y existente optimizado. Aunque en ningún caso se produce un sobredeslastre, el esquema UFLS existente alcanza las desviaciones de frecuencia más altas, incluso por debajo de 47 Hz. Los esquemas convencional optimizado y el basado en FSM presentan una respuesta similar, ambos desconectan menos carga que el existente, sin violar las restricciones. El esquema basado en FSM desprende la menor carga en el tercer escenario (S8G15), ya que detecta la gravedad de la perturbación antes y actúa más rápido, deteniendo la caída de frecuencia y evitando un mayor deslatre de carga. Por lo tanto, el esquema UFLS existente se ha optimizado con éxito para los escenarios representativos.

	Rendimiento de esquemas UFLS		
Caso	Deslastre total (MW)	Nº Relés	ΣΔωmin (Hz)
Existente	526.61	295	223.43
Optimizado	293.31	170	227.41
Basado en FSM	210.70	120	207.59

Tabla 4. Comparación de los diferentes diseños de esquemas UFLS del Sistema de potencia de La Palma

La Tabla 4 compara el rendimiento del sistema para los tres modelos de esquema UFLS aplicados a los 164 posibles escenarios N-1. Tanto el esquema convencional optimizado como el basado en FSM muestran una reducción significativa en la cantidad de carga deslastrada en comparación con el esquema existente, con el esquema basado en FSM deslastrando aún menos carga (60% de reducción frente a 30% de reducción). Esto también se refleja en el número de relés activados. Cabe destacar que el esquema basado en FSM muestra una suma de frecuencia mínima total más baja que los otros esquemas. Al disminuir el deslastre de carga, se esperaría el efecto contrario, ya que la reducción de la desconexión de carga generalmente conduce a una compensación con la frecuencia, lo que resultaría en desviaciones más negativas.

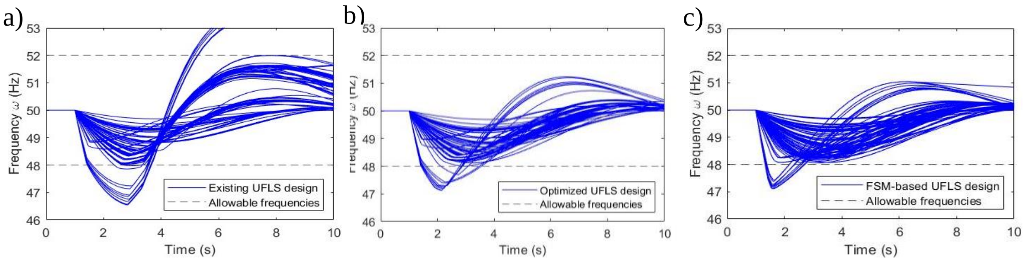

Figura 2. Respuesta en frecuencia global de los esquemas UFLS de La Palma: a) Existente, b) Convencional optimizado y c) Basado en FSM.

La Figura 2 ilustra las respuestas del sistema en términos de frecuencia para el esquema UFLS existente, su versión optimizada y la basada en FSM. Se observa que el esquema optimizado y el basado en FSM mantienen las desviaciones de frecuencia dentro de los límites permitidos, mientras que el esquema existente sufre inestabilidades de frecuencia, ya que los generadores no son capaces de ajustar adecuadamente su salida a la nueva demanda.

5.2. Sistema de potencia de Gran Canaria

Al igual que en el caso base, se usa el algoritmo K-Means de forma iterativa, identificando cuatro clústeres que representan todos los escenarios OC posibles. Debido a que la pérdida de un solo generador no afecta significativamente a la estabilidad de este sistema, se consideran múltiples contingencias. La Tabla 5 muestra los escenarios representativos OC. Los esquemas UFLS semi-adaptativos y estáticos se rediseñan bajo las mismas restricciones usadas en el sistema de La Palma. Una vez más, sin considerar el tamaño de los escalones como variables de decisión. Por lo que se adoptan las propuestas en [1]. Teniendo en cuenta que el peor escenario para la pérdida de generación simulada es del 51%, 10 escalones serían suficientes. No obstante, solo se ajustan 5. Estos se resaltan en negrita en la Tabla 6 y la Figura 3 ilustra la respuesta dinámica del sistema de Gran Canaria.

Escenario	Generador	P_{dem} (MW)	P_{loss} (MW) (%)
10	G23	527.64	49.92 (9.46)
21	G1, G2	536.20	140.48 (26.20)
23	G1-G3	517.41	204.90 (39.60)
21	G1-G4	536.20	269.47 (50.25)

Tabla 5. Escenarios representativos del sistema de potencia de Gran Canaria

Escalón	Subestación	ω_{thr} (Hz)	FSM_{thr} (s)	$t_{thr,F}$ (s)	$t_{thr,FSM}$ (s)	t_{open} (s)	Tamaño escalón (%)
1	1001 – 1007	**48.99**	**1.04**	**0.21**	**0.23**	0.2	3.43
2	1008 – 1015	**48.70**	**0.77**	**0.03**	**0.03**	0.2	5.27
3	1016 – 1023	**48.60**	**0.74**	**0.04**	**0.07**	0.2	5.03
4	1024 – 1030	**48.24**	**0.73**	**0.06**	**0.36**	0.2	5.68
5	1031 – 1035	**48.09**	**0.5**	**0.14**	**0.00**	0.2	4.17
6	1036 - 1047	48.66	-	0.5	-	0.2	9.95
7	1048 - 1053	48.60	-	0.6	-	0.2	5.46
8	1054 - 1058	48.55	-	0.7	-	0.2	3.05
9	1059 - 1066	48.50	-	0.8	-	0.2	4.07
10	1067 - 1074	48.35	-	0.9	-	0.2	5.89
11	1075 - 1090	48.00	-	1	-	0.2	10.34

Tabla 6. Esquema UFLS propuesto basado en FSM para el sistema de potencia de Gran Canaria

La Figura 3 se puede muestra que el esquema propuesto presenta una respuesta dinámica en frecuencia adecuada, en términos de evitar tanto el sobre-deslastre como el sub-deslastre. No obstante, cuando se aplica a todos los posibles escenarios OC, la respuesta en frecuencia no cumple con la restricción de mantenerse por encima de f_{LIM}, incluso considerando el margen de 2 s. Este mismo problema también se observó en [7]. Este problema surge como consecuencia de optimizar el esquema UFLS. A medida que se reduce la cantidad de carga desconectada, aumenta el número de escenarios con frecuencia mantenida baja. Para mitigar esto, [7] sugiere incluir un criterio adicional en la optimización que limite la frecuencia a no caer por debajo de 49 Hz por más de 5 s, medida que se aplica al esquema basado en FSM.

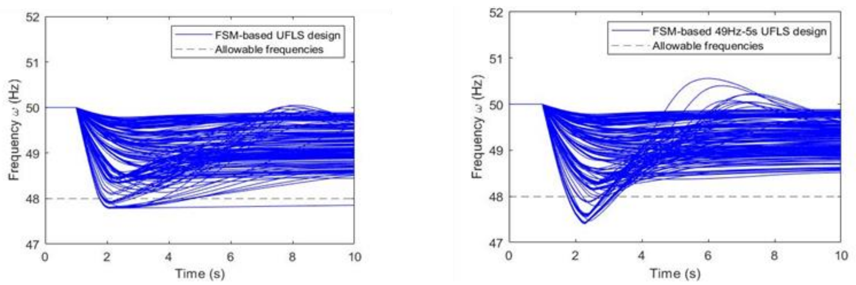

Figura 3. Respuesta en frecuencia de los esquemas UFLS en Gran Canaria: a) Basado en FSM, y b) Basado en FSM con la restricción 49Hz-5s

El criterio 49Hz-5s ayuda a mantener la frecuencia más cercana a 49 Hz en condiciones de estado estacionario. Sin embargo, varios escenarios aún se encuentran por debajo de este umbral, particularmente debido a las limitaciones de confiar únicamente en los relés FSM. Por el contrario, los esquemas que integran relés UF y RoCoF, como los observados en [7], gestionan mejor el deslastre de carga al considerar tanto los relés RoCoF como los de UF. Este enfoque dual garantiza frecuencias operativas más seguras, especialmente en escenarios en los que el sistema se estabiliza por debajo de 49 Hz. Por lo tanto, la integración de relés UF y FSM podría optimizar la respuesta del sistema en condiciones extremas, mejorando la estabilidad y confiabilidad del sistema de energía de Gran Canaria en estado estacionario.

	Rendimiento de esquemas UFLS		
Caso	Delastre total (MW)	Nº Relés	ΣΔωmin (Hz)
Existente	21,291.0	6498	334.90
Optimizado	8,916.9	2804	364.67
Basado en FSM	7,932.9	2557	390.02
Basado en FSM: 49Hz -5s	5,383	1654	198.39

Tabla 7. Comparación de los diferentes esquemas UFLS del sistema de potencia de Gran Canaria

6. Análisis de sensibilidad

Esta sección ofrece un análisis de sensibilidad de los esquemas UFLS respecto a las condiciones de diseño, considerando cuatro casos principales: i) el impacto del aumento de la penetración de FER, ii) la implementación de sistemas de almacenamiento de energía, iii) la modificación de la formulación de la función objetivo, y iv) la inclusión del tamaño del escalón como variable de decisión. En la Tabla 8 se describen y comparan los cuatro casos.

Rendimiento esquemas UFLS			
Caso	Deslastre total (MW)	Nº Relés	ΣΔωmin (Hz)
Caso Base	210.70	120	207.59
Aumento FER – I	356.84	183	188.82
Aumento FER – I (Optimizado)	319.80	156	208.80
Aumento FER – II	384.68	199	207.82
Aumento FER – II (Optimizado)	306.07	153	220.35
Caso base + SAE	93.19	60	132.48
Caso base + SAE (Optimizado)	79.28	56	139.21
Caso 1: $\sum(p_{shed} + \Delta\omega_{min})$	216.10	121	203.61
Caso 2: $\sum(p_{shed} + k_{eq}\Delta\omega_{min})$	220.99	124	201.95
Caso 3: $\sum(n_{count}\ p_{shed})$	215.40	122	209.80
Diseño escalones deslastre	203.88	143	217.32

Tabla 8. Comparación de los distintos diseños de esquemas UFLS basados en FSM

6.1. Aumento de la penetración de FER

En [6] se analiza cómo el aumento de la penetración de FER afecta al esquema UFLS basado en FSM de La Palma. Niveles más altos de FER resultan en mayores RoCoF y en desviaciones de frecuencia, subrayando la necesidad de investigar más a fondo su integración en el marco UFLS.

Se han considerado dos niveles adicionales de penetración de DPG, hasta el 24% y el 49% de la demanda total. Los esquemas UFLS fueron ajustados para cada nivel de DPG y comparados con el caso base (véase la Tabla 8). A medida que aumenta la penetración de FER, tanto el deslastre de carga como el número de errores aumentan, principalmente debido a frecuencias más bajas y desconexiones de carga excesivas, que conducen a sobredeslastres.

En el Escenario I (hasta 24%), el esquema UFLS optimizado elimina los sobredeslastres, mientras que el Escenario II (hasta 49%) todavía experimenta uno y cuatro casos donde la frecuencia cae por debajo de 48 Hz durante más de 2 s. El aumento significativo en la penetración de renovables en el Escenario II da lugar a mayores oscilaciones y tiempos de estabilización de frecuencia extendidos. Aunque hay menos sobredeslastres, la estabilidad de la frecuencia se ve comprometida, particularmente debido a la naturaleza aislada del sistema eléctrico de La Palma, que tiene baja inercia y reservas giratorias limitadas.

Esto pone de manifiesto que, sin la participación de las FER en el control de frecuencia primario, como el alivio de carga de los aerogeneradores [9], la estabilidad del sistema se ve comprometida. Para mejorar tanto la estabilidad como la eficiencia, las FER deberían aportar en reserva, lo que permitiría una reducción segura de la generación térmica.

6.2. Impacto de la implementación de almacenamiento

En esta sección se examina el impacto de la implementación de soluciones de almacenamiento de energía (SAE) en el rendimiento del esquema UFLS. En concreto, se incorpora un ultracondensador (UC) de 4 MW-5s en el caso base. Además, para analizar el efecto del almacenamiento en el proceso de diseño, se ha diseñado un esquema UFLS integrando SAE. La Figura 8 muestra que la incorporación de SAE en el esquema propuesto reduce el deslastre de carga en aproximadamente un 55%, lo que indica una mejora sustancial en el rendimiento del sistema de potencia. La mejora principal proviene de la simple inclusión de SAE, mientras que la optimización del esquema UFLS con SAE refina ligeramente los resultados. Note que, aunque la adición de SAE reduce el deslastre de carga, la optimización conduce a un comportamiento más oscilatorio, lo que resulta en mayores desviaciones de frecuencia mínima y máxima.

6.3. Variación de la formulación de la función objetivo

Esta sección explora formulaciones alternativas y más complejas con ponderación de parámetros. La adición de términos relacionados con la frecuencia da como resultado un diseño más conservador. Esto reduce las desviaciones de frecuencia, pero aumenta la cantidad de deslastre de carga. Se analizan tres enfoques:

- Caso 1: Añade un término relacionado con la frecuencia con el mismo factor de ponderación que la carga.
- Caso 2: Agrega un término relacionado con la frecuencia más conservador.
- Caso 3: El factor de ponderación de carga se ajusta en función del número de contingencias en cada escenario.

La Tabla 8 muestra que el Caso 1 disminuye la suma de las desviaciones de frecuencia mínimas, con la desviación máxima del sistema pasando de -2,90 Hz en el caso base a -2,77 Hz. Si bien el deslastre de carga aumenta ligeramente, la carga desconectada global sigue siendo menor que en el esquema existente y su versión optimizada. El enfoque más conservador, el Caso 2, da como resultado desviaciones de frecuencia más bajas y un aumento en la carga desconectada. Por último, multiplicar la carga de deslastre por el número de escenarios OC da como resultado un ligero aumento de la carga desconectada.

Los tres escenarios demuestran un sólido rendimiento del sistema, lo que garantiza un esquema UFLS robusto y eficiente. La opción más apropiada dependerá de los objetivos del esquema UFLS, ya sea que el reducir el deslastre de carga (P_{shed}) y/o en minimizar las desviaciones de frecuencia.

6.4. Diseño del esquema UFLS incluyendo el tamaño del escalón

En esta sección, se integra el tamaño de los escalones como variable de decisión en el esquema UFLS basado en FSM, permitiendo al algoritmo ajustar flexiblemente los valores óptimos. Esto redujo el porcentaje total de carga desconectada del 46,7% (caso base) al 41,61% en los seis escalones de UFLS.

Los tamaños ajustados por el algoritmo SA mostraron una reducción del 28% en el primer escalón (5,11%) y del 95% en el segundo (1,17%). Esto llevó a la activación de más relés, ya que en los escenarios analizados se activaron tanto el primer como el segundo escalón, a diferencia del caso base donde solo se activaba el primero. Los dos primeros escalones ahora representan un 6,28%, menos que el primer escalón del caso base por sí solo. Al aplicar este ajuste a las 164 perturbaciones, se logra reducir el deslastre de carga total en un 3,24% (mostrado en la Tabla 8), aunque conduce a una recuperación de frecuencia más lenta y oscilatoria. No obstante, la frecuencia se mantiene dentro de los límites aceptables (48 Hz durante 2 s) en todos los escenarios excepto en uno, donde el tiempo por debajo de 48 Hz es de 2,089 s. Se puede concluir que la mejora en la respuesta dinámica es limitada, ya que solo se logra una reducción del 3,24% en el deslastre de carga, lo que sugiere que la distribución actual de escalones ya ofrece un esquema UFLS eficiente.

Cabe destacar que este diseño carece de realismo, pues no incluye criterios específicos para ajustar de adecuadamente los tamaños de los escalones. El propósito de este enfoque fue evaluar su impacto global en la respuesta dinámica y en la cantidad de carga deslastrada.

7. Conclusiones

Este proyecto aborda la estabilidad de frecuencia en pequeños sistemas aislados. Para ello, se presenta un método para diseñar esquemas UFLS robustos y eficientes basados en FSM. El esquema propuesto se ha aplicado con éxito al sistema de La Palma, el cual muestra un buen rendimiento. Las principales conclusiones del proyecto son las siguientes:

- En La Palma, el esquema basado en FSM y el convencional optimizado, ofrecen una muy buena respuesta a las contingencias, con el primero reduciendo aún más el deslastre de carga. Además, este distingue entre escenarios críticos y no críticos.
- En Gran Canaria, el esquema convencional optimizado presenta una mejor respuesta en frecuencia dinámica en comparación con el propuesto, ya que gestiona el deslastre de carga de manera más efectiva al considerar tanto relés RoCoF como los UF.
- El análisis de sensibilidad mostró que incluir SAE en el diseño del esquema UFLS basado en FSM reduce significativamente el deslastre de carga. La principal mejora proviene de la simple inclusión del SAE. La optimización del esquema con SAE, aunque refina levemente los resultados, conduce a una respuesta más oscilatoria.
- El análisis de diferentes funciones objetivo enfatizó que la idoneidad de cada enfoque en el diseño de esquemas UFLS depende del objetivo que se persigue, es decir, si se busca reducir las desviaciones de frecuencia y/o el deslastre de carga.
- El estudio de escenarios con mayor penetración de FER en el esquema propuesto mostró un buen desempeño a niveles moderados de integración de FER. Sin

embargo, para un aumento sustancial, se concluyó que, para garantizar tanto la estabilidad como la eficiencia, las FER deberían contribuir al control primario.

- La relajación del diseño del tamaño de los escalones de deslastre, aunque mostró un buen rendimiento, resultó en una reducción mínima de la desconexión de carga, y esta ligera disminución condujo a un comportamiento más oscilatorio en comparación con el caso base, con períodos prolongados por debajo de los límites de frecuencia durante ciertas perturbaciones.

8. Referencias

[1] L. Sigrist, I. Egido and L. Rouco, «A Method for the Design of UFLS Schemes of Small Isolated Power Systems,» *IEEE Transactions on Power Systems*, vol. 27, nº 2, pp. 951-958, May 2012.

[2] Aderson, P.M (1999). Power System Protection. McGraw-Hill Companies

[3] U. Rudez, D. Sodin and R. Mihalic, “Estimating frequency stability margin for flexible under-frequency”, *Electric Power Systems Research*, vol. 194, 2021

[4] H. E. Lokay and V. Burtnyk, “Application of underfrequency relays for automatic load shedding,” *IEEE Trans. Power App. Syst*., vol. PAS-87, no. 3, pp. 720–726, Mar. 1968.

[5] L. Sigrist, I. Egido, E. F. Sanchez-Ubeda and L. Rouco, "Representative Operating and Contingency Scenarios for the Design of UFLS Schemes," in *IEEE Transactions on Power Systems*, vol. 25, no. 2, pp. 906-913, May 2010

[6] M. Vadillo, L. Sigrist and U. Rudez, "Design and comparison of UFLS schemes of isolated power systems based on frequency stability margin," *2023 IEEE Belgrade PowerTech*, Belgrade, Serbia, 2023, pp. 1-6

[7] L. Sigrist (2010), Design of underfrequency load-shedding schemes of small isolated power systems. Madrid (Spain).

[8] Ministry of Industry Tourism and Commerce of Spain, Resolution 9613 of 26 April 2006 Establishing the Operation Procedures for Insular and Extra Peninsular Power Systems, Official Bulletin of the State no 219 of 31 May 2006. [Online]. Available: http://www.ree.es.

[9] M. Rajabdorri, L. Sigrist, E. Lobato, M. d. C. Prats and F. Echavarren, "Viability of providing spinning reserves by RES in Spanish islandpower systems," *IET Renewable Power Generation*, vol. 15, 2021.

OPTIMAL TUNING OF UFLS SCHEMES BASED ON FREQUENCY STABILITY MARGIN

Author: Vadillo Díaz de Aguilar, Mónica.
Supervisor: Sigrist, Lukas.
Collaborating Entity: ICAI – Universidad Pontificia Comillas

ABSTRACT

The increasing penetration of renewable energy sources (RES) impacts system stability, particularly frequency stability in small isolated power systems such as the Canary Islands. Underfrequency load shedding (UFLS) are typically used as a las resort tool to protect power systems. The aim of this project is to optimize the parameters of an UFLS scheme based on the frequency stability margin (FSM) using heuristic algorithms, specifically simulated annealing, and compare its performance with the conventional UFLS scheme. The model is implemented both in the La Palma and the Gran Canaria power systems to assess its effectiveness in case of a disturbance (generator outage). The results of this study exhibit that implementing FSM in the La Palma's UFLS scheme significantly enhances its performance. In contrast, for Gran Canaria power system, although there is an improvement in load shedding reduction, the scheme is less effective than conventional approaches in diminishing large steady-state frequency deviations. Moreover, a sensitivity analysis of the FSM-based UFLS scheme for La Palma power system is presented, where the effect of varying key design parameters such as the level of RES penetration, the inclusion of storage, the objective function formulation, and the inclusion of the step size design, are studied.

Keywords: Design methodology, underfrequency load shedding, frequency stability margin, island power system protection

1. Introduction

Frequency stability is a critical concern for small isolated power systems. These systems are particularly vulnerable to disturbances that can cause substantial power imbalances, which compromise their security and reliability. The primary factors that jeopardize their stability and makes them more sensitive to disturbances include their low inertia, which can lead to rapid frequency decay during power disturbances, and their lack of interconnection, which constrains their ability to draw on the support of neighboring systems in the event of perturbances. This is further accentuated by the increasing penetration of renewable energy sources (RES), given that they typically do not provide inertia and barely contribute to the primary frequency control. Moreover, due to their small size and isolated nature, these systems are vulnerable to severe active power imbalances, where primary frequency control may not react quickly enough to restore power balance and maintain frequency within limits. Consequently, underfrequency load shedding (UFLS) schemes are typically employed to safeguard the power system's integrity.

UFLS schemes are a last-resort tool to prevent frequency instability and a complete system collapse. The majority of UFLS schemes today are conventional static and semi-adaptative schemes [1]. These schemes continuously measure frequency and/or the rate of change of frequency (RoCoF) by means of type 81 relays [2] and shed a predefined amount of load in case frequency and/or RoCoF fall below a certain threshold. The effectiveness of conventional UFLS schemes is heavily influenced by their design. An effective UFLS design must meet two key characteristics: robustness and efficiency. Selecting appropriate operating conditions enhances the scheme's robustness. Meanwhile, efficiency is achieved by fine-tuning the parameters of the UFLS scheme to minimize the amount of load shed while ensuring system stability [1].

Conventional UFLS schemes, while widely used, have several drawbacks. They lack adaptability [1], i.e., they are based on predefined load shedding amounts and do not adjust to the severity of disturbances. This can result in excessive or insufficient load disconnection. Advanced schemes offer an alternative solution in this regard, but require extensive communication and data collection, making them complex and potentially costly to implement. These schemes are mainly centralized, while conventional UFLS schemes are locally distributed. Conventional UFLS schemes can be enhanced to better distinguish between critical disturbances that require immediate action and those where load shedding can be postponed or even avoided. Recently, a novel adaptative UFLS approach using the Frequency Stability Margin (FSM) as a shedding criterion has been proposed in [3]. Unlike conventional methods that rely solely on frequency measurements, this approach incorporates the FSM – a frequency and RoCoF dependent criterion – to determine the remaining time before reaching the minimum allowable frequency (e.g. $f_{LIM} = 47.5\ Hz$). By comparing frequency measurements and FSM calculations against established thresholds, the system can initiate the appropriate load shedding actions.

There is no systematic method for designing UFLS schemes, but several approaches for conventional UFLS design can be found in the literature. Methods such as iterative trial and error, and screening processes [4] exist, but they do not guarantee an efficient performance. Deterministic optimization algorithms have been applied to optimize key parameters in conventional UFLS schemes. However, they depend on initial variable guesses and may be hindered by discontinuities in the objective function. Heuristic algorithms, such as genetic algorithms or simulated annealing (SA), provide a suitable alternative, demonstrating strong performance in objective functions with nonlinearities [1]. Nonetheless, they face challenges in small isolated power systems due to limited load step size.

Robust UFLS designs rely heavily on appropriate contingency selection. While various contingencies can be contemplated, in this project only generation outages are considered, as they have a significant impact on frequency deviations. Common practice involves evaluating operational conditions at different load-demand levels and designing the UFLS scheme based on the outages of the largest and smallest generating units. In [5], a clustering-based method is proposed to identify representative operating and contingency (OC) scenarios for UFLS design.

This project implements a FSM-based UFLS scheme in real isolated Spanish power systems. The proposed method is based on [1] where an efficient and robust approach for designing UFLS schemes is presented, but it has been adapted to include the FSM criterion proposed by [3]. To fine-tune the parameters of the UFLS scheme, SA is used, focusing on minimizing the amount of disconnected load.

2. Project definition

This project aims to enhance frequency stability in small isolated power systems by optimizing UFLS schemes. Based on previous research, which demonstrated the effectiveness of incorporating the FSM threshold, the project seeks to automate and improve the UFLS scheme proposed in [6] using advanced algorithms. The specific objectives are:

- Use data mining techniques to identify representative scenarios, pinpointing contingencies that effectively represent potential disturbances.
- Formulate the tuning of a UFLS scheme parameters as an optimization problem to be solved with heuristic algorithms for La Palma and Gran Canaria power system.

- Compare the performance of the FSM-based UFLS scheme with conventional static and semi-adaptive designs.
- Perform a sensitivity analysis to understand how variations in key variables affect the UFLS scheme's performance (increased RES penetration, storage implementation, changes in the objective function, and relaxation of constraints).

The methodology involves a comprehensive review of current UFLS practices, followed by the development of a new design and modeling approach. This integrates the FSM criterion with conventional static and semi-adaptive designs. The power system of La Palma (Canary Islands) serves as the base case for the implementation and optimization. MATLAB will be used for parameter optimization, while Simulink will simulate the complete power system.

3. System modeling

This section outlines the model used to represent and simulate small isolated power system with UFLS scheme. This model is able to capture the short-term frequency dynamics of small isolated power systems.

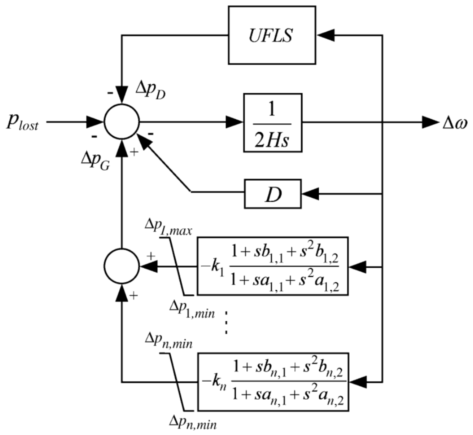

Figure 1. System-frequency dynamic of the power system [1]

The power system model comprises *n* generating units. Each generator is denoted by a second-order approximation of its turbine-governor system. In fact, frequency dynamics are mainly influenced by rotor and turbine-governor system dynamics. Excitation and generator transients can be neglected as they operate much faster than the turbine-governor system dynamics. Steam turbines are generally modeled by first-order models. Nonetheless, the generation mix also includes gas-driven and diesel-driven turbines, which might require the adoption of higher-order models [1].

The parameters of the model are detailed in Figure 1. The equivalent system inertia H can be determined, as frequency can be considered uniform [2]. The load-damping factor D is generally negligible due to its limited effect in steady-state conditions compared to the turbine-governor gain. Additionally, for each generator g, the gain k_g and parameters $a_{g,1}$, $a_{g,2}$, $b_{g,1}$ and $b_{g,2}$, are specified and can be obtained from more models or field tests. Furthermore, the model incorporates boundaries for the generator output constraints due to the limitations of primary spinning reserves, thus $\Delta p_{g,min}$ and $\Delta p_{g,max}$ are included.

4. Method for the design of the FSM – based UFLS scheme

This section presents the methodology for designing robust and efficient UFLS schemes. This involves two steps: i) selecting the suitable OC scenarios and, ii) optimizing the parameters (ω_{thr}, FSM_{thr}, $t_{f_{thr}}$, $t_{FSM_{thr}}$) using the SA algorithm.

4.1. Selection of OC scenarios

The adequate selection of OC scenarios is crucial to ensure the robustness of the UFLS scheme. Here, only generation outages are considered as contingency, given that they lead to the most significant frequency deviations in small isolated power systems [1].

To identify representative OC scenarios, the clustering-based method described in [5] is applied. This approach uses the K-means technique to determine the optimal number of clusters and the patterns that best represent the dynamic frequency responses of all possible contingencies. Subsequently, the real responses that accurately approximate the calculated patterns are identified.

4.2. Tuning of UFLS schemes parameters

The efficiency of the UFLS scheme relies on the adjustment of its parameters, which is performed for the selected representative OC scenarios. The UFLS tuning problem is expressed as an optimization problem with the following objective function to be minimized:

$$\sum_{i=1}^{M} \alpha_{f,i} \cdot P_{shed,i}(\boldsymbol{x}_d) \tag{1}$$

where $\alpha_{f,j}$ is the *ith* weighting factor, which is set to unity as in [1]; $P_{shed,i}$ represents the amount of shed load (pu) for the *ith* contingency and M denotes the total number of representative OC scenario. The decision variables, $\boldsymbol{x}_d$, include FSM, ω, $t_{\omega,int}$ and $t_{FSM,int}$. Therefore:

$$\boldsymbol{x}_d = [\omega \quad FSM \quad t_{int,\omega} \quad t_{int,FSM}]^T \tag{2}$$

The step size is not included as decision variable since, for small isolated power systems, it is typically defined by the utility and depends on the feeder connected to the relays [1]. The t_{open} has also not been included, given that it represents the opening signal delay, and it is typically set to 200 ms for all steps.

The constraints for the power system and UFLS scheme are similar to those proposed in [7]. The system constraints include: i) the minimum and ii) maximum allowable frequency values. Generally, the minimum admissible frequency constraint is accompanied by a maximum time delay during which the frequency can remain below this threshold. For small isolated power systems, common values are 47.5 Hz for a maximum of 3 s [8]. However, as in [1], this project adopts more conservative values of 48Hz – 2 s. The maximum allowable frequency is set at 52 Hz. These constraints are formulated for the M OC scenarios:

$$g_1(\boldsymbol{x}_d) = t_{\omega \le \omega_{min,allowable},i}(\boldsymbol{x}_d) - t_{\omega_{min,allowable}} \text{ for } i = 1, \dots, M \tag{3}$$

$$g_2(\boldsymbol{x}_d) = \omega_{max,i}(\boldsymbol{x}_d) - \omega_{max,allowable} \tag{4}$$

The UFLS scheme constraints are iii) FSM must remain above its minimum allowable value, which is set to 0, iv) FSM must not exceed its maximum allowable value, established at 1.2 s, v) UFLS scheme does not act once the frequency has exceeded its minimum value, as the frequency is restoring to its nominal value, vi) the amount of disconnected load is less than or equal to the amount of real power lost, and vii) priority of loads is respected.

$$g_3(\boldsymbol{x}_d, t) = FSM_{min,allowable} - FSM_{min,j}(\boldsymbol{x}_d) \tag{5}$$

$$g_4(\boldsymbol{x}_d) = FSM_{max,i}(\boldsymbol{x}_d) - FSM_{max,allowable} \tag{6}$$

$$g_5(\boldsymbol{x}_d) = t_{shed,j}(\boldsymbol{x}_d) - t_{\omega_{min},i}(\boldsymbol{x}_d) \tag{7}$$

$$g_6(\boldsymbol{x}_d) = A \cdot \boldsymbol{x}_d - \boldsymbol{\sigma_\omega} \tag{8}$$

Where:

$$A = \left[\begin{array}{ccccc|ccccc|ccc|c|c|c|ccc}
-1 & 1 & \cdots & & & 0 & & \cdots & & 0 & 0 & \cdots & 0 & \cdots & \cdots & \cdots & 0 & \cdots & 0 \\
0 & 0 & \vdots & & & 0 & & \vdots & & 0 & & & & & & & & & \\
0 & 0 & 0 & -1 & 1 & 0 & & \cdots & & 0 & & \vdots & & \vdots & \vdots & \vdots & & \vdots & \\
0 & & \cdots & & & -1 & 1 & \cdots & & & & \vdots & & \vdots & \vdots & \vdots & & \vdots & \\
0 & & \vdots & & & 0 & 0 & \vdots & & & & & & & & & & & \\
0 & & \cdots & & & 0 & 0 & 0 & -1 & 1 & 0 & \cdots & 0 & \cdots & \cdots & \cdots & 0 & \cdots & 0
\end{array}\right]$$

$$\boldsymbol{\sigma_\omega} = \begin{bmatrix} \sigma_\omega \\ \vdots \\ \vdots \\ \sigma_\omega \end{bmatrix}$$

$$g_7(\boldsymbol{x}_d) = p_{shed,i}(\boldsymbol{x}_d) - p_{loss,i} \tag{9}$$

The optimization problem is solved with the SA optimization algorithm. The constraints are taken into account by adding a penalty term to the objective function.

5. Application to isolated Spanish power systems

The methodology outlined above is applied to the power systems of La Palma and Gran Canaria, which are small isolated Spanish power systems with a peak demand of 35 MW (11 generators) and 530 MW (22 generators), respectively. The system operation conditions (SOC), and the parameters of the generating unit models are derived from [1]. The generation dispatches include decouple power generation (DPG) which accounts for up to 12% of total demand [1]. The resulting UFLS scheme for the La Palma power system will be referred to as the case base, which is used to perform a sensitivity analysis on the design conditions.

5.1. Base case – La Palma power system

The first step in the design is to identify the representative OC scenarios. For this purpose, the K-Means algorithm is applied iteratively, determining that four clusters are sufficient to cover the 164 possible OC scenarios. The selection includes N-1 contingencies, since the loss of a single generator can exceed 50% of the total demand. Note that during the OC scenarios selection process the UFLS scheme remains inactive. Table 1 presents the representative OC scenarios obtained through this clustering approach.

Scenario	Generator	P_{dem} (MW)	P_{loss} (MW) (%)
8	11	27.37	2.35 (9.24)
3	17	18.48	9.55 (51.68)
8	15	27.37	6.10 (22.29)
1	17	22.09	10.41 (47.13)

Table 1. Optimal OC Scenarios of the La Palma power system

To redesign the semi-adaptive and static UFLS scheme, the method proposed in Section 4 is applied. The decision variables include the frequency thresholds (ω_{thr}), the FSM thresholds (FSM_{thr}), and the intentional delays associated with each threshold ($t_{int,\omega_{thr}}$, $t_{int,FSM_{thr}}$). The UFLS scheme parameters are bounded as follows: i) 48 Hz $\leq \omega_{thr} \leq$ 49 Hz, ii) 0 s $\leq FSM_{thr} \leq$ 1.2 s, iii) 0 s $\leq t_{int,\omega_{thr}} \leq$ 0.5 s, and iv) 0 s $\leq t_{int,FSM_{thr}} \leq$ 0.5 s. The step size of the UFLS scheme stages is not considered as decision variables; therefore, those proposed posed in [1] will be utilized. Additionally, a relay opening time of 200 ms is considered.

The optimization constraints are: v) $\omega <$ 48 Hz for $t_{max} = 2$ s, vi) 47 Hz $< \omega \leq$ 52 Hz, vii) priority of load shedding, and viii) load shed [MW] < power generation loss [MW], and ix) load shedding should not occur once f_{min} is reached. Six load shedding steps are sufficient to stabilize frequency, since the worst-case scenario considered involves a generation loss of 51.68%. Table 2 displays the proposed UFLS scheme (tuned values are highlighted in bold) and Figure 2 c) illustrates its frequency response for all possible contingencies.

Stage	Substation	ω_{thr} (Hz)	FSM_{thr} (s)	$t_{thr,F}$ (s)	$t_{thr,FSM}$ (s)	t_{open} (s)	Step size (%)
1	2101	**49.00**	**0.80**	**0.03**	**0.20**	0.2	7.1
2	2102	**48.87**	**0.62**	**0.05**	**0.29**	0.2	0.6
3	3101	**48.72**	**0.32**	**0.02**	**0.06**	0.2	14.5
4	3102	**48.61**	**0.19**	**0.08**	**0.11**	0.2	3.6
5	2103	**48.44**	**0.17**	**0.14**	**0.08**	0.2	7.3
6	1101	**48.19**	**0.05**	**0.06**	**0.06**	0.2	13.6

Table 2. Proposed FSM-based UFLS scheme of the La Palma power system

The proposed scheme takes longer to activate the first two stages. While the third stage has a shorter response time compared to the conventional optimized one [1], the overall response time is still delayed. In subsequent cases, the FSM responds quicker. This highlights a key principle of the FSM-based scheme: allowing the system to recover naturally during minor contingencies while responding quickly in more severe cases.

		Existing UFLS scheme		Optimized UFLS scheme		FSM – based UFLS scheme	
Scenario	Generator (MW) (%)	ω_{min} (Hz)	P_{shed} (MW) (# relays)	ω_{min} (Hz)	P_{shed} (MW) (# relays)	ω_{min} (Hz)	P_{shed} (MW) (# relays)
8	2.35 (9.24)	49.13	0 (0)	49.13	0 (0)	49.13	0 (0)
3	9.55 (51.68)	45.74	10.94 (7)	47.01	8.63 (6)	47.12	8.63 (6)
8	6.10 (22.29)	48.01	7.06 (4)	47.79	6.08 (3)	48.30	1.94 (1)
1	10.41 (47.13)	46.59	13.08 (7)	47.21	10.32 (6)	47.37	10.32 (6)

Table 3. Output of the different UFLS schemes applied to the La Palma power system

Table 3 provides additional information on the performance of the proposed, existing, and optimized UFLS schemes. Although no over-shedding occurs in any case, the existing UFLS scheme reaches the highest frequency deviations, even below 47 Hz. The conventional optimized and FSM-based schemes show a similar response, both shedding less load than the existing one, without violating performance constraints. The FSM-based scheme sheds the least load in the third contingency, as it detects the severity of the disturbance earlier and acts faster, arresting the frequency and preventing further load shedding. Thus, the existing UFLS scheme has been successfully optimized for the representative OC scenarios.

	UFLS performance		
Case	Total shed (MW)	Nº Relays	$\Sigma\Delta\omega min$ (Hz)
Existing	526.61	295	223.43
Optimized	293.31	170	227.41
FSM – based	210.70	120	207.59

Table 4. Comparison of the different UFLS scheme designs of the La Palma power system

Table 4 compares the system performance of the three UFLS scheme models when applied to the 164 possible N-1 scenarios. The amount of load shed is significantly reduced in the conventional optimized and FSM-based schemes compared to the existing one, with the FSM-based scheme shedding even less load (60% reduction vs 30% reduction). This is also reflected in the number of activated relays. It is notable that the FSM-based scheme shows a lower total minimum frequency sum than the other schemes. By diminishing load shedding, the opposite effect would be expected, as reducing load disconnection typically leads to a trade-off with frequency, resulting in more negative deviations.

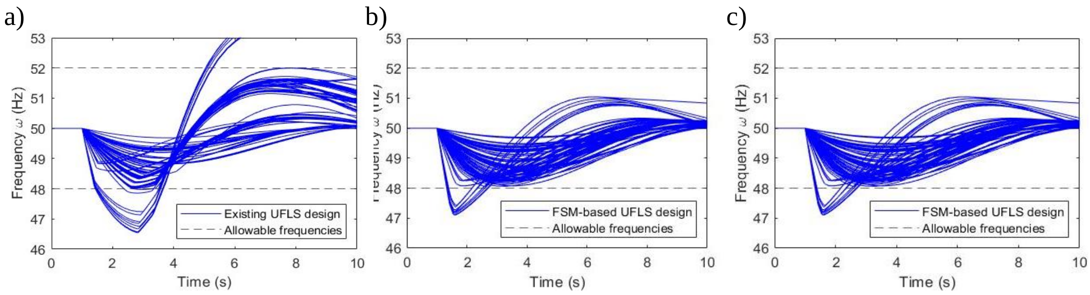

Figure 2. Overall frequency response of the La Palma UFLS schemes: a) Existing, b) Conventional optimized and c) FSM-based.

Figure 2 illustrates and compares the system responses in terms of frequency of the existing UFLS scheme, its optimized version and the FSM-based one. It can be seen that, in the case of the FSM and the conventional optimized UFLS schemes, the frequency deviations remain within the maximum and minimum allowed frequency values. By contrast, the existing UFLS scheme causes frequency instabilities, since the generators cannot reduce their output to the new level of load demand.

5.2. Gran Canaria power system

Similar to the base case, the K-Means algorithm is used iteratively, resulting in four clusters that represent all possible OC scenarios. Multiple contingencies are considered, as the loss of a single generator barely compromises system stability. Table 5 presents the representative OC scenarios derived from clustering.

The semi-adaptive and static UFLS schemes are redesigned using the same constraints as those used for the La Palma power system. Again, the step size of the UFLS scheme stages is not considered as decision variables; therefore, those proposed [1] are adopted. Considering that the worst-case scenario for the simulated generation loss is 51%, 10 steps will be sufficient, but only 5 stages are adjusted. These are highlighted in bold in Table 6 and Figure 3 illustrates the dynamic response of the Gran Canaria system.

Scenario	Generator	P_{dem} (MW)	P_{loss} (MW) (%)
10	G23	527.64	49.92 (9.46)
21	G1, G2	536.20	140.48 (26.20)
23	G1-G3	517.41	204.90 (39.60)
21	G1-G4	536.20	269.47 (50.25)

Table 5. Optimal OC Scenarios of the Gran Canaria power system

Stage	Feeders	ω_{thr} (Hz)	FSM_{thr} (s)	$t_{thr,F}$ (s)	$t_{thr,FSM}$ (s)	t_{open} (s)	Step size (%)
1	1001 – 1007	**48.99**	**1.04**	**0.21**	**0.23**	0.2	3.43
2	1008 – 1015	**48.70**	**0.77**	**0.03**	**0.03**	0.2	5.27
3	1016 – 1023	**48.60**	**0.74**	**0.04**	**0.07**	0.2	5.03
4	1024 – 1030	**48.24**	**0.73**	**0.06**	**0.36**	0.2	5.68
5	1031 – 1035	**48.09**	**0.5**	**0.14**	**0.00**	0.2	4.17
6	1036 - 1047	48.66	-	0.5	-	0.2	9.95
7	1048 - 1053	48.60	-	0.6	-	0.2	5.46
8	1054 - 1058	48.55	-	0.7	-	0.2	3.05
9	1059 - 1066	48.50	-	0.8	-	0.2	4.07
10	1067 - 1074	48.35	-	0.9	-	0.2	5.89
11	1075 - 1090	48.00	-	1	-	0.2	10.34

Table 6. Proposed FSM-based UFLS scheme of the Gran Canaria power system

From Figure 3 it can be inferred that the proposed scheme demonstrates a suitable dynamic frequency response in terms of avoiding both over-shedding and undershedding. Nonetheless, when applied to all possible OC scenarios, the frequency response does not meet the constraint of remaining above the frequency limit, even considering the 2s margin. The same issue was also observed in [7]. This arose as a consequence of optimizing the UFLS scheme. As the amount of disconnected load is reduced, the number of scenarios with low maintained frequency increases. To address this, [7] proposed including an additional criterion in the optimization, which consists of limiting the frequency from falling below 49 Hz for more than 5 s. Therefore, the same measure is applied to the FSM-based scheme.

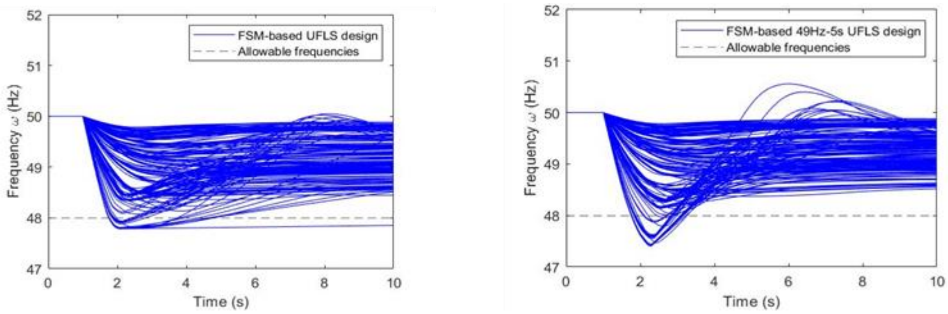

Figure 3. Overall frequency response of the Gran Canaria UFLS schemes: a) FSM-based b) FSM-based with the 49Hz-5s constraint

Applying the 49Hz-5s criterion helps to arrest frequency closer to 49 Hz in steady-state conditions. However, several scenarios still fall below this threshold, particularly due to the limitations of relying solely on FSM relays. In contrast, schemes that integrate both UF and RoCoF relays, such as those observed in [7], better manage load shedding by considering both RoCoF and UF relays. This dual approach ensures safer operational frequencies, particularly in scenarios where the system stabilizes below 49 Hz. Therefore, integrating both UF and FSM relays would optimize the system's response under extreme conditions, enhancing the stability and reliability of the Gran Canaria power system in steady state.

	UFLS performance		
Case	Total shed (MW)	Nº Relays	ΣΔωmin (Hz)
Existing	21,291.0	6498	334.90
Optimized	8,916.9	2804	364.67
FSM – based	7,932.9	2557	390.02
FSM – based: 49Hz -5s	5,383	1654	198.39

Table 7. Comparison of the different UFLS scheme designs of the Gran Canaria power system

6. Sensitivity Analysis

This section provides a sensitivity analysis of UFLS scheme designs regarding the designed conditions. The analysis focuses on four main cases: i) the impact of increasing RES penetration, ii) the implementation of energy storage systems, iii) the modification of the objective function formulation, and iv) the inclusion of step size as a decision variable. Table 8 outlines and compares the four cases.

UFLS performance			
Case	Total shed (MW)	Nº Relays	ΣΔωmin (Hz)
Base Case	210.70	120	207.59
Increased RES – I	356.84	183	188.82
Increased RES – I (Optimized)	319.80	156	208.80
Increased RES – II	384.68	199	207.82
Increased RES – II (Optimized)	306.07	153	220.35
Base case + ESS	93.19	60	132.48
Base case + ESS (Optimized)	79.28	56	139.21
Case 1: $\sum(p_{shed} + \Delta\omega_{min})$	216.10	121	203.61
Case 2: $\sum(p_{shed} + k_{eq}\Delta\omega_{min})$	220.99	124	201.95
Case 3: $\sum(n_{count}\ p_{shed})$	215.40	122	209.80
Step size design	203.88	143	217.32

Table 8. Comparison of different FSM-based UFLS schemes designs

6.1. Increasing RES penetration

The impact of increased RES penetration on the La Palma FSM-based UFLS scheme has been examined in [6]. Higher RES levels lead to higher RoCoF and frequency deviations, indicating the need for further exploration of their integration into the UFLS framework.

Two additional DPG penetration levels – up to 24% and 49% of total demand – have been considered. UFLS schemes have been tuned for each DPG, and performance have been compared with the base case (see Table 8). As RES penetration increases, both load shedding and the number of errors rise, primarily due to lower frequencies and excessive load disconnections, which lead to overshoots.

The optimized UFLS scheme for Scenario I eliminates overshoots, while Scenario II still experiences one overshoot and four cases where the frequency drops below 48 Hz for more than 2 s. The significant increase in RES penetration (up to 49%) in Scenario II results in greater oscillations and extended frequency stabilization times. Despite fewer overshoots, frequency stability is compromised, particularly due to the isolated nature of La Palma's power system, which has low inertia and limited spinning reserves.

This highlights that, without integrating RES into primary frequency control, such as wind deloading [9], system stability is compromised. To enhance both stability and efficiency, RES should be integrated into spinning reserves, allowing for a safe reduction of thermal generation.

6.2. Impact of implementing storage

The impact of implementing energy storage solutions (ESS) on the performance of the UFLS scheme is examined in this section. Specifically, a 4 MW-5s ultracapacitor (UC) is incorporated into the base case. Furthermore, to analyze the effect of storage on the design process, a UFLS scheme has been designed under these generation conditions.

Figure 8 shows that incorporating ESS into the proposed scheme reduces load shedding by approximately 55%, indicating a substantial improvement in power system performance. The primary enhancement comes from the simple inclusion of ESS, while optimizing the UFLS scheme with ESS slightly refines the results. Note that although adding ESS reduces load shedding, the optimization leads to more oscillatory behavior, resulting in increased minimum and maximum frequency deviations.

6.3. Varying the objective function formulation

This section explores alternative and more complex formulations with parameter weighting. Adding frequency-related terms results in a more conservative design. This reduces frequency deviations but increases the amount of load shed. Three approaches are analyzed:

- Case 1: Adds a frequency-related term with the same weighting factor as the load.
- Case 2: Adds a frequency-related term with a greater emphasis on frequency.
- Case 3: Load weighting factor adjusts based on the number of contingencies in each scenario.

Table 8 shows that Case 1 decreases the sum of minimum frequency deviations, with the maximum system deviation dropping from -2.90 Hz in the base case to -2.77 Hz. While load shedding increases slightly, the overall disconnected load remains lower than in both the existing scheme and its optimized version. The most conservative approach, Case 2, results in lower minimum frequency deviations and an increase in disconnected load. Finally, multiplying the shed load by the number of operational contingency scenarios results in a slight increase in the disconnected load.

The three scenarios demonstrate strong system performance, ensuring a robust and efficient UFLS scheme. The most appropriate option will depend on the objectives of the UFLS scheme—whether the focus is on reducing load shedding (P_{shed}) and/or on minimizing frequency deviations.

6.4. UFLS scheme design including step size

This section integrates step size design as a decision variable in the FSM-based UFLS scheme. It is included as an unbounded variable, allowing the algorithm to flexibly determine optimal values. As a result, the total percentage of load disconnected across the six UFLS steps diminished from 46.7% in the base case to 41.61%.

The step sizes proposed by the SA algorithm showed a 28% reduction in the first step (to 5.11%) and a 95% increase in the second (to 1.17%). As a result, more relays are activated, since, unlike in the base case in scenarios—where only the first step was triggered—both the first and second steps are activated here. Together, they account for 6.28%, lower than the base case's first step alone. When applied to 164 disturbances, this adjustment reduces total load shedding by 3.24% (as shown in Table 8) but leads to slower frequency recovery and more oscillatory behavior. Nonetheless, the frequency remains within acceptable limits (48 Hz for 2 s) in all but one scenario, where the time below 48 Hz is 2.089 s. It can be concluded that the improvement in the dynamic response is limited, as only a 3.24% reduction in load shedding is achieved, which suggests that the current distribution of steps already offers an efficient UFLS scheme.

Note that this design lack realism, as it does not incorporate specific criteria for effectively adjusting step sizes. The objective of this approach was to evaluate the overall effect on the dynamic response and the amount of load shed.

7. Conclusions

This project examines the problem of frequency stability, a major concern for small isolated power systems. To address this, it presents a method for designing robust and efficient FSM-based UFLS schemes. The proposed UFLS scheme has been successfully applied to the La Palma power system, showing a good performance. The key findings of the project are:

- The FSM and the conventional optimized UFLS schemes, designed for the La Palma power system, provide a very good response to contingencies, with the FSM-based UFLS scheme achieving an even greater reduction in the amount of load shed. Moreover, it is able to distinguish between critical and non-critical scenarios.
- For the Gran Canaria power system, the conventional optimized UFLS scheme provides a better dynamic frequency response compared to the proposed one, as it manages load shedding more effectively by considering both RoCoF and UF relays.
- The sensitivity analysis showed that including ESS into the power system when designing the FSM-based UFLS scheme significantly reduces load shedding. However, the primary enhancement comes from the simple inclusion of ESS, while optimizing the UFLS scheme with ESS slightly refines the results and leads to a more oscillatory behavior.
- The analysis of different objective function formulations emphasized that the suitability of each approach in UFLS scheme design depends on the primary goal, i.e., whether the focus is on reducing frequency deviation and/or load shedding.
- The application of the proposed scheme to scenarios with higher RES penetration showed a good performance at moderate levels of RES integration. However, for a substantial increase, it was concluded that, to ensure both stability and efficiency, RES should contribute to primary frequency control.
- The relaxation of the step size design, although it showed good performance, resulted in minimal reduction of load shedding, and this slight reduction led to more oscillatory behavior compared to the base case, with extended periods below frequency limits during certain disturbance.

8. References

[1] L. Sigrist, I. Egido and L. Rouco, «A Method for the Design of UFLS Schemes of Small Isolated Power Systems,» *IEEE Transactions on Power Systems*, vol. 27, nº 2, pp. 951-958, May 2012.

[2] Aderson, P.M (1999). Power System Protection. McGraw-Hill Companies

[3] U. Rudez, D. Sodin and R. Mihalic, "Estimating frequency stability margin for flexible under-frequency", *Electric Power Systems Research*, vol. 194, 2021

[4] H. E. Lokay and V. Burtnyk, "Application of underfrequency relays for automatic load shedding," *IEEE Trans. Power App. Syst*., vol. PAS-87, no. 3, pp. 720–726, Mar. 1968.

[5] L. Sigrist, I. Egido, E. F. Sanchez-Ubeda and L. Rouco, "Representative Operating and Contingency Scenarios for the Design of UFLS Schemes," in *IEEE Transactions on Power Systems*, vol. 25, no. 2, pp. 906-913, May 2010

[6] M. Vadillo, L. Sigrist and U. Rudez, "Design and comparison of UFLS schemes of isolated power systems based on frequency stability margin," *2023 IEEE Belgrade PowerTech*, Belgrade, Serbia, 2023, pp. 1-6

[7] L. Sigrist (2010), Design of underfrequency load-shedding schemes of small isolated power systems. Madrid (Spain).

[8] Ministry of Industry Tourism and Commerce of Spain, Resolution 9613 of 26 April 2006 Establishing the Operation Procedures for Insular and Extra Peninsular Power Systems, Official Bulletin of the State no 219 of 31 May 2006. [Online]. Available: http://www.ree.es.

[9] M. Rajabdorri, L. Sigrist, E. Lobato, M. d. C. Prats and F. Echavarren, "Viability of providing spinning reserves by RES in Spanish islandpower systems," *IET Renewable Power Generation*, vol. 15, 2021.

.

Contents

Figure Index

Table Index

Chapter 1. INTRODUCTION

1.1 PROBLEM STATEMENT

The urgent need to mitigate the impact of climate change and prevent irreversible environmental damage is driving countries to reduce their greenhouse gas (GHG) emissions. As global electricity demand continues to rise, particularly with the anticipated electrification of heating and transport sectors [1], the imperative to decarbonize the electricity supply becomes increasingly critical. The focus on renewable energy is decisive, as evidenced by the 2015 Paris Agreement, where countries agreed to reduce GHG emissions to limit global temperature rise to 2ºC above pre-industrial levels, with the ambition to limit it to 1.5ºC [2]. The European Union (EU) has further strengthened this commitment by setting ambitious targets to achieve carbon neutrality by 2050. In this landscape, the energy sector emerges as a key player, accounting for around 75% of total CO_2 emissions in the EU in 2022 [3]. Without proactive measures, these emissions will continue to rise in line with the growing energy demand of a growing global population. Therefore, increasing the penetration of renewable energy sources (RES) in the energy mix is not only urgent, but essential to meet the global sustainability goals.

The commitment to intensify the penetration of RES is even more critical in the context of recent geopolitical tensions. Particularly, the conflict between Russia and Ukraine has highlighted the vulnerabilities of nations that depend on imported gas and oil. This has accelerated the transition towards RES, as countries seek to control their energy resources and diversify them to ensure stability and an uninterrupted power supply. Accordingly, the European Commission has strengthened the EU Renewable Energy Directive [4]. This new agreement, enclosed within the "Fit for 55" measures, aims to reduce at least 55% of GHG emissions by 2030 and to increase the RES penetration target from 32% to 42.5%.

Accelerating the penetration of RES not only mitigates dependency on external energy suppliers, but also brings several advantages. These include decreased dependency on fossil fuels, lower carbon-dioxide emissions, and economic benefits such as reduced energy costs and operational expenses.

Nonetheless, the shift from synchronous generators to decoupled power generators presents significant challenges. Given that RES depend on climate conditions and weather changes, they provide a highly variable and intermittent generation. This lack of predictability leads to significant problems for systems with higher RES penetration, since conventional generators must face higher variations in net demand, and subsequently pose an obstacle to the deployment of wind and photovoltaic (PV) technology. Recent events in the Spanish power grid illustrate these challenges. Red Eléctrica de España (REE), the Spanish system operator, activated its Demand Response Mechanism, which temporarily halted part of the industry due to energy supply shortages, for the second time in less than two months, driven, among other factors, by lower-than-forecasted wind production and unexpected high electricity demand [5]. This incident is the third one since September 2023, highlighting the risks and uncertainties that RES introduce to supply-demand balance.

Moreover, RES are integrated into the grid through power electronic devices, which lack rotational components and, consequently, does not contribute to the system's overall inertia. This can hamper system stability, particularly frequency stability, as reduced inertia can lead to greater frequency variations. Low inertia level indeed worsens the ability of the power system to arrest power disturbances, leading to faster frequency decays. Furthermore, to date, RES do not provide primary frequency reserve and thus contribute to primary frequency control although this control is technically possible and new installation are required to be able to provide frequency control if needed [6]. Hence, these energy sources cannot provide effective inertia. Finally, with insufficient inertia and primary frequency control capabilities, an active power disturbance could cause a drop in power system frequency that in turn could activate frequency protections of generating units, which could result in a blackout.

These issues are generally less critical in continental systems due to their large size, their big number of generating units, and their highly meshed grids. However, frequency instability significantly hampers isolated power systems. Given their small size and the relatively large size of the generators, these systems are highly vulnerable to active power imbalances, such as generation outages. Furthermore, their isolated nature makes them particularly sensitive to the rapid fluctuations caused by RES such as wind and PV power. A clear example of this is the case of the Canary Islands, where the power system is currently facing increasing frequency stability issues due to a higher likelihood of imbalances [7]. As a result, the equilibrium between demand and supply could be compromised, underscoring the need for advanced frequency control strategies.

To protect the power system against frequency drops after large active power imbalances and to avoid a complete system collapse, underfrequency load shedding (UFLS) schemes are commonly used as a last-resort tool. This project, therefore, aims to address the system protection problem of small isolated power systems by exploring a better response of UFLS schemes.

1.1.1 ADDRESSING FREQUENCY INSTABILITY IN ISOLATED POWER SYSTEMS

Frequency stability is a major concern in small isolated power systems. Frequency stability can be defined as the ability of the system to keep frequency within acceptable limits after either a normal (load variation) or an abnormal (faults, generator tripping) disturbance cause a power imbalance between power generation and demand [8]. When an incident occurs, the frequency drops at a rate determined by the inertia of the synchronous generators and the amount of generation lost. Afterwards, the primary frequency control is activated to arrest and stabilize frequency decay. This can be achieved if two conditions are met, i) the spinning reserve of the remaining generating units is sufficient to replace the generator lost, and ii) the generators increase power fast enough to prevent the frequency from dropping below acceptable limits to avoid a complete system collapse [8]. The challenge is greater in small isolated power systems, which cannot rely on neighboring systems for support. In the event of a contingency, the rate of change of frequency (RoCoF) is larger than in highly meshed and interconnected power systems. This occurs because isolated systems have lower inertia, as they typically have fewer generator units connected to the system. Furthermore, in these systems, the loss of an individual generating unit can significantly impact the power supply of a substantial part of total demand. For example, in the La Palma power system, a single generating unit can meet up to 51.68% of total demand. The loss of both inertia and a significant portion of generation contributes to an increase in RoCoF [9], requiring more rigorous frequency regulation from spinning reserves to prevent the frequency from falling below 47.5 Hz, limit established by REE [10].

This is further intensified by the increasing penetration of RES, given that they usually do not provide inertia and hardly contribute to the primary frequency control. To address this limitation of primary frequency control, UFLS schemes are commonly employed to preserve the integrity of the power system.

1.1.2 ACCELERATING RES DEPLOYMENT IN THE CANARY ISLANDS

The power system of the Canary Islands consists of six small and slightly meshed isolated power systems. Its transmission grid includes substations and lines with voltages of 66 kV or higher, electrical interconnections between the islands and transformers that operate at 220/132/66 kV [11].

The power generation in the Archipelago relies heavily on thermal generation, especially diesel engines and gas turbines. In 2022, approximately 75% of the islands' installed capacity corresponded to thermal power plants [12]. This dependency is further hindered by the obsolescence of their infrastructure. The equipment in these plants are the oldest in the country and they are the only ones still operating on fuel-oil. According to a study conducted by the Canary Islands Technological Institute [13], half of the electricity generation units in the thermal power plants exceeded their operational lifespan before 2020. These units are over 40 years old and have not yet been replaced. As a result, on July 30, 2023, the island of La Gomera experienced a complete blackout lasting several hours due to a fire in the auxiliary service room at the El Palmar thermal power station [14]. This incident highlights the urgent need for infrastructure upgrades and a diversification of energy sources to enhance system resilience. The dependency on outdated single-source generation increases the risk of failures and limits the emergency response capabilities of the island's power system.

This system collapse is not an isolated incident in the Canary Islands, unfortunately, it occurs more frequently than it should. A clear example of this are the two blackouts that Tenerife suffered in a period of less than 10 months between 2019 and 2020 [15]. Another factor that threatens this type of system is the intermittency and lack of accurate prediction of renewable generation, which makes grid planning and operation difficult. This issue will worsen over time, as the plans to increase RES penetration in the Canary Islands are very ambitious. Therefore, this transition represents a great challenge for the transmission system operator (TSO), since in a few years it will have to deal with the operation of weak grids, with a large amount of uncontrollable generation within a context of diminished natural inertia [16].

One might think that the future development of a total interconnection between the islands would solve the problem of robustness, ensure stability and guarantee the energy supply of the Canary Islands' power system. However, given the geographical nature of the Canary Archipelago, this is not an option, as there are depths of more than 2 km between most of the islands [17]. This interconnection is only possible between some islands such as Lanzarote and Fuerteventura which are already interconnected, and Tenerife and La Gomera that are currently in the process of being electrically connected and are expected to be linked by 2025 [18]. In addition, the possibility of establishing a future connection between Gran Canaria and Tenerife has not been completely ruled out. Nonetheless, islands such as La Palma, El Hierro and Gran Canaria are excluded from the possibility of interconnection. Consequently, other solutions must be explored to strengthen the grid.

In the light of this situation, TSOs now face the challenge of adapting the grid to host all the expected RES. In particular, the Canary Islands Government has defined several objectives to achieve an energy mix with a high presence of renewables. These are collected in the "Energy transition plan for the Canary Islands" (PETCan, Spanish acronym), which is updated every year.

These goals are crucial, as the subtropical-ultraperipheral location of the archipelago, as well as its isolation, make the Canary Islands a region particularly vulnerable to the impacts of climate change. For this reason, the Canary Archipelago must play an active role in the transformation towards an adapted and resilient society. In line with this, in August 2019, the Canarian Government declared the climate emergency [19], bringing forward the objective of decarbonizing the Canary Islands economy by 2040 and setting the goal of strengthening the resilience of its social and economic systems, in order to achieve a thorough energy transition towards a clean, sustainable, affordable and secure power system.

Currently in the Canary Islands, energy production is the largest contributor to its overall GHG emissions, accounting for more than 85% of the total [20]. Therefore, several milestones have been established to achieve climate neutrality. Among them, it can be highlighted that by 2040 92% of the final energy consumption should derive from renewable energies. It is estimated that by 2030 this share will be 37%, compared to the current 20% [21]. The Canary Islands are working to promote renewable energies by encouraging the implementation of new renewable plants, as well as the repowering of existing ones, in addition to increasing storage capacity.

All these, combined with the annual growth in energy demand, make it extremely urgent to implement the necessary power system back-up measures. There is a clear bottleneck in the achievement of these objectives, and this is the capacity of the grid to support the high penetration of renewable energies. Therefore, even if new PV or wind farms are developed, it will be impossible to achieve the targets set if works are not carried out to renew and prepare the grid for the energy transition. In this regard, the concept of "virtual inertia" is emerging. This resource addresses the need to compensate for the lack of contribution from RES to primary control. Unlike traditional power plants, RES typically do not provide reserve capacity nor system inertia, as they are connected to the grid through power electronics, which lack rotational parts. Virtual inertia seeks to emulate the behavior of the primary motor to virtually improve the inertia in the control loop, thereby stabilizing the frequency of the system [22]. Additionally, there is extensive research in the literature on optimizing and enhancing the efficiency of existing resources. One notable technique explored in this context are UFLS schemes, which will be the focus of this project.

1.2 STATE OF THE ART

UFLS schemes are a last-resort tool that are typically used to guarantee frequency stability in the event of a large disturbance. When frequency and/or RoCoF fall below a certain threshold, UFLS schemes shed a certain amount of load, thereby reducing system recovery time and the number of affected consumers. As a result, fewer consumers are affected by the loss of generation, and system recovery is achieved in minutes rather than hours, which would be the case in the event of a blackout. UFLS schemes not only safeguard generation and load-side equipment but also enhance the reliability of the power system, minimizing the socio-economic impact on utilities and customers.

Conventional UFLS schemes have shown their ability to prevent widespread blackouts, as they can avoid large-scale outages by disconnecting loads in a controlled manner. Furthermore, they contribute to maintaining frequency stability during severe disturbances. However, conventional schemes have significant shortcomings. The most important is their lack of adaptability, as conventional UFLS schemes cannot adapt their measurements according to the severity of the disturbance, since they shed a predefined amount of load with a set time delay when the magnitude of the measured local voltage drops below a fixed threshold [23], which can lead to excessive or insufficient disconnections. In addition, voltage peaks can be originated when restoring power, damaging equipment.

In the following sections, the different types of UFLS schemes that exist in the literature will be explored. This analysis aims to provide a comprehensive understanding of the various approaches to UFLS schemes.

1.2.1 TYPE OF UFLS SCHEMES

Several UFLS schemes exist within the literature to protect the power system from a complete collapse. These can be divided into two main groups i) manual and ii) automatic. Manual UFLS schemes are typically applied to restore frequency problems and seldom used to limit frequency deviations, whereas automatic techniques are primarily used to arrest frequency decay and reestablish the balance between generation and demand in the steady state. As it can be seen in Figure 1 the latter can be further categorized into conventional and advanced. Conventional UFLS schemes are decentralized, i.e. the shedding decisions are based on local measurements and do not require communication [24]. Conversely, advanced schemes are commonly centralized, which implies that the information is collected and transmitted to the control center to estimate the magnitude of the disturbance [25]. Besides, advance schemes are highly adaptative, i.e. they adjust their response according to actual power system conditions.

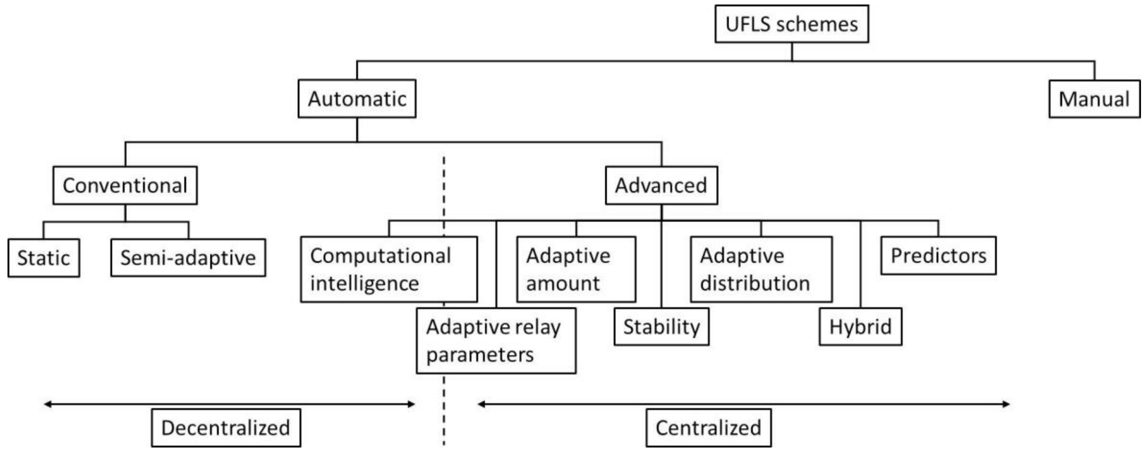

Figure 1. Classification of UFLS techniques [24]

Advanced UFLS schemes not only consider frequency and RoCoF, but also additional information and measurements (e.g. power generation, voltage, etc.). These schemes use a variety of external signal and algorithms to dynamically adapt the load shedding pattern. They estimate the generation outage immediately after a disturbance and adjust the shedding schedule accordingly. Such approaches not only aim to achieve an adequate frequency recovery, but they also account for other factors, such as enhancing the voltage stability margin [26]. Nevertheless, conventional schemes remain the most widely used to date [24]. Therefore, this project will focus on conventional UFLS schemes.

Conventional UFLS schemes can be either static or semi-adaptative. They rely on type 81 frequency relays and, in the case of semi-adaptive schemes, additionally use RoCoF relays. The relays shed a specific share of load by sending an activation signal to the breaker whenever the systems frequency and/or RoCoF decay and exceeds their respective threshold for a certain time [27].

The static UFLS schemes operation principle relies on measuring frequency deviation. They are characterized by being quick and easy to implement, as the load to be shed and the parameters of the relays are defined by off-line contingency simulations. Nevertheless, this approach may result in either too much or too little load to be shed in response to unexpected contingencies. By contrast, semi-adaptative UFLS schemes also consider the RoCoF, which enhance system performance. This helps to distinguish between minor and major disturbances and allows for quicker frequency response, given that in the event of large disturbances the load is shed earlier. As a result, many UFLS configurations now combine elements of both static and semi-adaptive schemes. However, despite the improved response, these schemes still face challenges with over-delays.

Similar to static UFLS schemes, semi-adaptative UFLS schemes trigger load to restore the power balance. The activation signal is determined by frequency and RoCoF thresholds and the intentional time delays. The timing of load shedding is determined by the frequency and RoCoF thresholds along with intentional time delays, and these parameters are step dependent. Each step specifies a certain percentage of load to be shed, based on the medium voltage feeder in small power systems. When the frequency drops below the predefined threshold and continues to violate it after the time delay, load shedding is triggered. The goal of the UFLS scheme is to disconnect the minimum necessary load to prevent a complete system collapse, ensuring that the shed load does not exceed the loss of generation. The requirements for load shedding vary across different power systems and are designed according to their individual characteristics, setting specific frequency thresholds and load shedding limitations accordingly. In small isolated power systems, the criterion for selecting load step size is usually not applicable, and the minimum and maximum frequency thresholds vary depending on the system. A common minimum frequency threshold is 48 Hz. Note that it is important to coordinate this frequency thresholds with turbine underfrequency protections to prevent excessive shedding and over-frequency situations [28].

1.2.2 DESIGN OF CONVENTIONAL UFLS SCHEMES

An effective UFLS scheme design must be both robust and efficient. Robustness is attained by carefully selecting OC scenarios that accurately represent the power system performance. Whereas efficiency involves optimizing the scheme to minimize load shedding while maintaining system stability. The literature offers various methods for designing UFLS schemes, broadly categorized into experimental and optimal designs. Both approaches primarily rely on simulating the power system's behavior under hypothetical contingencies to evaluate and enhance the performance of the UFLS scheme. The main difference between the two approaches lies in their methodology. Experimental designs are based on the selection of the best scheme within a set of options or on trial-and-error practices, in which frequency and RoCoF thresholds, intentional time delays, and step sizes are manually adjusted by repetitive testing and adjustment. Screening processes are also reported, where a series of candidate schemes are evaluated to select the most effective one based on predefined criteria. In contrast, optimal designs use algorithms to tune the parameters of the UFLS schemes.

1.2.2.1 Methodology for optimal design

The primary goal of UFLS schemes is to minimize the amount of disconnected load. These schemes can be designed using various methods, including deterministic and heuristic algorithms, which typically optimize parameters such as frequency thresholds, intentional time delays, and step sizes.

Deterministic algorithms like quasi-Newton and steepest descent methods have been used to address optimization problems [29] [30] [31]. Although they are accurate, their performance depends heavily on the initial values of the decision variables [31], increasing the risk of getting trapped in local minima. Furthermore, given the step-like behavior of UFLS schemes, the optimization problem becomes discontinuous and nonlinear, making frequency gradient-based methods unsuitable for this application. Hence, heuristic algorithms are more adequate in these cases [31] [32].

Heuristic optimization algorithms, such as genetic algorithms (GA) or simulated annealing (SA), provide a suitable alternative, demonstrating strong performance in objective functions with nonlinearities [33]. These methods can dynamically adjust to power system contingencies and variations, providing greater flexibility and effectiveness under changing conditions.

Given that this study is focused on small isolated power systems, optimizing step sizes is not included in the problem due to the difficulty of achieving appropriate step sizes by reorganizing the load blocks of available generators. Nevertheless, various methods for tuning this criterion have been explored in the literature, from experimental to optimal approaches. Heuristic algorithms have been applied to optimize step sizes, with examples including GA for single-stage UFLS schemes and hierarchical genetic algorithms to minimize deflection loading and maximize the lowest oscillation frequency. Scenario-based optimization also considers step size variations as scenarios, modeling feeder load changes and outages using Normal-Bernoulli distribution functions [34].

1.2.2.2 Typical UFLS design criteria

The process of designing the conventional UFLS scheme consists in tuning several parameters for each of the UFLS steps, including (i) the frequency threshold, (ii) the intentional delay, and (iii) the amount of load to be shed.

According to the European Network of Transmission System Operators for Electricity (ENTSO-E), the first UFLS stage should be initiated at 49 Hz [35] to prevent unnecessary load shedding during transient or minor incidents. Further, the minimum frequency threshold should not be set below 47 Hz. This ensures that the power system operates within the range of 47.5 Hz to 52 Hz, as established by the Spanish Ministry of Energy, Tourism, and Digital Agenda for isolated power systems [36].

As for time delays, these are pivotal to guarantee a good performance of the UFLS scheme. They allow the system to recover naturally from incidents, thereby reducing the amount of load shed and override transients. They should not be excessively large, a value between 0 and 0.5 s is generally sufficient. Additionally, an extra delay accounts for the time it takes the system to execute the activation after receiving the signal, typically set to 0.2 s.

When it comes to the steps, the required number of stages is characteristic of each power system, as the system size determines the number of steps needed. For small power systems, it is common to implement between three and six stages. Their size is another crucial factor, given that if it is too large, it will result in overshedding, while if it is too small, it will lead to undershedding. Typically, in these power systems, the step size is determined by the utility and the available feeders. However, in small systems, it can be challenging to find load blocks that match the desired shedding power. Generally, each step is assigned a size between 5% and 15%, and according to ENTSO-E, the first step should shed at least 5%.

Finally, regarding the adjustment of the frequency stability margin threshold, it is crucial to define the value of f_{LIM} used to calculate FSM at each moment. According to REE [10], the minimum frequency should not fall below 47.5 Hz for more than 3 s. However, since the case study involves a small isolated power system, a more conservative approach is adopted, thus, similar to [37], a threshold of 48 Hz for 2 s is adopted. This ensures that the system does not become unstable during the opening delay and avoids that there appear low steady-state frequencies. Such low frequencies can cause mechanical stress on generator components, like the rotor and stator, potentially leading to overheating and damage the equipment [38]. This threshold ensures that the generator operates within safe limits, reducing the risk of component damage. With regard to the FSM threshold, this will depend on each power system, for the case of study values between 0 s and 1.2 s would be appropriate. Setting very high values for FSM is not advisable because the condition would be easily met, and the load shedding decision would rely mainly on the frequency threshold. Furthermore, given the definition of FSM, i.e. the time it takes for the frequency to fall below f_{LIM}, values below 0 would not make any sense.

All these conditions will be taking into account in the following chapter when optimizing the power system under study.

1.2.2.3 OC scenario selection

A key step in the optimization of UFLS schemes is the selection of representative scenarios, so that a few contingencies represent the frequency response of the entire power system. These scenarios must gather sufficient information to ensure that, when used for tuning, an optimal, robust and efficient UFLS scheme is achieved.

In the field of power systems, several types of contingencies, such as generation losses, line disconnection, etc., can be considered. Nevertheless, in small and isolated power systems, generator losses cause the largest frequency deviations [39].

1.3 OBJECTIVES

This project focuses on frequency stability, a critical aspect in the protection of small isolated power systems. It particularly addresses UFLS schemes. Previous research [40] demonstrated that including a criterion based on the frequency stability margin in the UFLS scheme offered good performance. However, this scheme was manually tuned. Therefore, this project seeks to improve conventional static and semi-adaptive schemes by implementing the frequency stability margin and optimizing the UFLS scheme through algorithms in a small isolated power system. The specific objectives are:

- Use data mining techniques to identify representative OC scenarios, i.e., to find those contingencies that best represent all other possible disturbances.
- Study the impact of increasing penetration of RES.
- Formulate the tuning of UFLS scheme parameters as an optimization problem, which will be solved by means of heuristic algorithms.
- Conduct a sensitivity analysis to assess how variations in certain variables affect the outcomes of the UFLS scheme.

1.4 METHODOLOGY

In a first step, a review of the different types of current practices used for the adjustment of UFLS schemes will be carried out. Subsequently, a new design and modeling approach will be presented based on a combination of the frequency stability margin criterion outlined in [41] and the design of conventional static semi-adaptive proposed by [37].

The implementation and optimal adjustment of this criterion will be done using as a base case the isolated power system of La Palma, located in the Canary Islands. The necessary tools for the modeling will be, on the one hand, MATLAB, for the optimization of the parameters by means of simulated annealing and the development of the code, and on the other hand, Simulink, for the simulation of the complete power system.

Once the code is developed and an optimal FSM-based UFLS scheme is achieved, a comparative analysis between the performance of the proposed scheme and the current scheme, both the existing one and an optimized version of it, will be conducted. Finally, a sensitivity analysis will be carried out to evaluate the effectiveness of the UFLS scheme response and its performance. This analysis will include the consideration of increased penetration of RES, changes in the objective function, and relaxation of constraints, among other factors.

1.5 PROJECT OUTLINE

The project is organized into six chapters. The first chapter introduces the topic, providing an overview of the context and the current state of the art in the power system protection field.

The second chapter covers the modeling aspects, detailing power system modeling and conventional UFLS schemes, including their principles of operation and the FSM-based UFLS scheme.

The third chapter presents the proposed FSM-based UFLS scheme design methodology, explaining the selection of OC scenarios, the optimization of UFLS scheme parameters, and the application of these methodologies to real power systems, specifically the La Palma and Gran Canaria power systems. Additionally, the chapter discusses the results, providing a description of the power systems and comparing the proposed UFLS schemes with the conventional ones.

Chapter four presents a sensitivity analysis on several aspects such as the effect of increasing RES penetration, the impact of implementing storage, varying the objective function formulation, and designing load stages.

Finally, the last chapter summarizes the conclusions drawn from this research.

Chapter 2. MODELING

This chapter presents the model used for representing and simulating small isolated power systems. The analysis and design of the UFLS schemes will be conducted using the non-linear multi-generator system frequency dynamics (SFD) model proposed in [33], as it enables to reflect short-term frequency dynamics of small power systems. In addition, the operational principles of the conventional UFLS scheme employed to mitigate frequency deviations, will be explained. Furthermore, the principles of the FSM-based criterion and the modifications required to implement it to the current power system model will be outlined.

2.1 POWER SYSTEM MODELING

The SFD model accurately captures the short-term frequency dynamics of small isolated power systems. Figure 2 shows the power system model that consists of *n* generating units, where each generator is represented by a second-order approximation of its turbine-governor system. In fact, frequency dynamics are mainly influenced by the rotor and turbine-governor system dynamics. Excitation and generator transients can be neglected since they operate much faster than the turbine-governor system dynamics. Steam turbines are generally modeled by means of first-order models. Nonetheless, within the generation mix, there are gas-driven and diesel-driven turbines, which might necessitate the adoption of higher-order models [33].

In Figure 2, the parameters of the SFD model are identified. These include the equivalent inertia, H_{eq}, which can be established given the assumption of uniform frequency. It can be defined as follows:

$$H_{eq} = \sum_{i=1}^{n} \frac{H_i \cdot M_{base,i}}{S_{base}} \quad (1)$$

Here, H_i represents the inertia in (s), $M_{base,i}$ is the base rating of the *ith* generating unit in (MW), and S_{base} is the sum of the ratings of all generators in (MW). The initial RoCoF, $\Delta\omega_0$, is determined as follows:

$$\Delta\dot{\omega}_0 = -\frac{\Delta p_{loss}}{2H_{eq}} \tag{2}$$

This equation illustrates the impact of equivalent inertia on the dynamic frequency response. It suggests that a decrease in inertia leads to a more rapid initial frequency decay and influences the minimum frequency.

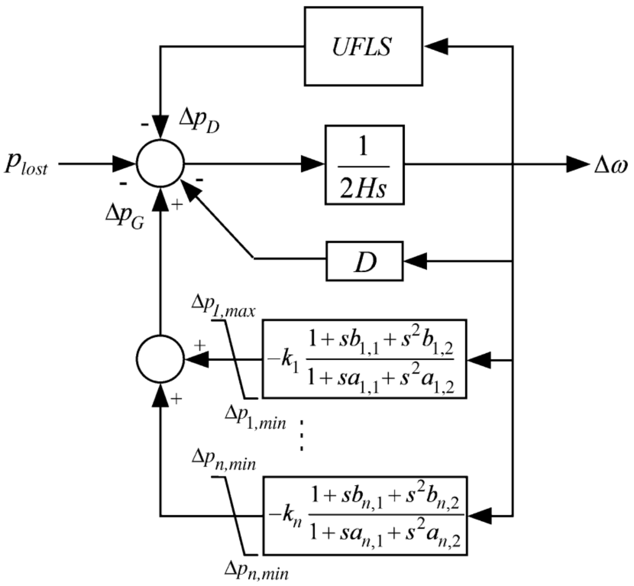

Figure 2. System-frequency dynamic of the power system [33]

While the load-damping factor, *D*, is a model parameter, it is often negligible, as its impact in steady state is minimal compared to the droop of the turbine-governor systems [33]. This is demonstrated by the following equation:

$$\Delta\omega_{ss} = -\frac{\Delta p_{loss}}{\sum_{i=1}^{n} k_{g,i} + D} \tag{3}$$

$\Delta\omega_{ss}$ represents the steady-state frequency deviation, and $k_{g,i}$ denotes the gain of the *ith* generator model with respect to S_{base}. It can be stated that the influence of the load-damping factor is minimal when compared to the gain of the turbine-governor system, given that $\sum_{i=1}^{n} k_{g,i}$ is larger than D.

Moreover, for each generator *g*, the model specifies the gain k_g and parameters $a_{g,1}$, $a_{g,2}$, $b_{g,1}$ and $b_{g,2}$, which can be derived from more accurate models or field tests. Additionally, the model includes generator-output boundaries, since primary spinning reserved are limited, hence, $\Delta p_{g,min}$ and $\Delta p_{g,max}$ are also taken into account.

The model depicted in Figure 2 will be implemented in Simulink as a block diagram. The necessary parameters for running simulations in this tool are stored in Excel files, encompassing generator parameters, various generation dispatch scenarios, energy storage system parameters (considered in the sensitivity analysis in Chapter 4. and UFLS scheme data. Detailed information on the block diagram of the power system model implemented in Simulink is provided in APPENDIX I

2.2 CONVENTIONAL UFLS SCHEMES

Currently, conventional statice and semi-adaptive UFLS schemes are used, where underfrequency relays sense frequency and acts on a breaker, interrupting load. This section describes the model for conventional UFLS schemes as well as the one for FSM-based UFLS schemes.

2.2.1 PRINCIPLES OF OPERATION

The approach that will be used in this project is based on the load shedding model introduced by [37], where a method to optimize a static and semi-adaptive UFLS scheme is presented. In the following subsections, the operating principle of this model will be examined, along with a comprehensive description of the frequency stability margin-based scheme proposed in this research.

2.2.1.1 Conventional UFLS schemes

The UFLS scheme proposed in [37] is based on optimized load shedding, which, in the event of a disturbance, automatically sheds an optimal amount of load. The operating principle of this scheme is based on frequency and ROCOF thresholds, intentional delays, and the amount of load to be shed, which is a step-dependent criterion, where a percentage of total demand is shed at each step according to the medium voltage feeder. This model is implemented using Matlab/Simulink to simulate the system's response.

A detailed explanation of the operating principle of the UFLS scheme is presented in Figure 3. In case of an incident, the system received the information that a frequency deviation caused by the generation loss is taking place. Then, the UFLS scheme measures locally the frequency deviation through the UF relays, and the frequency deviation and RoCoF through the RoCoF relays and compares the measurements with predefined thresholds for each type of relay. When the first limit is reached, an intentional time delay is activated, giving the system the possibility to recover by itself. Should this not be successful, the relay is activated. Afterwards, once the trigger signal is sent, a second delay is activated, which represents the time it takes for the activation to become effective. Thus, the time it takes for the system to give a response is equal to the sum of the two delays. As it can be seen, the purpose of this tool is not to restore the frequency drop, but to stop it, i.e. the reconnection of the shed load is not contemplated. The detailed model to be simulated in Simulink can be found in the APPENDIX I.

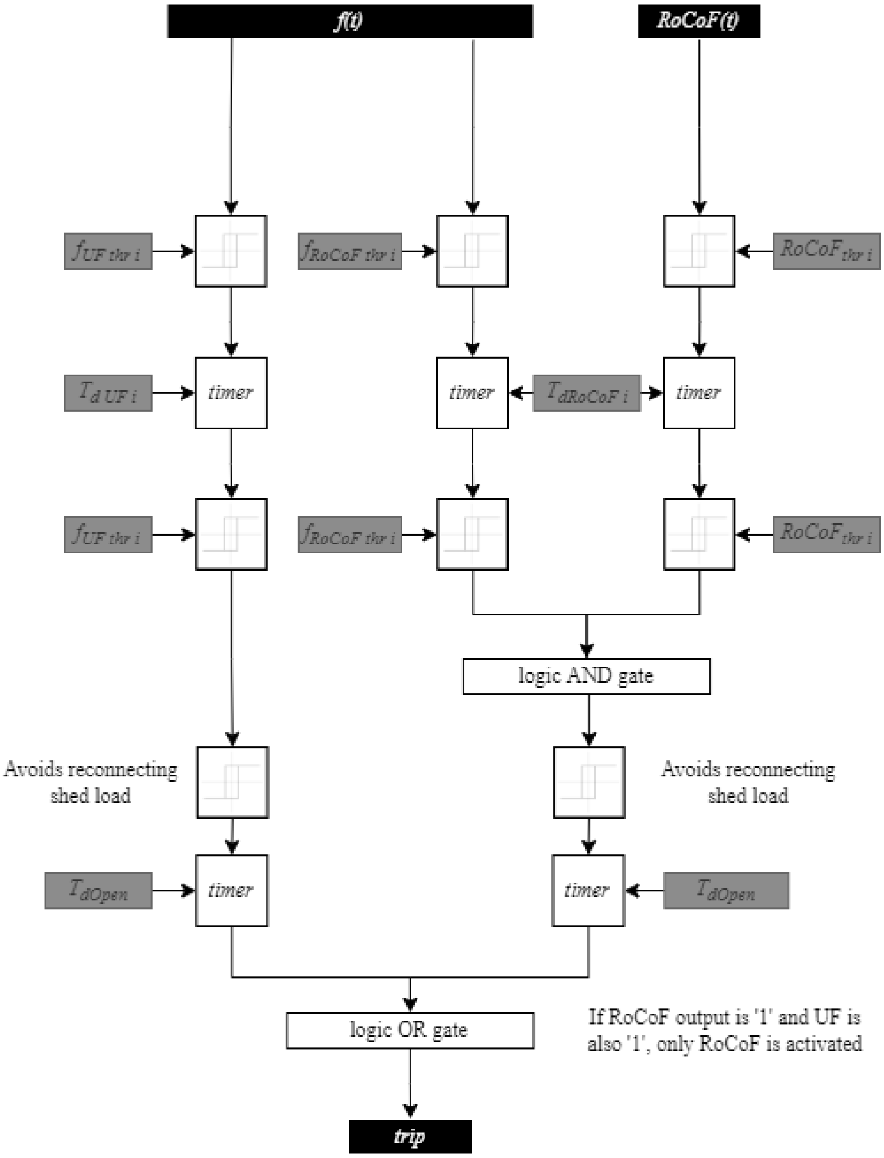

Figure 3. Logical block diagram: Conventional UFLS scheme operating principle [40]

2.2.1.2 FSM-based UFLS schemes

The load shedding schemes based on frequency stability margin (FSM) are quite similar to those presented in the previous section, in particular, to those based on RoCoF. The reason behind this is that the frequency stability margin is, in essence, another interpretation of RoCoF. This criterion, first proposed in [41], aims to reduce over-delay and give the system the ability to decide whether the contingency under consideration is severe and requires the activation of load shedding steps, or if, conversely, it is able to handle it without disconnecting load or can delay its activation.

As mentioned above, this criterion uses a similar reasoning to that of RoCoF-based schemes, but the main difference between the two models lies in the way the information is processed. While in the first approach the frequency decay rate is directly compared to a predefined threshold, in this second approach, instead of directly applying the RoCoF, it is used to calculate the FSM in real time at each relay. The FSM is defined as the time remaining until the frequency reaches the minimum set limit (47.5 Hz, as proposed in [41]). This definition and its corresponding calculation can be clearly visualized in Figure 4 and is calculated according to the following equation:

$$FSM(t) = \frac{f_{LIM} - f\ (t)}{RoCoF\ (t)} \tag{4}$$

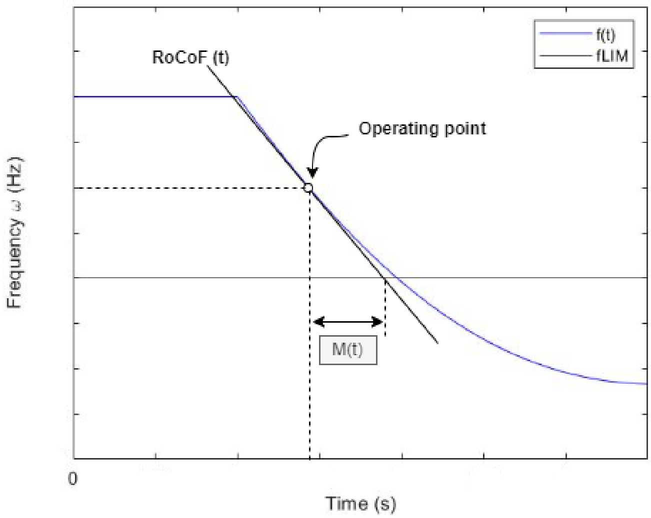

Figure 4. Calculation of the frequency-stability margin [40]

As can be inferred from the equation (4), the criterion compares and evaluates the frequency instantly with the defined threshold and weights it according to the rate at which the frequency decays.

The rationale followed by the FSM-based scheme for load shedding is shown in Figure 5. It measures locally the frequency deviation caused by the incident and calculates at each instant the FSM, comparing each measurement with its respective predefined thresholds. These delay thresholds offer the possibility to reduce the amount of load to be disconnected, since it gives the system the opportunity to naturally recover. If the violation persists after this time elapses and if both thresholds are violated, the shedding signal is sent to the relay. Afterwards, a final delay simulates the time it takes for the trigger signal to become active. The block diagram designed to perform the simulation is provided in the APPENDIX I.

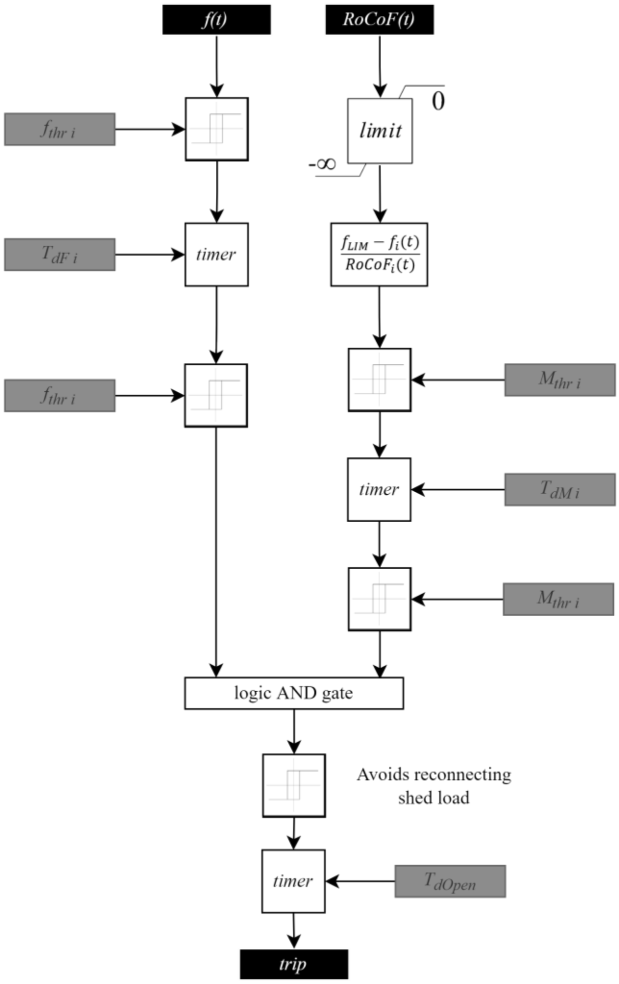

Figure 5. Logical block diagram: FSM-based UFLS scheme operating principle [40]

Chapter 3. METHODOLOGY FOR THE DESIGN OF FSM-BASED UFLS SCHEMES

In the section 1.2, a review of the literature has been conducted. It is clear that there is not a systematic and general method to tune UFLS schemes, but numerous methodologies exist. In this chapter, the design of a robust and efficient UFLS scheme, based on the simulation of several hypothetical disturbances in a small isolated power system, is presented. The design consists of two phases: i) the adequate selection of representative scenarios, and ii) the application of an optimization algorithm. The selection of OC scenarios will be done through clustering techniques, and the algorithm that will be used is adaptive simulated annealing. Finally, the optimization algorithm will be applied to two small isolated power systems with different sizes.

3.1 SELECTION OF OC SCENARIOS

Operating and contingency scenarios are a set of disturbances under diverse operating conditions, each defined by its corresponding generation dispatch scenario. The adequate selection is crucial to guarantee the robustness of the UFLS scheme. There are several types of contingencies that can be considered as OC scenarios, such as generation outages, line tripping, etc. Nonetheless, in small isolated power systems generator losses lead to great frequency deviations [39]. Thus, only generator outages will be considered as contingency.

According to the literature, a widely adopted practice to select OC scenarios consist in determining systems conditions under different load-demand level, such as a minimum and maximum, and to design the UFLS scheme by considering outages of the largest, medium-size and the smallest generator for each specific system conditions [42]. Nonetheless, this method does not ensure the selection of suitable OC scenarios. As an alternative, authors have proposed different methods, some based on Data Mining techniques, to guarantee the adequate selection. Data mining techniques allow to summarize relevant information from data bases. Cluster analysis (CA) is a method within Data Mining. This practice seeks to partition the data base into a limited set of clusters that share common features. Within CA several techniques can be applied (e.g. K-means, hierarchical clustering, fuzzy c-means) [43]. One of the most widely used is K-means clustering, which is a distance-based unsupervised algorithm [44]. By applying K-means algorithm, the data-frame is split into a predefined (K) number of clusters, and this method can be formulated as follows:

$$\min(QE) \tag{5}$$

Where

$$QE = \sum_{c=1}^{K_N} QE_c = \sum_{c=1}^{K_N} \sum_{\substack{e \in Learning\ Set \\ e \in Cluster\ c}} \|\boldsymbol{x}_e - \boldsymbol{x}_c\|^2 \tag{6}$$

QE represents the sum of squared distances, also known as the quadratic sum of inaccuracy, between all data points in the database and their respective cluster centroids.

To determine the optimal K value, the elbow graph method is applied. This uses the within-cluster sum of square (WCSS), i.e. the sum of square distance between the cluster centroid and the points in a cluster. The ideal K value will correspond to the elbow shape in the graph. Beyond this point, a higher K value will not significantly reduce the WCSS.

The K-means technique is applied again for the optimal value of K. This method provides an approximation of the most suitable scenarios, which does not correspond to any specific simulation. Therefore, it is necessary to identify and select those OC scenarios that best fit the clusters.

3.1.1 APPLICATION EXAMPLE

The method presented in the preceding section is applied to the power system of La Palma to illustrate how it works. The latter is a small isolated power system that consists of eleven generators. The power system is simulated utilizing the SFD model depicted in 2.1 with real generation dispatches provided in Table 3. The simulation covers all possible scenarios, including simulated outages for each individual generator under consideration.

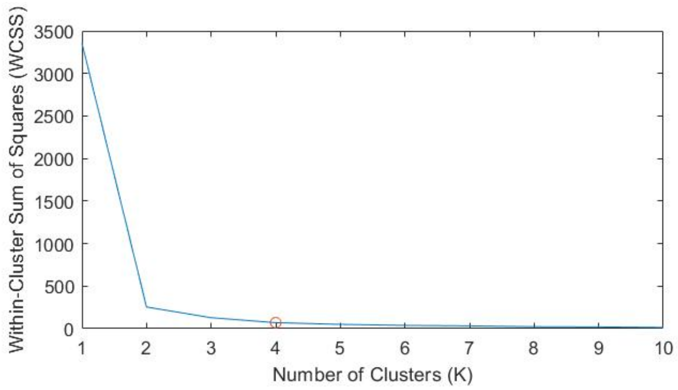

Figure 6. Elbow graph: Determination of the number of clusters using K-means algorithm

The initial step in applying the clustering method is to determine the number of clusters needed to represent the entire power system. To achieve this, the K-Means method is applied with a sufficiently large number of clusters, e.g., 10. The quantization error is plotted against the number of clusters, known as the elbow graph, and the point where the decrease in WCSS starts to flatten out is identified. In Figure 6, this occurs at K = 4.

Once the value of K is known, the K-means technique is applied again. This method offers an approximation of the most suitable scenarios. Consequently, those scenarios exhibiting a similar performance are identified as OC scenarios (see Figure 7)

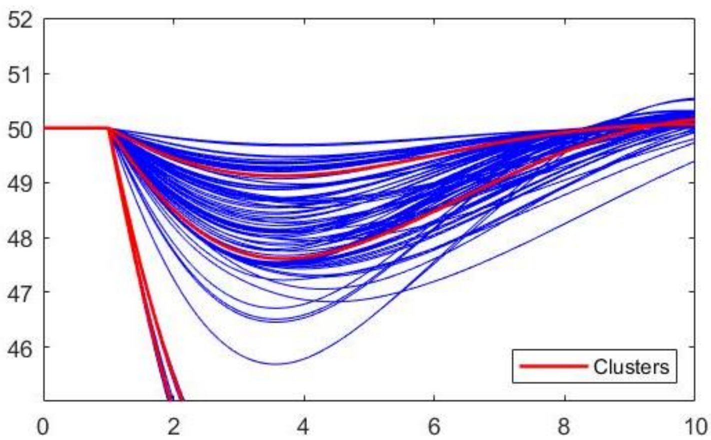

Figure 7. K-means: Cluster identification

The clusters plotted in red (Figure 7) do not correspond to any specific scenario, they are an approximate representation based on quantization errors. Thus, it is necessary to identify real contingencies that have a similar frequency response to those identified by K-means. These are presented in Table 1.

Scenario	Generator	P_{dem} (MW)	P_{loss} (MW) (%)
8	11	27.37	2.35 (9.24)
3	17	18.48	9.55 (51.68)
8	15	27.37	6.10 (22.29)
1	17	22.09	10.41 (47.13)

Table 1. Optimal OC Scenarios of the La Palma power system

These scenarios will be utilized as contingencies for the design in subsequent sections of the La Palma UFLS scheme.

3.2 OPTIMIZATION OF UFLS SCHEMES PARAMETERS

The goal of the optimization problem is to design the UFLS scheme of a small isolated power system such that the amount of load to be shed is minimized, and the best frequency response is obtained after a contingency occurs. As introduced in 1.2.2, to address non-linear and discontinuous problems it is convenient to use heuristic algorithms. Moreover, this approach allows to optimize the UFLS parameters, while avoiding getting trapped in local minima. Whitin it, there exist different algorithms that can be used to tackle the problem, such as genetic algorithms, greedy algorithms, simulated annealing, tabu search algorithms, etc. Thus, adaptative simulated annealing will be the one chosen to optimize the UFLS scheme.

The optimization problem to be addressed is as follows:

$$\min_{x} f(\boldsymbol{x}_d) \;\; s.t. \tag{7}$$

$$lb \leq \boldsymbol{x}_d \leq ub$$

$$h_l(\boldsymbol{x}_d) = 0, \quad l = 1, \dots, m_e$$

$$g_l(\boldsymbol{x}_d) \leq 0, \quad l = m_e + 1, \dots, m_t$$

Where $f(\cdot)$ is the objective function, $\boldsymbol{x}_d$ are te decision variables, lb and ub are the low and upper boundaries, $h_l(\cdot)$ and $g_l(\cdot)$ represent the equality and inequality constraints, respectively, m_e is the number of equality contraints and m_t the number of constraints. When optimizing UFLS schemes, the decision variables are the parameters of the relays. In the proposed design, these are:

- $\omega_{threshold}$, the frequency threshold and, $t_{int,\omega}$, the intentional time delay related to frequency.
- $FSM_{threshold}$, the frequency stability margin threshold and, $t_{int,FSM}$, the intentional time delay associated to FSM.

The step size has not been included as decision variable since, for small isolated power systems, like the La Palma power or the Gran Canaria power systems, the step size is typically defined by the utility and depends on the feeder connected to the relays. Thus, finding feeder blocks that add up to the desired step size would be challenging [39]. Generally, these step sizes are set within the range of 5-15%. The predefined steps sizes presented in [39] will be the ones used to tune the UFLS scheme. The t_{open} has also not been included, given that it represents the opening signal delay, and it is typically set to 0.2s for all steps.

3.2.1 OBJECTIVE FUNCTION

The main goal of the UFLS scheme is to protect the power system against instability by shedding the minimum amount of load. In accordance with this, various formulations can be proposed, some more complex than others, as described in [39]. However, this study will consider the following objective function:

$$f(\boldsymbol{x}_d) = \sum_{j=1}^{M} \alpha_{f,j} \cdot P_{shed,j}(\boldsymbol{x}_d) \tag{8}$$

Where $\alpha_{f,j}$is the weighting factor, $P_{shed,j}$ the amount of shed load (pu) for the jth contingency, and M represents the total number of representative OC scenario. As in [39], $\alpha_{f,j}$ is set to unity, since the objective is to minimize the load to be shed. The decision variables, $\boldsymbol{x}_d$, include frequency (ω), frequency stability margin (FSM), and the corresponding intentional time delays ($t_{\omega,int}$, $t_{FSM,int}$). Therefore:

$$\boldsymbol{x}_d = \begin{bmatrix} \omega_{threshold} \\ FSM_{threshold} \\ t_{int,\omega} \\ t_{int,FSM} \end{bmatrix}$$

3.2.2 CONSTRAINTS

The optimization problem includes applying boundaries to guide the decision variables. In addition to ensuring that the decision variables, $\boldsymbol{x}_d$, fall within the upper, ub, and lower, lb, boundaries, they are also subjected to additional constraints. These constraints can be categorized into two types: strict constraints, i.e. those which must always be fulfilled, and flexible constraints, which are those that allow for a certain degree of deviation.

- The frequency deviation must remain within the minimum ($\Delta\omega_{min,allowable}$) and maximum ($\omega_{max,allowable}$) allowable values. Additionally, for the minimum frequency deviation ($\Delta\omega_{min,j}$), a maximum time ($t_{max,j}$) is defined during which frequency can fall below the minimum threshold.

$$g_1(\boldsymbol{x}_d, t) = \Delta\omega_{min,allowable} - \Delta\omega_{min,j}(\boldsymbol{x}_d) \quad \text{for } t < t_{max,j}, \qquad j = 1, \dots, M \tag{9}$$

$$g_2(\boldsymbol{x}_d) = \Delta\omega_{max,j}(\boldsymbol{x}_d) - \omega_{max,allowable} \tag{10}$$

  Here, $\Delta\omega_{min,j}$ and $\Delta\omega_{max,j}$ represent the minimum and maximum frequency deviations for the jth contingency, respectively.

- The frequency stability margin must stay within the minimum ($FSM_{min,allowable}$) and maximum ($FSM_{max,allowable}$) allowable limits.

$$g_3(\boldsymbol{x}_d, t) = FSM_{min,allowable} - FSM_{min,j}(\boldsymbol{x}_d), \ \ j = 1, \dots, M \tag{11}$$

$$g_4(\boldsymbol{x}_d) = FSM_{max,j}(\boldsymbol{x}_d) - FSM_{max,allowable} \tag{12}$$

Where, $FSM_{min,j}$ and $FSM_{max,j}$ denote the minimum and maximum frequency stability margin value for the *jth* contingency, respectively.

- The priority of loads to be shed should be respected.
- The amount of shed load has to be smaller than or equal to the amount of lost power.
- The UFLS scheme should only act if the frequency has not surpassed its minimum value.

$$g_5(\boldsymbol{x}_d) = t_{shed,j}(\boldsymbol{x}_d) - t_{\omega_{min},j}(\boldsymbol{x}_d) \text{ for } j = 1, \dots, M \tag{13}$$

$$g_6(\boldsymbol{x}_d) = A \cdot \boldsymbol{x}_d - \boldsymbol{\sigma_\omega} \tag{14}$$

Where:

$$A = \left[\begin{array}{ccccc|ccccc|ccc|c|c|c|ccc}
-1 & 1 & \cdots & & & 0 & & \cdots & & 0 & 0 & \cdots & 0 & \cdots & \cdots & \cdots & 0 & \cdots & 0 \\
0 & 0 & \vdots & & & 0 & & \vdots & & 0 & & & & & & & & & \\
0 & 0 & 0 & -1 & 1 & 0 & & \cdots & & 0 & & \vdots & & \vdots & \vdots & \vdots & & \vdots & \\
0 & & \cdots & & & -1 & 1 & \cdots & & & & \vdots & & \vdots & \vdots & \vdots & & \vdots & \\
0 & & \vdots & & & 0 & 0 & \vdots & & & & & & & & & & & \\
0 & & \cdots & & & 0 & 0 & 0 & -1 & 1 & 0 & \cdots & 0 & \cdots & \cdots & \cdots & 0 & \cdots & 0
\end{array}\right]$$

$$\boldsymbol{\sigma_\omega} = \begin{bmatrix} \sigma_\omega \\ \vdots \\ \vdots \\ \sigma_\omega \end{bmatrix}$$

$$g_7(\boldsymbol{x}_d) = p_{shed,j}(\boldsymbol{x}_d) - p_{loss,j} \tag{15}$$

$$\begin{bmatrix} \omega_{threshold,min} \\ FSM_{threshold,min} \\ t_{int,\omega,min} \\ t_{int,FSM,min} \end{bmatrix} \leq \boldsymbol{x}_d \leq \begin{bmatrix} \omega_{threshold,max} \\ FSM_{threshold,max} \\ t_{int,\omega,max} \\ t_{int,FSM,max} \end{bmatrix}$$

3.2.3 ADAPTATIVE SIMULATED ANNEALING

SA algorithm is applied to solve the optimization problem. To ensure that the constraints are evaluated in the algorithm, a penalty term is added to the objective function. The resulting energy function is as follow:

$$E(\boldsymbol{x}_d) = f(\boldsymbol{x}_d) + \phi\big(g_l(\boldsymbol{x}_d)\big);\;\; l = m_e + 1, \dots, m_t \tag{16}$$

$\phi(\cdot)$ is the penalty term, which is given by:

$$\phi = \sum_{i=1}^{R}\left(\sum_{j=1}^{M} \delta_j \left(\mu \cdot C_{1,j} + C_{2,j} \cdot g_j(x)\right)\right) \tag{17}$$

Where δ_j represents whether the constraint j is active ($\delta_j = 1$) or not ($\delta_j = 0$). $C_{1,j}$ and $C_{2,j}$ are penalty constants that can take different values according to the severity of the parameter violation, μ is an iteration-dependent factor, $g_j(\cdot)$ is the ith constraint function, R is the number of OC scenarios, and M the number of constraints. $C_{1,j}$ guarantees that the violations of hard-conditions are penalized more heavily than violations of soft-constraints.

Here, $C_{1,j}$ takes a high value when hard constraints (e.g. amount of load to be shed, allowable frequencies) are infringed, a medium value for intermediate constraints (e.g. priority constraint) and a lower value for less severe violations (e.g. instant of shedding). If the penalty constant $C_{2,j}$ is set to 0, the penalty function will depend only on the number of constraint violations. In this case, $C_{2,j}$ takes the same values as $C_{1,j}$. The iteration-dependent factor is penalized as the number of iterations k increase, and it can be defined as follows:

$$\mu = \mu_0 \cdot k \tag{18}$$

Where μ_0 represents, for the initial decisions variables, $\boldsymbol{x}_{\boldsymbol{d}_0}$, the difference between the objective function and the penalty function.

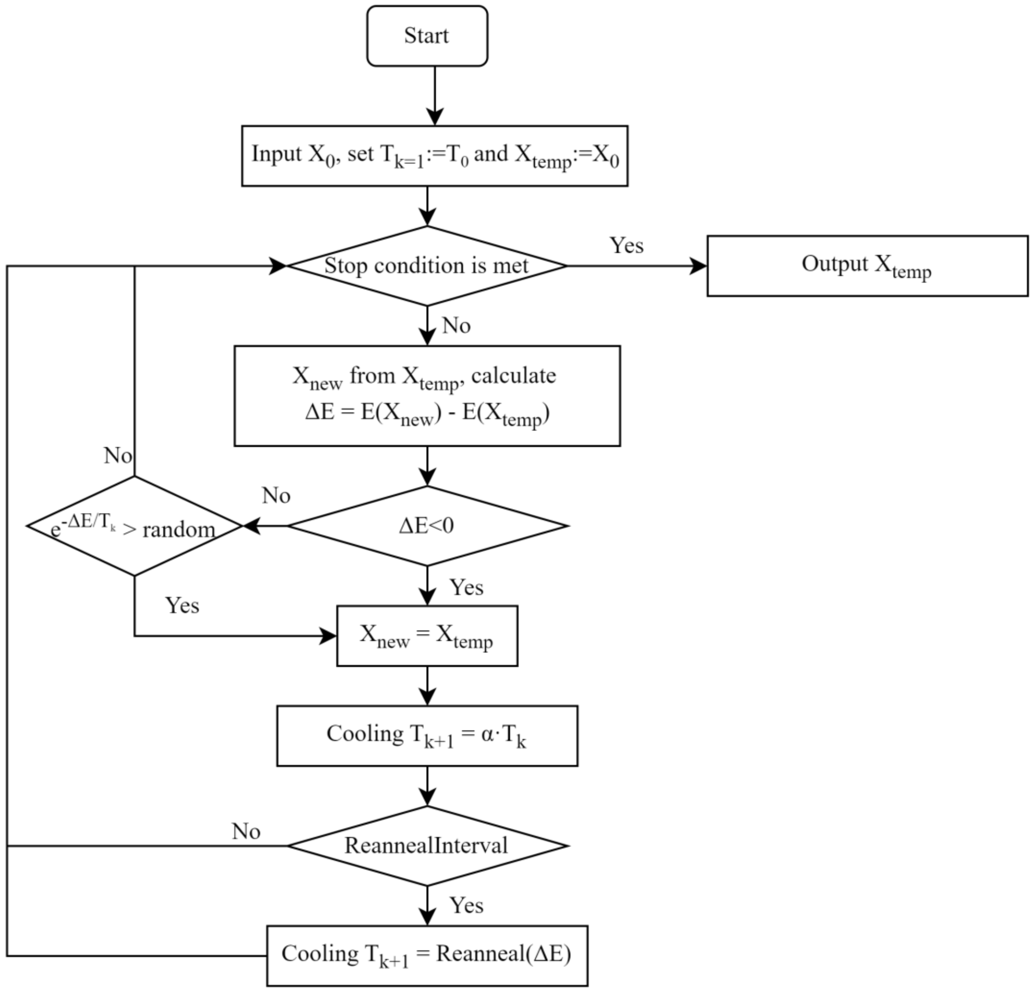

Figure 8. Flow chart: Adaptative Simulated Annealing

The algorithm works as follows. The value of the objective function for the initial decision variables is assigned to the initial temperature, T_o. Subsequently, the stop criterion is evaluated, if a set of constraints related to the satisfaction of a certain improvement of the objective function are fulfilled. If the stop constraint is not satisfied, the algorithm calculates the new value of temperature.

At each iteration k, the temperature is lowered according to a geometric cooling scheme, wherein the reduction factor, α_τ, is a random constant within the range of 0.8 and 0.97. After various disturbed configurations, the Reannealing mechanism is activated, typically with a reannealing interval set to 100 iterations [39].

3.3 APPLICATION TO REAL POWER SYSTEMS

After modeling the power system and providing a detailed explanation of the new shedding criterion, the design of the novel UFLS scheme is carried out for a selected set of disturbances identified in section 3.1.1 through clustering techniques. This scheme will be applied to both the power systems of La Palma and Gran Canaria. These are two completely isolated systems of different sizes, with the former having a peak demand of 35 MW compared to the 530 MW peak demand of Gran Canaria. The main goal is to tune the parameters of the FSM-based UFLS scheme for each island to achieve an optimal response, i.e., to minimize the shed load while ensuring that the constraints outlined in 3.2.2 are met.

The SFD model presented in 2.1 will be used with the parameters of the generators for each island. Additionally, decoupled power generation will be included in the generation dispatches, as omitting it would not accurately represent the current status of RES penetration. Furthermore, in [45], the importance of including DPG when designing an accurate UFLS scheme based on frequency stability margin was evident. In [45] was observed how the penetration of RES clearly impacted the stability of the system and frequency recovery capacity.

Both power systems will be represented using the Simulink tool through a block diagram (see APPENDIX I). The model has a single bus that connects all demand and generation. The inputs include the turbine-governor system, which provides spinning reserve to restore power balance in case an incident occurs; the energy storage system, initially excluded from the base case study but later incorporated in the sensitivity analysis; the perturbation, representing the outage of a generating unit; and finally, the UFLS scheme, which acts after a disturbance when primary frequency control is not able to arrest frequency within acceptable limits. The output of the model is the frequency response, which is determined by the mentioned inputs and the inertia of the rotor. Note that replacing the conventional UFLS scheme with FSM-based UFLS scheme will only affect the UFLS scheme block, the other blocks will remain unchanged.

3.3.1 LA PALMA POWER SYSTEM

The La Palma power system is one of the smallest power systems of the Canary Island. It is isolated and consists of eleven generators. The primary sources of generation on the island include diesel engines and a gas turbine [12]. Table 2 presents the parameters of the generator units to be utilized and Table 3 illustrates the generation dispatches to be simulated. The latter were obtained in [37] with values from the 2009 renewable energy penetration, which was approximately 9.5% in the Canary Islands as a whole. However, according to updated data from the Canary Islands Government, this figure increased to approximately 23% in 2022 [12]. In the case of La Palma, renewable penetration has risen by almost 80% from the 5.67 MW it had in 2009, reaching today an installed capacity of 10.3 MW of solar and wind energy. Despite the change, the proposed scheme will continue to use the 2009 values for adjustments, as these values serve as the basis for the conventional optimized, and original schemes. This allows for a consistent comparative performance analysis. It would be inappropriate to compare schemes adjusted based on different generation dispatches. In the generation dispatches under consideration, DPG contributes 40% of its installed capacity, covering approximately 10% of demand with RES. In addition, the absence of solar energy contribution during the night has been taken into account.

In the sensitivity analysis that will be carried out in later chapters, updated data will be contemplated and the increase in RES penetration will be studied.

Given the small size of the La Palma power system, the loss of a generator unit can severely compromise its stability. Hence, considering individual outages would be sufficient to represent a disturbance that can jeopardize the security of the power system.

Generator	H (s)	K	b1 (s)	b2 (s)	a1 (s)	a2 (s)	Pmin (MW)	Pmax (MW)
G11	1.75	20	1.44	0	18.60	3.98	2.5	4.0
G12	1.75	20	1.44	0	18.60	3.98	2.5	4.0
G13	1.75	20	1.44	0	18.60	3.98	2.5	4.0
G14	1.73	20	1.44	0	18.60	3.98	3.0	4.5
G15	2.16	20	1.32	0	18.40	2.7	3.5	7.0
G16	1.88	20	1.43	0	18.70	3.85	3.5	7.0
G17	2.10	20	1.32	0	18.30	2.71	7.0	12.0
G18	6.50	21.25	0.89	0	5.66	3.48	0.0	22.8
G19	2.10	20	1.32	0	18.30	2.71	7.0	12.0
G20	2.10	20	1.32	0	18.30	2.71	7.0	12.0
G21	2.10	20	1.32	0	18.30	2.71	7.0	12.0

Table 2. Parameters of the generator model of the La Palma power system [39]

S. O. C.	G11	G12	G13	G14	G15	G16	G17	G18	G19	G20	G21	DPG	$P_{G_{tot}} = P_{D_{tot}}$
1	2.35	0	0	0	3.41	3.69	10.41	0	0	0	0	2.23	22.09
2	0	0	0	0	3.41	4.26	9.26	0	0	0	0	2.23	19.16
3	0	0	0	0	3.41	3.29	9.55	0	0	0	0	2.23	18.48
4	0	0	0	0	3.41	3.69	8.96	0	0	0	0	2.23	18.29
5	0	0	0	0	3.41	3.29	9.35	0	0	0	0	2.23	18.28
6	0	0	0	0	3.41	3.29	9.61	0	0	0	0	2.23	18.54
7	2.35	0	0	0	3.41	3.29	10.02	0	0	0	0	2.23	21.30
8	2.53	0	0	0	6.10	5.84	0	0	6.63	4	0	2.27	27.37
9	2.35	0	0	2.82	5.00	4.92	0	0	6.63	6.7	0	2.27	30.69
10	2.41	0	0	2.82	5.73	5.59	0	0	6.63	6.7	0	2.27	32.15
11	2.46	0	0	2.82	5.88	5.69	0	0	6.63	6.7	0	2.27	32.45
12	2.49	0	0	2.82	5.99	5.77	0	0	6.63	6.7	0	2.27	32.67
13	2.58	0	0	2.82	6.27	5.96	0	0	6.63	6.7	0	2.27	33.23
14	2.4	0	0	2.82	5.69	5.56	0	0	6.63	6.7	0	2.27	32.07
15	2.35	2.35	0	2.82	5.20	5.12	0	0	6.63	4	0	2.27	30.74
16	2.35	2.35	0	2.82	4.82	4.74	0	0	6.63	4	0	2.27	29.98
17	2.35	2.35	0	2.82	4.30	4.22	0	0	6.63	4	0	2.27	28.94
18	2.35	2.35	0	0	3.37	3.29	9.21	0	6.63	0	0	2.27	29.47
19	2.35	2.35	0	0	3.37	3.29	8.68	0	6.63	0	0	2.27	28.94
20	2.35	2.35	0	0	3.41	3.29	9.35	0	6.63	0	0	2.23	29.61
21	2.35	2.35	0	0	3.83	3.71	11.38	0	6.63	0	0	2.23	32.48
22	2.35	2.35	0	0	3.70	3.58	11.38	4.85	6.63	0	0	2.23	37.07
23	2.35	2.35	0	0	3.75	3.63	11.38	0	6.63	0	0	2.23	32.32
24	2.35	2.35	0	0	3.41	3.29	6.63	0	6.63	0	0	2.23	26.89
25	0	0	0	0	3.41	3.29	9.16	0	0	0	0	2.23	18.09
26	2.35	2.35	0	0	3.70	3.58	11.38	4.85	6.66	0	0	2.23	37.10

Table 3. Generation dispatch scenarios of the La Palma power system with DPG [39]

The OC scenarios representing all possible contingencies are shown in Table 1. The parameters of the La Palma UFLS scheme are optimized considering the following constraints:

- $\omega < 48$ Hz or $t_{max} = 2$ s.
- 47 Hz $< \omega \leq$ 52 Hz.
- Priority of load shedding.
- The load shed [MW] < The power generation loss [MW].

The parameters of the UFLS scheme are constrained within upper and lower limits as described below:

- 48 Hz ≤ Frequency threshold ≤ 49 Hz
- 0 s ≤ FSM threshold ≤ 1.2 s
- 0 s ≤ Intentional time delay for frequency threshold ≤ 0.5 s
- 0 s ≤ Intentional time delay for FSM threshold ≤ 0.5 s

The step size of the UFLS scheme stages that were proposed in [39] will be consider. Given that the worst-case scenario considered involves a loss of 51,68% generation, six load shedding steps are enough to stabilize frequency. Table 4 displays the optimized UFLS scheme (the tuned values are highlighted in bold) and Figure 9 illustrates its frequency response for all possible contingencies. The design modified frequency (ω_{thr}) and FSM thresholds (FSM_{thr}) and their associated time delays ($t_{thr,F}$ and $t_{thr,FSM}$).

Stage	Substation	ω_{thr} (Hz)	FSM_{thr} (s)	$t_{thr,F}$ (s)	$t_{thr,FSM}$ (s)	t_{open} (s)	Step size (%)
1	2101	**49.00**	**0.80**	**0.03**	**0.20**	0.2	7.1
2	2102	**48.87**	**0.62**	**0.05**	**0.29**	0.2	0.6
3	3101	**48.72**	**0.32**	**0.02**	**0.06**	0.2	14.5
4	3102	**48.61**	**0.19**	**0.08**	**0.11**	0.2	3.6
5	2103	**48.44**	**0.17**	**0.14**	**0.08**	0.2	7.3
6	1101	**48.19**	**0.05**	**0.06**	**0.06**	0.2	13.6

Table 4. Proposed FSM-based UFLS scheme of the La Palma power system

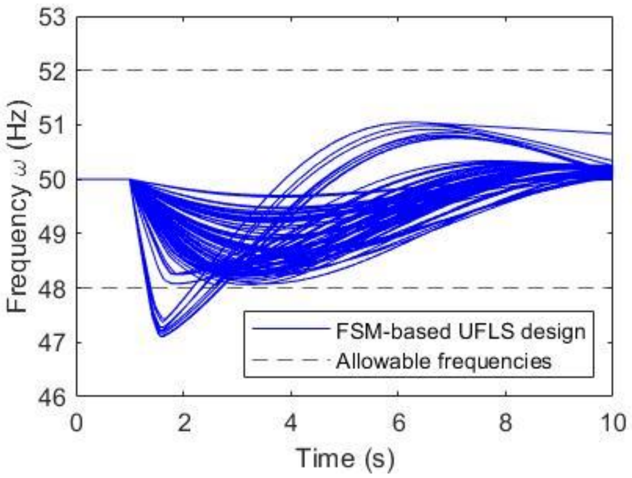

Figure 9. Overall frequency response of the La Palma FSM – based UFLS scheme

From Figure 9 it can be seen that the proposed scheme offers an adequate dynamic frequency response, since in no case overshedding or undershedding occurs. The admissible limits, both maximum and minimum, are respected, remaining at all times below 52 Hz and above 48 Hz. Note that in some cases the frequency drops below the minimum threshold but always for less than 2 s. Therefore, it can be concluded that the proposed scheme offers a good performance.

3.3.1.1 Comparison with the existing and the optimized UFLS scheme

This section presents a comparative analysis between the proposed scheme, the existing scheme, and its optimized version. The introduction of the frequency stability margin aims to enable rapid differentiation between severe and non-severe disturbances. This allows the system to delay load shedding, providing flexibility for natural recovery, or to act quickly in case of drastic RoCoF changes in order to prevent the system from a complete collapse. This is achieved by comparing at each point the frequency with the set $f_{LIM} = 48$ Hz and evaluating this gradient with the rate at which the frequency falls at each instant, i.e., measuring the time the system takes to fall below the frequency limit.

First of all, it is of great interest to compare the dynamic response for the different representative scenarios (see Table 5 and Figure 10). Table 5 shows and compares the amount of shed load and the minimum frequency deviations for the proposed FSM-based design, the existing scheme and its optimized version for the representative outages, whereas Figure 10 exhibits the time responses. It is observed that the best frequency response is offered by the proposed model and by the one optimized by [37]. Indeed, in scenario S1G17 and S3G17 both schemes offer similar dynamic responses. Although the amount of load shed is the same for the optimized and FSM-based scheme, the effect of including the FSM criterion is observed in the minimum frequency of both OC scenarios. In the case of the proposed scheme, lower frequency deviations are achieved, since it is able to quickly detect the severity of the occurrence and send the activation signal to the relays earlier.

As for scenario S8G11, given that the share of generation lost is quite low, the three schemes behave similarly. They recognize that shedding load is unnecessary, allowing the system to recover by itself.

Regarding the representative scenarios chosen by means of K-means, the difference between the conventional optimized scheme and the proposed one can be appreciated in S8G15. With the proposed one only one relay is activated, while in the conventional optimized formulation three relays are needed to arrest frequency decay. Here, as shown in Figure 10, what occurs is that the proposed scheme sheds load earlier than the other two schemes by activating the first step, thereby allowing the system to recover. Conversely, the conventional schemes delay the load shedding, and when the first disconnection step is finally activated, the frequency deviation is already substantial, having exceeded f_{LIM} = 48 Hz. As a result, the system requires disconnecting more load to ensure a stable frequency response.

		Existing UFLS scheme		Optimized UFLS scheme		FSM – based UFLS scheme	
Scenario	Generator (MW) (%)	ω_{min} (Hz)	P_{shed} (MW) (# relays)	ω_{min} (Hz)	P_{shed} (MW) (# relays)	ω_{min} (Hz)	P_{shed} (MW) (# relays)
8	2.35 (9.24)	49.13	0 (0)	49.13	0 (0)	49.13	0 (0)
3	9.55 (51.68)	45.74	10.94 (7)	47.01	8.63 (6)	47.12	8.63 (6)
8	6.10 (22.29)	48.01	7.06 (4)	47.79	6.08 (3)	48.30	1.94 (1)
1	10.41 (47.13)	46.59	13.08 (7)	47.21	10.32 (6)	47.37	10.32 (6)

Table 5. Output of the different UFLS schemes applied to the La Palma power system

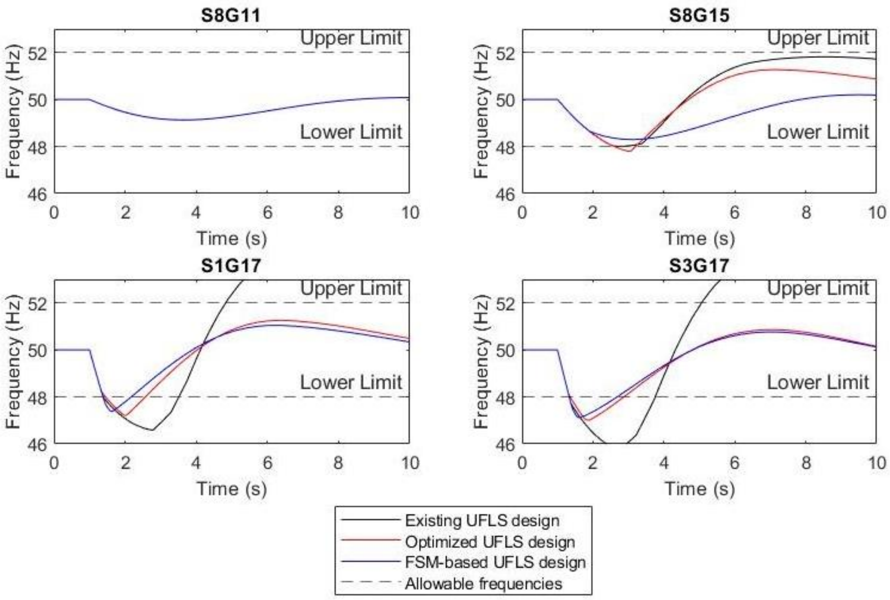

Figure 10. Output of the different UFLS schemes applied to the La Palma power system

Finally, when comparing the overall performance of the three schemes (see Table 6 and Figure 11), it can be clearly seen that the best answer is provided by the proposed scheme. Table 6 and Figure 11show and compare the total amount of shed load, the number of relays used and the accumulated minimum frequency deviations ($\Sigma\Delta\omega_{min}$) for the three designs and all possible outages. However, the conventional optimized scheme also shows a significant improvement over the existing UFLS scheme. Specifically, the proposed scheme achieves a 60% reduction in the amount of disconnected load compared to the existing scheme and nearly 30% compared to conventional optimized one. It is notable that the FSM-based scheme shows a lower total minimum frequency sum than the other schemes. By diminishing load shedding, the opposite effect would be expected, as reducing load disconnection typically leads to a trade-off with frequency, resulting in more negative deviations.

	UFLS performance		
Case	Total shed (MW)	Nº Relays	ΣΔωmin (Hz)
Existing	526.61	295	223.43
Optimized	293.31	170	227.41
FSM – based	210.70	120	207.59

Table 6. Comparison of the different UFLS scheme designs of the La Palma power system

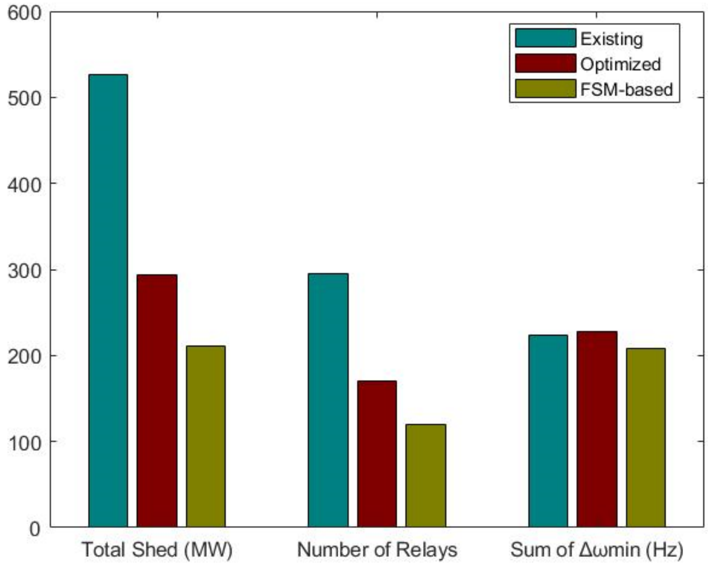

Figure 11. Performance of the different UFLS scheme designs of the La Palma power system

Note that, with respect to the results of the manually adjusted scheme described in [45], a robust scheme without over-shedding including RES has been achieved. It should be highlighted that, like the other model, a reduction of the disconnected load is attained compared to the existing scheme and its optimized version. With the scheme presented in this project, the disconnected load has been further reduced.

3.3.2 GRAN CANARIA POWER SYSTEM

The proposed method presented in the previous section is now implemented in the Gran Canaria power system, the second-largest power system of the Canary Islands. Similar to the one of La Palma, it is isolated, but it is considerably larger as it comprises 22 generator units. The parameters of the generator models are detailed in Table 8 and the generation dispatches are provided in Table 7.

S. O. C.	G1	G2	G3	G4	G5	G6	G7	G8	G9	G10	G11	G12	G13	G14	G15	G16	G17	G18	G19	G20	G21	G22	GDP	$P_{G_{tot}} = P_{D_{tot}}$
1	38.45	38.45	54.57	54.57	54.57	9.7	9.7	0	0	0	13.58	0	26.55	26.55	0	0	0	19.01	19.01	0	0	0	41.39	406.1
2	27.84	27.84	51.14	51.14	51.14	9.7	9.7	0	0	0	13.58	0	26.55	26.55	0	0	0	18.23	18.23	0	0	0	41.39	373.03
3	27.84	27.84	48.16	48.16	48.16	9.7	9.7	0	0	0	13.58	0	26.55	26.55	0	0	0	14.09	14.09	0	0	0	41.39	355.81
4	27.84	27.84	45.62	45.62	45.62	9.7	9.7	0	0	0	13.58	0	26.55	26.55	0	0	0	14.09	14.09	0	0	0	41.39	348.19
5	27.84	27.84	44.77	44.77	44.77	0	0	9.7	9.7	0	13.58	0	26.55	26.55	0	0	0	14.09	14.09	0	0	0	41.39	345.64
6	27.84	27.84	47.41	47.41	47.41	0	0	9.7	9.7	0	13.58	0	26.55	26.55	0	0	0	14.09	14.09	0	0	0	41.39	353.56
7	30.5	30.5	54.5	54.5	54.5	0	0	9.7	9.7	0	13.58	0	26.55	26.55	0	0	0	19.01	19.01	0	0	0	41.39	389.99
8	53.63	53.63	54.7	54.7	54.7	0	0	9.7	9.7	0	13.58	0	26.55	26.55	0	0	0	19.01	19.01	0	0	0	49.92	445.38
9	52.75	52.75	54.7	54.7	54.7	0	0	9.7	9.7	0	13.58	0	50.56	50.56	0	0	0	19.01	19.01	0	0	0	49.92	491.64
10	70.24	70.24	55.04	55.04	55.04	0	0	9.7	9.7	0	13.58	0	50.56	50.56	0	0	0	19.01	19.01	0	0	0	49.92	527.64
11	70.24	70.24	64.01	64.01	64.01	0	0	9.7	9.7	0	13.58	0	50.56	50.56	0	0	0	19.01	19.01	0	0	0	49.92	554.55
12	70.24	70.24	65.27	65.27	65.27	0	0	9.7	9.7	0	18.47	0	50.56	50.56	0	0	0	19.01	19.01	0	0	0	49.92	563.22
13	70.24	70.24	65.27	65.27	65.27	0	0	9.7	9.7	0	25.28	0	50.56	50.56	0	0	0	19.01	19.01	0	0	0	49.92	570.03
14	70.24	70.24	65.27	65.27	65.27	0	0	9.7	9.7	0	23.48	0	50.56	50.56	0	0	0	19.01	19.01	0	0	0	49.92	568.23
15	70.24	70.24	63.05	63.05	63.05	0	0	9.7	9.7	0	13.58	0	50.56	50.56	0	0	0	19.01	19.01	0	0	0	49.92	551.67
16	70.24	70.24	55.58	55.58	55.58	0	0	9.7	9.7	0	13.58	0	50.56	50.56	0	0	0	19.01	19.01	0	0	0	49.92	529.26
17	67.81	67.81	54.83	54.83	54.83	0	0	9.7	9.7	0	13.58	0	50.56	50.56	0	0	0	19.01	19.01	0	0	0	49.92	522.15
18	69.22	69.22	54.84	54.84	54.84	0	0	9.7	9.7	0	13.58	0	50.56	50.56	0	0	0	19.01	19.01	0	0	0	49.92	525
19	68.7	68.7	54.84	54.84	54.84	0	0	9.7	9.7	0	13.58	0	50.56	50.56	0	0	0	19.01	19.01	0	0	0	49.92	523.96
20	70.24	70.24	56.62	56.62	56.62	0	0	9.7	9.7	0	13.58	0	50.56	50.56	0	0	0	19.01	19.01	0	0	0	41.39	523.85
21	70.24	70.24	64.49	64.49	64.49	0	0	9.7	9.7	0	13.58	0	44.93	44.93	0	0	0	19.01	19.01	0	0	0	41.39	536.2
22	70.24	70.24	65.27	65.27	65.27	0	0	9.7	9.7	0	33.28	0	50.56	50.56	0	0	0	19.01	19.01	0	0	0	41.39	569.5
23	70.24	70.24	64.42	64.42	64.42	0	0	9.7	9.7	0	13.58	0	35.64	35.64	0	0	0	19.01	19.01	0	0	0	41.39	517.41
24	64.53	64.53	54.8	54.8	54.8	0	0	9.7	9.7	0	13.58	0	26.55	26.55	0	0	0	19.01	19.01	0	0	0	41.39	458.95

Table 7. Generation dispatch scenarios of the Gran Canaria power system with DPG [39]

Generator	H (s)	K	b1 (s)	b2 (s)	a1 (s)	a2 (s)	Pmin (MW)	Pmax (MW)
G1	5.6	16.67	0	0	5.35	1.75	27.84	74.24
G2	5.6	16.67	0	0	5.35	1.75	27.84	74.24
G3	5.084	20.21	0	0	0.43	0.09	3.23	67.6
G4	5.084	20.21	0	0	0.43	0.09	3.23	67.6
G5	5.084	16.67	0	0	5.35	1.75	3.23	67.6
G6	5.084	20.21	0	0	0.43	0.09	9.7	68.7
G7	5.084	20.21	0	0	0.43	0.09	9.7	68.7
G8	5	34.13	2.39	0	3.99	1.87	5.81	32.34
G9	5	35.2	2.66	0	4.32	2.08	5.81	32.34
G10	3	16.67	1.09	0	5.99	5.47	13.5	28.02
G11	3	16.67	1.09	0	5.99	5.47	13.58	37.28
G12	3	16.67	1.09	0	5.99	5.47	13.58	37.28
G13	4	16.67	1.12	0	6.06	5.64	26.55	55.56
G14	4	16.67	1.12	0	6.06	5.64	26.55	55.56
G15	1.5	25	0	0	0.35	0.01	4.58	11.34
G16	1.5	25	0	0	0.35	0.01	4.58	11.34
G17	1.5	25	0	0	0.35	0.01	4.58	11.34
G18	1.5	25	0	0	0.35	0.01	14.09	20.51
G19	1.5	25	0	0	0.35	0.01	14.09	20.51
G20	5	39.91	2.51	0	4.02	1.95	5.81	21.56
G21	5	32	2.25	0	3.85	1.75	5.81	32.34
G22	5	32	2.25	0	3.85	1.75	5.81	32.34

Table 8. Parameters of the generator model of the Gran Canaria power system [39]

As the frequency response will be compared with the existing and its optimized version presented in [37], the same generation dispatches will be used to ensure a rigorous comparison. Therefore, DPG generation will again be considered to cover 10% of the total demand.

Given the size and robustness of the Gran Canaria power system, considering only individual outages would not be sufficient to cause frequency deviations that could compromise the security of the power system. Therefore, multiple and simultaneous generator losses will be considered.

As a different power system is considered, it is necessary to identify the OC scenarios to represent the case study. For this purpose, the K-means algorithm is applied. Having to select the scenarios with multiple generation losses, the possible combinations are extremely large.

Thus, the selection is limited to scenarios where generation losses range between 9% and 51% of the total generation within each dispatch.

Once again, it is necessary to determine the optimal number of representative scenarios to be considered. Thus, the elbow diagram is used. As it can be seen in Figure 12, a $K = 4$ is sufficient to represent all possible scenarios. The OC scenarios derived from the CA analysis are detailed in Table 9.

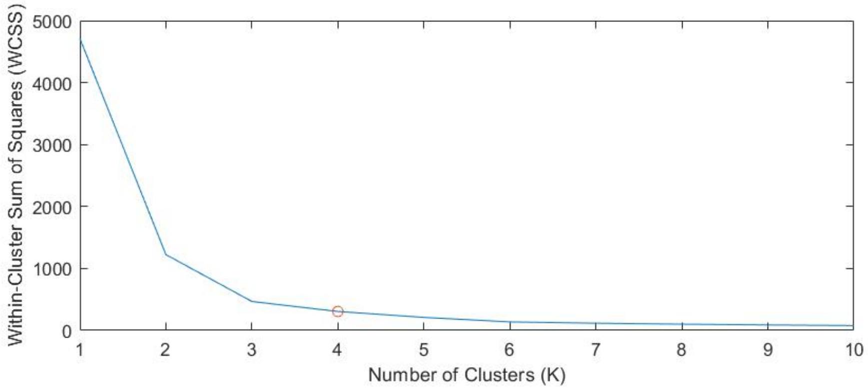

Figure 12. Elbow graph: Determination of the number of clusters using K-means algorithm

Scenario	Generator	P_{dem} (MW)	P_{loss} (MW) (%)
10	G23	527.64	49.92 (9.46)
21	G1, G2	536.20	140.48 (26.20)
23	G1- G3	517.41	204.90 (39.60)
21	G1-G4	536.20	269.47 (50.25)

Table 9. Representative OC scenarios of the Gran Canaria power system

Once the OC scenarios are identified, the next step is to optimize the Gran Canaria UFLS scheme parameters. To this end, the following constraints will be considered:

- $\omega < 48$ Hz or $t_{max} = 2$ s.
- 47 Hz $< \omega \leq 52$ Hz.
- Priority of load shedding.
- The load shed [MW] < The power generation loss [MW].

The parameters of the UFLS scheme are constrained within upper and lower limits as described below:

- 47 Hz ≤ Frequency threshold ≤ 49 Hz
- 0 s ≤ FSM threshold ≤ 1.2 s
- 0 s ≤ Intentional time delay for frequency threshold ≤ 0.5 s
- 0 s ≤ Intentional time delay for FSM threshold ≤ 0.5 s

Again, the step size of UFLS scheme proposed in [39] will be assumed, these can be seen in Table 10. Given that the worst-case scenario for the simulated generation loss is 51%, 10 steps will be sufficient. However, only 5 stages will be adjusted. These are highlighted in bold in Table 11 and the overall dynamic response of the Gran Canaria power system is depicted in Figure 13.

Stage	Substation	ω (Hz)	t_{int} (s)	t_{open} (s)	Step size (%)	Cumulative (%)
1	1001 - 1007	49.00	0.1	0.2	3.43	3.43
2	1008 - 1015	48.92	0.15	0.2	5.27	8.70
3	1016 - 1023	48.85	0.2	0.2	5.03	13.73
4	1024 - 1030	48.79	0.3	0.2	5.68	19.41
5	1031 - 1035	48.72	0.4	0.2	4.17	23.58
6	1036 - 1047	48.66	0.5	0.2	9.95	33.53
7	1048 - 1053	48.60	0.6	0.2	5.46	38.99
8	1054 - 1058	48.55	0.7	0.2	3.05	42.04
9	1059 - 1066	48.50	0.8	0.2	4.07	46.11
10	1067 - 1074	48.35	0.9	0.2	5.89	52.00
11	1075 - 1090	48.00	1	0.2	10.34	62.34

Table 10. Original UFLS scheme [37]

Stage	Feeders	ω_{thr} (Hz)	FSM_{thr} (s)	$t_{thr,F}$ (s)	$t_{thr,FSM}$ (s)	t_{open} (s)	Step size (%)
1	1001 – 1007	**48.99**	**1.04**	**0.21**	**0.23**	0.2	3.43
2	1008 – 1015	**48.70**	**0.77**	**0.03**	**0.03**	0.2	5.27
3	1016 – 1023	**48.60**	**0.74**	**0.04**	**0.07**	0.2	5.03
4	1024 – 1030	**48.24**	**0.73**	**0.06**	**0.36**	0.2	5.68
5	1031 – 1035	**48.09**	**0.5**	**0.14**	**0.00**	0.2	4.17
6	1036 - 1047	48.66	-	0.5	-	0.2	9.95
7	1048 - 1053	48.60	-	0.6	-	0.2	5.46
8	1054 - 1058	48.55	-	0.7	-	0.2	3.05
9	1059 - 1066	48.50	-	0.8	-	0.2	4.07
10	1067 - 1074	48.35	-	0.9	-	0.2	5.89
11	1075 - 1090	48.00	-	1	-	0.2	10.34

Table 11. Proposed FSM-based UFLS scheme of the Gran Canaria power system

When analyzing the parameters of the FSM-based UFLS scheme, it becomes evident that the activation of the first step is delayed by applying a longer intentional time delay. Notably, steps 2, 3, and 4 have very similar FSM values. Considering the FSM parameters, the frequency thresholds, and the intentional delays, steps 2 and 3 will be activated in close succession. However, step 4, despite having a similar FSM value, is assigned a longer delay, allowing the system to have a longer time to recover by itself. In the final step, the FSM threshold is directly violated once it reaches 0.5 s, while a frequency delay of 0.14 s is applied to assess whether the frequency can recover on its own or whether it continues to breach the threshold. In this last step, the load-shedding decision is mainly focused on the frequency value.

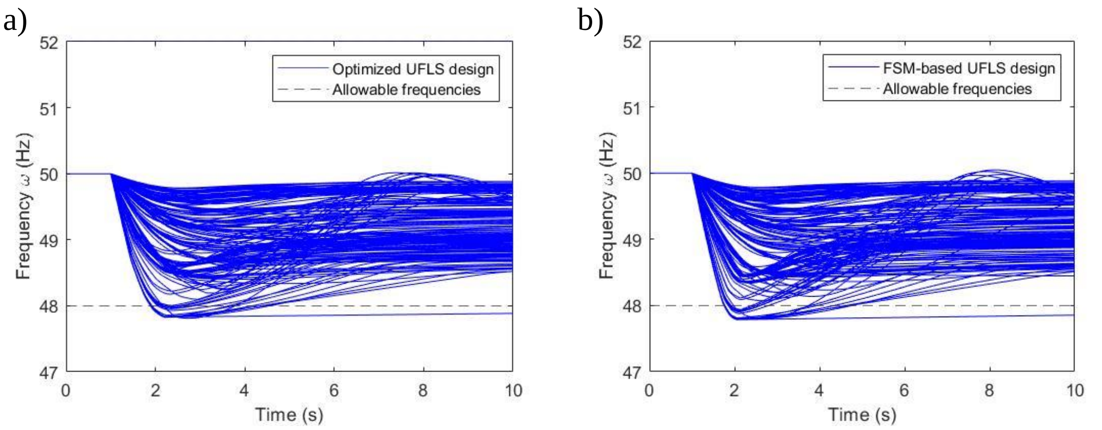

Figure 13. Overall frequency response of the Gran Canaria a) Optimized and b) FSM – based UFLS scheme

From Figure 13 it can be inferred that the proposed scheme demonstrates a suitable dynamic frequency response in terms of avoiding both over-shedding and undershedding. Nonetheless, when applied to all possible OC scenarios, the frequency response does not meet the constraint of remaining above the frequency limit, even considering the 2 s margin. The same issue was also observed in [37]. This arose as a consequence of optimizing the UFLS scheme. As the amount of disconnected load is reduced, the number of scenarios with low maintained frequency increases. However, as indicated when defining the constraints, it is not acceptable to have low steady-state frequency values. To address this, [37] proposed including an additional criterion in the optimization problem, which consists of limiting the frequency from falling below 49 Hz for more than 5 s. Therefore, the same measure is applied to the FSM-based scheme.

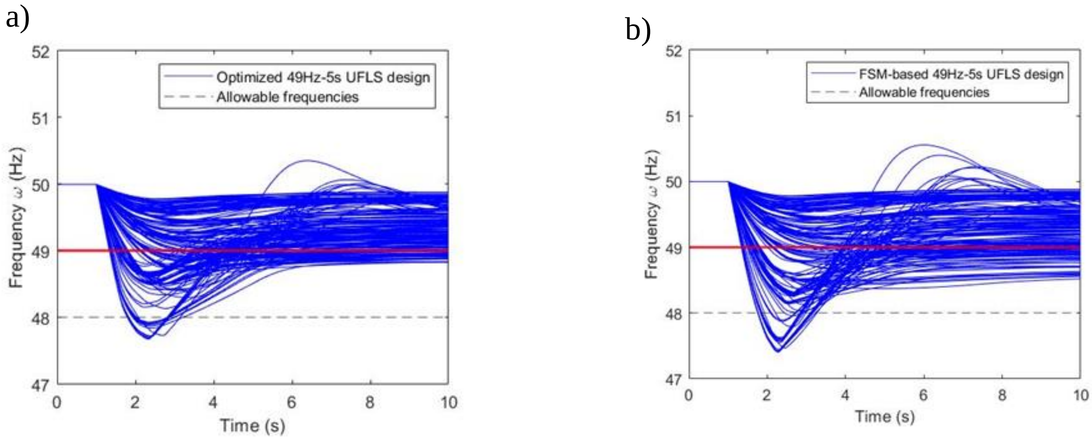

Figure 14. Overall frequency response of the Gran Canaria a) Opmized and b) FSM – based, 49 Hz-5s UFLS scheme

By applying the 49 Hz – 5s criterion, the frequency is arrested closer to 49 Hz in steady-state (see Figure 14). However, many scenarios still fall below 49 Hz, unlike the dynamic response observed in [37]. This discrepancy occurs because the proposed model in this project only includes FSM relays, whereas the scheme described in [37] incorporates both UF and RoCoF relays. This combination of relays allows the system to better manage load shedding, especially when the RoCoF is low, but the frequency deviation is large. This results in achieving safer frequencies. In contrast, the FSM-based model cannot reach the same result. Given that it relies solely on FSM relays, reducing the deviation would require setting very high FSM values, transforming the scheme into a UF-based model, where load shedding would depend on frequency rather than on both criteria. For instance, in scenarios where the frequency stabilizes at 48.5 Hz, FSM values greater than 20 s would be required, making it impossible for the proposed scheme to shed enough load to reduce the deviation in the steady state. This is because the adjustment is designed to stop shedding load once t_{min} is reached. The problem arises with disturbances like the S21 G1-G2 scenario, where the FSM-based scheme does not disconnect any load since no restrictions are violated, as the frequency stabilizes on its own above f_{LIM}. Additionally, in this case, the frequency drop is moderate, resulting in a high FSM value, which prevents any relay from activating. The issue here is that the frequency remains at 48.66 Hz in the steady state. In this scenario, with a loss of 140 MW, activating some load shedding steps could have helped reduce the steady-state deviation, but due to the FSM nature, none are activated. In contrast, with the UF scheme, 73 MW is shed without violating any restrictions, resulting in a small steady-state deviation.

Therefore, it can be concluded that, to achieve greater robustness in power systems like the one of Gran Canaria, it would be necessary to include UF relays in the model. Implementing a solution that integrates both UF and FSM relays would stabilize the system more effectively in scenarios of sustained low frequency, such as when the frequency stabilizes at 48.5 Hz, overcoming the limitations of a scheme based solely on FSM relays. Another option would be to explore the response obtained by removing the restriction that stops shedding once the minimum frequency is reached in the optimal design of the FSM-based scheme. Both approaches could contribute to reducing the risk of failures and optimizing the system's response in extreme conditions, ensuring safer and more stable operation in island systems like Gran Canaria in steady-state.

3.3.2.1 Comparison with the existing and the optimized UFLS scheme

This section compares the performance of the FSM-based UFLS scheme with both the existing scheme and its optimized version, as well as with the proposed scheme incorporating an additional 49 Hz - 5s constraint. Figure 15 shows the time responses in terms of frequency of the representative outages for the FSM-based scheme and for the existing scheme and its optimized version. In Figure 15 it can be seen that, by introducing the FSM criterion, load shedding is delayed. The best frequency response, in terms of minimized load disconnection, is achieved by both the FSM-based model and the one optimized by [33]. Notably, in scenarios S23 G1-G3 and S21 G1-G4, both schemes exhibit a similar dynamic response. In the first case, however, the amount of disconnected load is slightly higher in the FSM-based scheme, with an increase of 2.60%. This difference arises because the conventional optimized scheme employs both UF and RoCoF relays, enabling more activation combinations that reduce the amount of load shed.

By analyzing minimum frequencies, the impact of incorporating the FSM criterion becomes evident, as it results in deeper frequency drops. This occurs because the system delays load shedding, allowing the frequency to approach f_{LIM} more closely. This effect is particularly pronounced in the scheme with the 49H – 5s criterion, which, although it reaches lower frequency values, increases load shedding (see Table 12 which shows the amount of shed load and minimum frequency deviations for each representative outage). This additional load shedding helps arrest frequency deviations to achieve values of 49 Hz or above in the steady state. In scenario S21 G1, G2, both the conventional optimized and the proposed schemes do not shed load, as the frequency recovers naturally. However, despite this natural recovery, the large steady-state frequency deviation compromises system stability.

As for scenario S10 G23, given that the share of generation lost is quite low, the three schemes behave similarly. They recognize that shedding load is unnecessary, allowing the system to recover by itself.

		Existing UFLS scheme		Optimized UFLS schemes		FSM – based UFLS scheme	
Scenario	Generator (MW) (%)	ω_{min} (Hz)	P_{shed} (MW) (# relays)	ω_{min} (Hz)	P_{shed} (MW) (# relays)	ω_{min} (Hz)	P_{shed} (MW) (# relays)
10	49.92 (9.46)	49.73	0 (0)	49.73	0 (0)	49.73	0 (0)
21	140.48 (26.20)	48.82	73.63 (23)	48.66	0 (0)	48.66	0 (0)
23	204.90(39.60)	48.57	173.55 (47)	48.48	69.35 (20)	48.34	71.15 (23)
21	269.47 (50.25)	47.95	278.92 (74)	47.82	126.48 (35)	47.79	126.48 (35)

Table 12. Output of the different UFLS schemes applied to the Gran Canaria power system

		Optimized 49Hz-5s UFLS schemes		FSM – based 49Hz-5s UFLS scheme	
Scenario	Generator (MW) (%)	ω_{min} (Hz)	P_{shed} (MW) (# relays)	ω_{min} (Hz)	P_{shed} (MW) (# relays)
10	49.92 (9.46)	49.73	0 (0)	49.73	0 (0)
21	140.48 (26.20)	48.75	18.41 (7)	48.79	18.41 (7)
23	204.90 (39.60)	49.49	88.21 (26)	48.15	71.05 (23)
21	269.47 (50.25)	47.70	179.85 (47)	47.43	179.85 (47)

Table 13. Output of the 49Hz – 5s UFLS schemes applied to the Gran Canaria power system

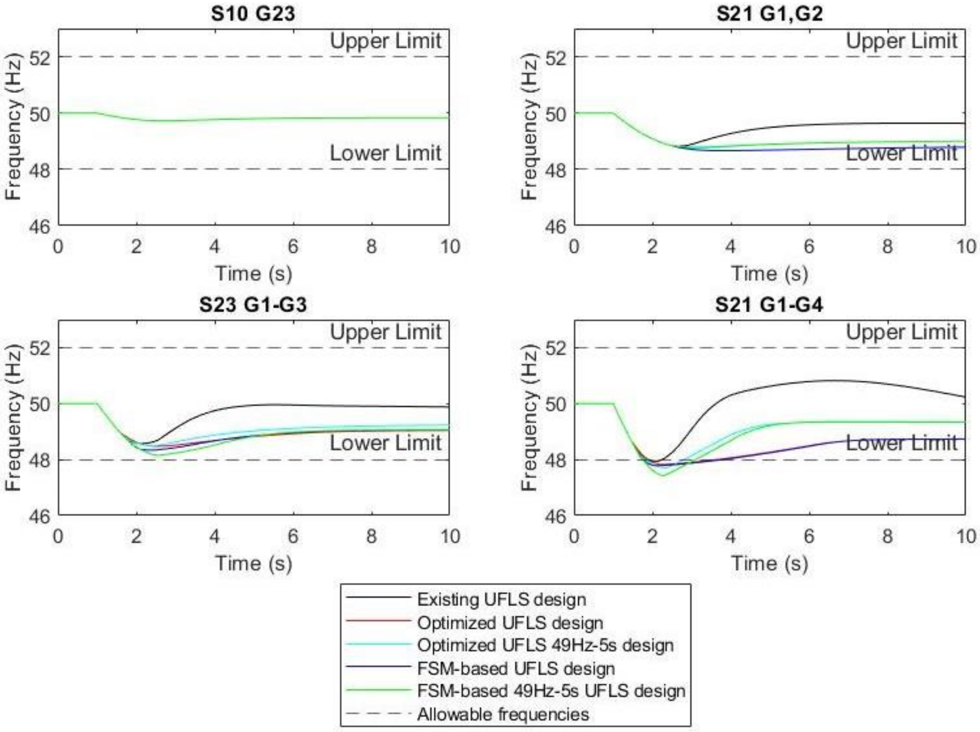

Figure 15.Output of the different UFLS schemes applied to the Gran Canaria power system

Finally, when comparing the overall performance of the five schemes (see Table 14 and Figure 16), it can be seen that, although the FSM-based scheme sheds more load than the conventional optimized scheme in representative scenarios, it ultimately reduces load shedding when applied across all possible contingencies. Table 14 and Figure 16 depict and compare the total amount of shed load, the number of relays used and the accumulated minimum frequency deviations ($\Sigma\Delta\omega$min) for the five designs and all possible outages. However, the optimized scheme also shows a significant improvement over the existing UFLS scheme.

Both the FSM-based and conventional optimized schemes effectively minimize load shedding. However, as noted previously, they also result in lower steady-state frequency values, which can compromise system stability. Considering both frequency and load shedding, the 49Hz – 5s scheme offers the best outcome. While it maintains frequency values below 49 Hz and increases load shedding by 28% (still lower than the existing scheme), it results in fewer low-frequency cases. Comparing the application of this criterion in both the FSM-based and optimized schemes, it can be observed that, while both shed similar load levels, the optimized scheme performs better by reducing the cases where frequency falls below 49Hz in the steady-state.

	UFLS performance		
Case	Total shed (MW)	Nº Relays	ΣΔωmin (Hz)
Existing	7,999	2444	170.46
Optimized	4,328	1312	184.08
Optimized: 49Hz - 5s	6,017	1820	182.24
FSM – based	4,200	1321	190.06
FSM – based: 49Hz -5s	5,383	1654	198.39

Table 14. Comparison of the different UFLS scheme designs of the Gran Canaria power system

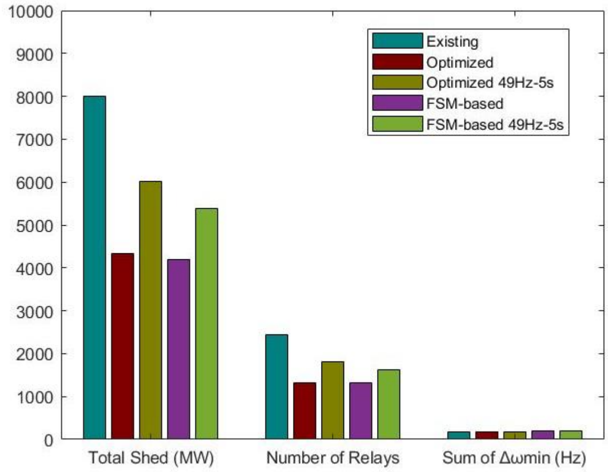

Figure 16. Performance of the different UFLS scheme designs of the Gran Canaria power system

Chapter 4. SENSITIVITY ANALYSIS

When it comes to power system modeling, sensitivity analysis is essential, especially when it involves the evaluation of the robustness and efficiency of UFLS schemes in small isolated power systems. Thus, this section is focused on exploring the power system response to variations in certain key parameters that directly influence the operation and efficiency of the proposed UFLS scheme. Given the critical nature of UFLS schemes in maintaining system stability after substantial disturbances, it is imperative to understand how variations in system configuration and conditions can impact system performance.

This analysis focuses on four specific areas that are fundamental to the secure and efficient operation of power systems: i) the increased penetration of RES, ii) the implementation of energy storage systems, iii) the variation in the formulation of the UFLS model objective function, and iv) the optimized design of load stages.

4.1 INCREASING RES PENETRATION

The global shift to renewables is progressively changing the landscape of power systems. This transformation, marked by a steady growth in the integration of RES into the energy mix, responds not only to sustainability objectives but also to the need to diversify energy sources and reduce dependence on fossil fuels. In this context, the Canary Islands is not an exception. During the last year, the installation of renewable capacity in the archipelago has experienced a significant increase, reaching 23% of the total installed capacity in 2022 [12]. This trend is projected to intensify, aiming to achieve the ambitious target of 100% renewable energy by 2050.

Focusing on the island of La Palma, recent data [12] reveals that its installed capacity stands at 116 MW, with approximately 9.5% from renewable sources – comprising 7 MW of wind power, 3.3 MW of solar power, and 0.8 MW of mini-hydro power (excluded from generation dispatches). La Palma is further committed to increasing the penetration of renewable energies. Indeed, it has been designated as one of the 30 island territories supported by the Clean Energy Secretariat of the European Union, with the goal of making the island 100% renewable by 2030 [46]. In addition, two wind projects are expected to be built, which will add up to 16.45 MW to the total installed capacity of the island. With these two new plants, it is estimated that 30% of the power generation of La Palma will be renewable [47].

Given this evolution, it is crucial to evaluate how increased renewable penetration will impact system stability and efficiency. Limiting analysis to a 10% renewable scenario is insufficient, as projections suggest much higher penetration. This necessitates examining high-RES scenarios to understand their effects on the design and operation of UFLS schemes.

The aim of this section is to assess the impact of increased RES capacity on frequency response and evaluate the performance of the UFLS scheme, ensuring system stability without over- or under-shedding. Two scenarios will be analyzed: *Scenario A*, based on updated generation dispatches reflecting higher renewable generation (see Table 15), and *Scenario B*, which doubles renewable power output while adjusting synchronous generation to match the demand level of *Scenario* A.

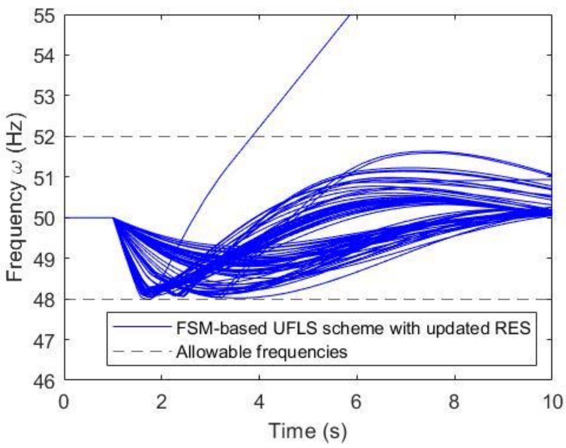

Figure 17. Scenario A: Overall frequency response

From Figure 17, it can be inferred that increasing RES penetration (from 4 – 10% to 10 – 24% of total demand) generally results in a good performance, except in one contingency where over-shedding occurs. In this scenario, the UFLS scheme failed to maintain frequency stability, as it shed more load than needed. Specifically, 10.35 MW of load was disconnected, while the system had only lost 7.40 MW. Activating 5 relays, rather than 6, would have been sufficient to restore stability without causing excessive load shedding. Aside from this case, the frequency remains within acceptable limits, meeting the necessary restrictions.

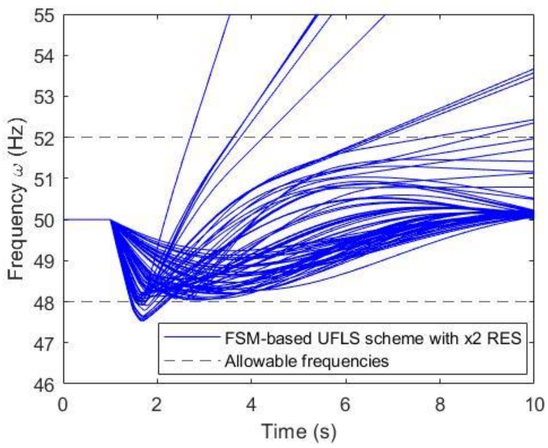

Figure 18. Scenario B: Overall frequency response

However, when analyzing the dynamic response of *Scenario B* (see Figure 18), the situation changes. The UFLS scheme results in overshedding on several occasions, compromising the stability of the power system. This response is expected, given that the UFLS scheme was designed and tuned for a power system with much lower RES compared to the current scenario (21 – 49% of total demand).

Both Figure 17 and Figure 18 show that increasing RES penetration in the La Palma power system with the proposed UFLS scheme leads to higher RoCoF values and greater frequency deviations

Table 15 presents a comparative analysis of these results with the conventional optimized UFLS scheme. It is evident that the optimized UFLS scheme performs better, as no over-shedding occurs in *Scenario A*, and while more load is shed in *Scenario B*, fewer overshoots are observed compared to the FSM-based UFLS scheme response. Additionally, it can be seen that the optimized scheme takes a more conservative approach, not only by shedding more load in the higher RES penetration scenario but also by maintaining more conservative frequency minimums. In contrast, the FSM-based scheme leads to larger frequency deviations as it allows the frequency to recover on its own before activating any frequency relay.

		UFLS performance			
UFLS scheme type	Case	Total shed (MW)	Nº Relays	ΣΔωmin (Hz)	# Overshoots
Proposed FSM - based	Scenario A	354.15	186	197.59	1
	Scenario B	380.37	186	218.13	14
Optimized ROCOF/UF	Scenario A	356.84	183	188.82	0
	Scenario B	384.68	199	207.82	12

Table 15. Comparison of UFLS scheme performance with different RES levels

These findings lead to several conclusions. On one hand, they highlight the critical need to adjust the UFLS scheme using real and up-to-date data on RES penetration. This allows for precise and appropriate fine-tuning to address drastic contingencies in the power system. On the other hand, the results underscore the importance of investing in and strengthening the infrastructure of power systems, as well as the tools needed for maintaining system security, before significantly increasing RES penetration. This process must be carried out in parallel: as RES penetration grows, the grid infrastructure must be improved to ensure users are not affected by blackouts or other instability issues. Strengthening both infrastructure and safety mechanisms is essential to ensure a reliable transition to higher levels of RES penetration.

In light of this, it would be appropriate to update the generation dispatch inputs in the simulator to identify the optimal UFLS scheme under the new generation conditions. The result of tuning the FSM-based UFLS scheme, considering the updated RES penetration levels, are presented in Table 16.

		UFLS performance			
UFLS scheme type	Case	Total shed (MW)	Nº Relays	ΣΔωmin (Hz)	# Overshoots
Optimized FSM-based UFLS scheme with updated RES	Scenario A	319.80	156	208.80	0
	Scenario B	306.07	153	220.35	1

Table 16. Performance of the FSM-based UFLS scheme adjusted with the new RES penetration scenarios.

From Table 16 it can be inferred that load shedding is reduced compared to the results obtained by applying both the proposed and the conventional optimized scheme. This is achieved by compromising frequency stability. By optimizing the scheme for the two new scenarios, it is possible to avoid overshoots in *scenario A*, but not in **scenario B**, where an overshoot still occurs in one particular case. Although attempts have been made to adjust the simulator to mitigate this overshoot, this remains the most favorable dynamic response, with fewer errors when applied to all 164 scenarios in terms of overshoots and violations of constraints. However, it is important to note that both *scenarios A and B* exhibit increased oscillatory behavior (see Figure 19) leading to a longer stabilization time for the frequency response compared to the base case (see Figure 9).

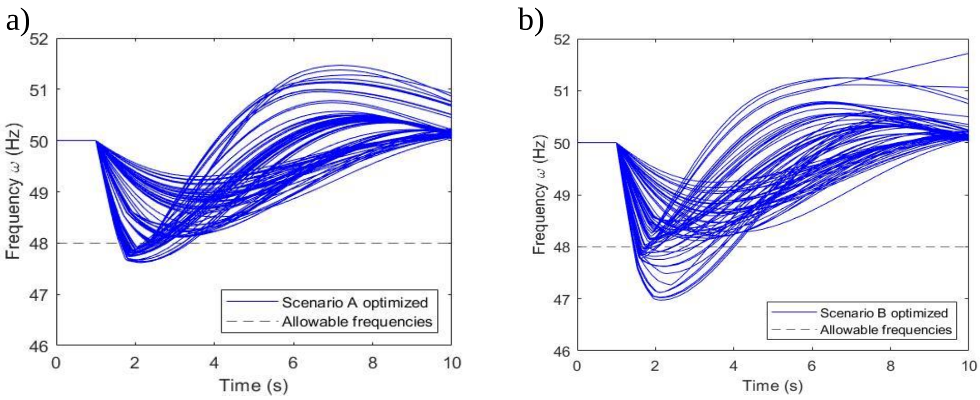

Figure 19. Overall frequency response with increased RES: a) Scenario A, b) Scenario B

Note that the scenario with higher penetration of renewables shed less load than scenario A, but again, this is achieved by compromising frequency stability. As it can be seen in Figure 19 (b), the adjusted UFLS scheme for *scenario B* presents a slower recovery and requires more time to recover naturally. In *scenario B*, unlike *scenario A*, where there are no violations, this slower response leads to four instances where the 48Hz – 2s constraint is infringed, i.e., frequency remains under 48 Hz during 2.0069 s, 2.3209 s, 2.3910 s and 2.2382 s. The difficulty in finding an optimal scheme for scenario B with no or minimal errors lies in the substantial increase in the penetration of RES (from 4 – 10% to 21 – 49% of total demand).

Given that the power system of La Palma is isolated, grid operation faces additional challenges due to the system's low inertia and the limited spinning reserve capacity provided by thermal units. The penetration of RES without adequate integration into primary control mechanisms, such as wind energy deloading for primary reserve, compromises system stability [48].

S. O. C.	G11	G12	G13	G14	G15	G16	G17	G18	G19	G20	G21	DPG	$P_{G_{tot}} = P_{D_{tot}}$
1	2.35	2.35	2.35	0.00	0.00	0.00	6.63	6.63	0.00	0.00	0.00	2.84	23.15
2	2.35	0.00	2.35	0.00	0.00	0.00	7.03	6.63	0.00	0.00	0.00	3.51	21.87
3	2.35	0.00	2.35	0.00	0.00	0.00	6.63	6.63	0.00	0.00	0.00	3.31	21.27
4	2.35	0.00	2.35	0.00	0.00	0.00	6.63	6.63	0.00	0.00	0.00	3.25	21.21
5	2.35	0.00	2.35	0.00	0.00	0.00	6.63	6.63	0.00	0.00	0.00	3.23	21.19
6	2.35	0.00	2.35	0.00	0.00	0.00	7.40	6.63	0.00	0.00	0.00	3.43	22.16
7	2.35	0.00	2.35	0.00	3.30	0.00	8.56	6.63	0.00	0.00	0.00	3.42	26.61
8	2.35	2.35	2.35	0.00	3.30	0.00	11.04	6.63	0.00	0.00	0.00	3.67	31.69
9	2.35	2.35	2.35	0.00	3.87	0.00	11.20	6.63	0.00	0.00	0.00	4.20	32.95
10	2.35	2.35	2.35	0.00	3.30	0.00	10.44	6.63	0.00	0.00	0.00	5.48	32.90
11	2.35	2.35	2.35	0.00	3.30	0.00	8.68	6.63	0.00	0.00	0.00	6.67	32.32
12	2.35	0.00	2.35	0.00	3.30	0.00	9.56	6.63	0.00	0.00	0.00	7.31	31.50
13	2.35	0.00	2.35	0.00	3.30	0.00	9.15	6.63	0.00	0.00	0.00	7.60	31.38
14	2.35	0.00	2.35	0.00	3.30	0.00	9.58	6.63	0.00	0.00	0.00	7.81	32.02
15	2.35	0.00	2.35	0.00	3.30	0.00	9.26	6.63	0.00	0.00	0.00	7.69	31.58
16	2.35	0.00	2.35	0.00	3.30	0.00	8.30	6.63	0.00	0.00	0.00	7.14	30.07
17	2.35	0.00	2.35	0.00	3.30	0.00	8.40	6.63	0.00	0.00	0.00	6.51	29.53
18	2.35	0.00	2.35	0.00	3.30	0.00	9.89	6.63	0.00	0.00	0.00	5.49	30.00
19	2.35	0.00	2.35	0.00	0.00	0.00	8.89	6.63	6.63	0.00	0.00	4.29	31.14
20	2.55	0.00	3.04	0.00	0.00	0.00	11.20	6.63	6.63	0.00	0.00	3.84	33.89
21	2.55	2.55	3.25	0.00	0.00	0.00	11.20	6.63	6.63	0.00	0.00	3.82	36.62
22	2.35	2.35	2.35	0.00	0.00	0.00	10.81	6.63	6.63	0.00	0.00	3.77	34.89
23	2.35	0.00	2.35	0.00	0.00	0.00	9.41	6.63	6.63	0.00	0.00	3.84	31.21
24	0.00	0.00	2.35	0.00	0.00	0.00	7.97	6.63	6.63	0.00	0.00	3.53	27.10
25	2.35	2.35	2.35	0.00	0.00	0.00	6.63	6.63	0.00	0.00	0.00	2.84	23.15
26	2.35	0.00	2.35	0.00	0.00	0.00	7.03	6.63	0.00	0.00	0.00	3.51	21.87

Table 17. Generation dispatch scenarios of the La Palma power system with updated demand and DPG

In this project, the increased penetration of RES was implemented without introducing any additional backup beyond adjustments to the UFLS scheme, resulting in a system with weak primary control and reduced inertia, ultimately jeopardizing overall stability. A deeper analysis should consider this aspect, as [48] emphasize that integrating RES into spinning reserves can reduce thermal generation by up to 40%, thereby enhancing both system efficiency and stability.

4.2 IMPACT OF ENERGY STORAGE SYSTEMS (ESS) ON THE DESIGN OF UFLS SCHEMES

In line with the trend outlined in the previous section, the commitment to include batteries both as standalone units and in hybrid wind and solar plants is becoming increasingly evident. The advantages of batteries are numerous, both in economic and technical terms. From a technical point of view, they can act alternatively as an energy source or as a load, so that generation-demand mismatches can be balanced. On the economic side, they give a competitive advantage to those who own them by being able to sell energy at times of low renewable production, when the energy market price is higher. This is crucial for encouraging more renewable plants to opt for hybridization, as energy prices during peak renewable production hours are plummeting. In Spain, for the first time in history, a negative energy price was recorded for three hours, reaching a value of -0.01 €/MWh between 2 pm and 5 pm in April 2024 [49].

Given this new paradigm and the fact that La Palma already has a 4MW-5s ultracapacitor, it is of great interest to study the impact of including storage in the proposed UFLS scheme. Therefore, with the aim of further reducing or even eliminating the need for load shedding while preserving system integrity, an ultracapacitor is connected to the system. To achieve the maximum performance from an ultracapacitor, its control parameters must be optimized. However, this research does not focus on the optimization itself but on observing how the proposed scheme behaves when a storage device is included. Consequently, the optimal parameters proposed in [50], which were optimized using the same power system and similar contingencies, will be used.

To include storage in the model, the following transfer function is included as input in the singles bus:

$$-\frac{1}{R_{ESS}}\frac{1+s(2\cdot R_{ESS}\cdot H_{ESS}+T_f)}{1+s\left(T_f+T_c\right)+s^2\left(T_f+T_c\right)} \quad (19)$$

Here R_{ESS} accounts for the droop, H_{ESS} is the vitual inertia, T_f is the filter time constant of the UC, and T_c represents the equivalent time constant of the converter and the current control of the UC. Another key parameter of the ultracapacitor is the tail control coefficient, E_{tail}, which progressively decreases the active power injection of the ESS as it depletes.

The values assigned to these parameters, along with the nominal characteristics of the UC, are presented in Table 18.

R_{ESS} (-)	H_{ESS} (s)	E_{tail} (%)	T_f (s)	T_c (s)	P_n (MW)	E_{max} (MWs)
0.022	9.82	71.06	0.2	0.2	4	20

Table 18. ESS parameters [50]

Now, the effect of storage is studied through two scenarios. The first one involves incorporating storage into the power system with the FSM-based UFLS scheme from section 3.3.1, i.e., maintaining the load-shedding parameters from the base case. Whereas in the second scenario, a new set of UFLS parameters is designed and optimized from scratch, taking into account energy storage in the power system simulations.

	UFLS performance			
Case	Total shed (MW)	Nº Relays	ΣΔωmin (Hz)	Max{Δωmin} (Hz)
Base case	210.70	120	207.59	-2.90
Base case with ESS	93.19	60	132.48	-2.31
Optimized FSM-based UFLS with ESS	79.28	56	139.21	-2.99

Table 19. FSM-based UFLS performance comparison with and without energy storage

From Table 19 it can be inferred that incorporating storage into the proposed scheme, load shedding is reduced by approximately 55%, which is a considerable improvement. Note that the difference between scenarios 1 and 2 is not very significant. The primary improvement comes from simply including storage. While optimization fine-tunes and reduces load shedding, scenario 1 already offers a good response on its own. Therefore, it can be concluded that integrating ESS enhances the efficiency, flexibility, and security of the electrical system.

While it is observed that adding storage reduces the frequency of instances where the load shedding scheme must be activated, it is observed that, by reducing the load disconnection load through the optimization, the sum of the minimum frequency deviations, as well as the maximum deviation in absolute terms, increases. The reason behind this is that by decreasing load shedding, the dynamic response reaches more negative values.

4.3 VARYING THE FORMULATION OF THE OBJECTIVE FUNCTION

The objective function considered in the base case is rather simple, thus it is convenient to explore other formulations. In the literature, more complex configurations with detailed weighting of the parameters can be found [37]. Adding weighting factors allows not only to reduce the disconnected load, but also to focus on other aspects, such as frequency deviation. Including a frequency-related term leads to a more conservative design, which may compromise the amount of load to be shed in order to reduce frequency deviations. Thus, with this new formulation it is expected that the load shed will increase, and frequency deviations will be reduced. The alternative objective function that will be studied is as follows:

$$f(\mathbf{x}_d) = \sum_{j=1}^{M} \alpha_{f,j} \cdot p_{shed,j}(\mathbf{x}_d) + \sum_{j=1}^{M} \beta_{f,j} \Delta\omega_{min,j}(\mathbf{x}_d) \tag{20}$$

Here $\alpha_{f,j}$ and $\beta_{f,j}$ represent the weighting factors thar can be calculated as described below:

$$\alpha_{f,j} = \frac{p_{loss,max} - p_{loss,min}}{p_{loss,j}} \tag{21}$$

$$\boldsymbol{\beta}_{f,j} = \begin{bmatrix} 0 & \cdots & 0 & k_{eq,M} \\ \vdots & & k_{eq,M-1} & \\ 0 & \iddots & & \vdots \\ k_{eq,1} & 0 & & 0 \end{bmatrix} \boldsymbol{\alpha}_f \tag{22}$$

Similar to [37], three different approaches will be studied. First, an objective function with $\alpha_{f,j}$ and $\beta_{f,j}$ set to the unity is considered (Case 1). Then, an objective function with a greater emphasis on the frequency term is used, where the weighting coefficient for the frequency-dependent term is equal to k_{eq} (case 2), i.e. only $\alpha_{f,j}$ is assumed as one. Finally, similar to the base case, the third approach will not optimize $\Delta\omega_{min}$, but will weight the shed load based on the number of contingencies in the scenario, so that scenarios with a larger number of disturbances reduce the amount of load they can shed (Case 3).

	UFLS performance			
Case	Total shed (MW)	# Relays	ΣΔωmin (Hz)	Max{Δωmin} (Hz)
Base case: $\sum(p_{shed})$	210.70	120	207.59	-2.90
Case 1: $\sum(p_{shed} + \Delta\omega_{min})$	216.10	121	203.61	-2.77
Case 2: $\sum(p_{shed} + k_{eq}\Delta\omega_{min})$	220.99	124	201.95	-2.51
Case 3: $\sum(n_{count}\, p_{shed})$	215.40	122	209.80	-3.01

Table 20. UFLS scheme performance based on the objective function formulation

As observed in Table 20, for Case 1, the sum of the minimum frequency deviations decreases with the new formulation, with the maximum system deviation being -2.77 Hz compared to -2.90 Hz in the base case. To achieve the new objective of minimizing the minimum system frequency deviation, the load shedding has slightly increased. Note that despite the rise in load shedding, the total load disconnected remains lower than that of the conventional optimized design and the existing one. As for Case 2, the effect of including the k_{eq} parameter is perceived, since a more conservative approach is attained compared to Case 1, where the minimum frequency is reduced, and the disconnected load is increased. Finally, by multiplying the shed load by the number of OC scenarios, a worse performance than the base case is obtained in terms of load shedding and minimum frequency. Although this approach indirectly accounts for the contribution of backup generator units providing inertia and spinning reserve to the system, it results in a slight increase in the amount of load to be disconnected.

4.4 UFLS SCHEME DESIGN INCLUDING THE STEP SIZE

In previous sections, it was emphasized that, given the characteristics of the power system under study, the step sizes are assumed to be known and constant. However, these change due to generator outages, generator load variations, or breaker failures [34]. Thus, the assumption that feeder load variation is proportional to demand is not realistic since different types of customers are supplied by the feeders depending on the hour and the day. Variations in step sizes are primarily influenced by changes in feeder loads, which can significantly degrade the effectiveness of UFLS schemes. For example, smaller step sizes may result in insufficient load shedding, leading to critically low frequency levels.

Given that step size is a critical parameter, this section also considers the step size as a decision variable. To do so, the optimizer determines the optimal values for the system, assuming complete flexibility in selecting the load to be shed. In this way, the amount of load shed is expected to diminish, and consequently, the total sum of frequency deviations is expected to increase. This is because reducing the disconnected load causes the system to tend towards lower frequency values. Similarly, by changing the step size, the initial step may decrease, resulting in an increase in the total number of active relays. The resulting UFLS scheme, along with its dynamic frequency response, can be seen in Table 21.

Stage	Substation	ω_{thr} (Hz)	M_{thr} (s)	$t_{thr,F}$ (s)	$t_{thr,M}$ (s)	t_{open} (s)	Step size (%)
1	2101	**48.99**	**0.57**	**0.08**	**0.13**	0.2	**5.11**
2	2102	**48.82**	**0.51**	**0.16**	**0.31**	0.2	**1.17**
3	3101	**48.66**	**0.39**	**0.03**	**0.13**	0.2	**14.92**
4	3102	**48.53**	**0.24**	**0**	**0.03**	0.2	**4.61**
5	2103	**48.39**	**0.14**	**0.08**	**0.15**	0.2	**7.49**
6	1101	**48.09**	**0.12**	**0.04**	**0.10**	0.2	**8.31**

Table 21. FSM-based UFLS scheme including step size

With this new design, the load distributed across the six UFLS steps is reduced, reaching 41.61% compared to 46.7% in the base case. The effect of the load disconnection reduction can be seen in Figure 20 and Table 22. It is observed that in all cases where load shedding is required, it is reduced, resulting in a slower frequency recovery and lower frequencies.

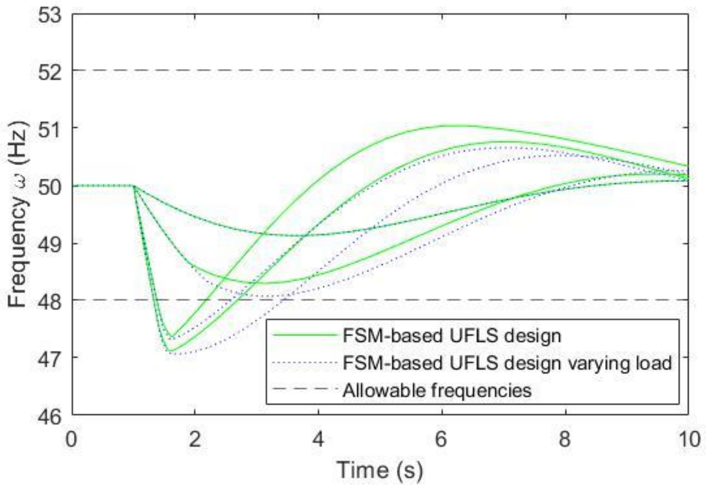

Figure 20. Comparison of the dynamic response of the OC scenarios

		FSM – based UFLS scheme		FSM – based UFLS scheme varying load	
Scenario	Generator (MW) (%)	ω_{min} (Hz)	P_{shed} (MW) (# relays)	ω_{min} (Hz)	P_{shed} (MW) (# relays)
8	2.35 (9.24)	49.13	0 (0)	49.13	0 (0)
3	9.55 (51.68)	47.12	8.63 (6)	47.07	7.69 (6)
8	6.10 (22.29)	48.30	1.94 (1)	48.07	1.40 (1)
1	10.41 (47.13)	47.37	10.32 (6)	47.32	9.19 (6)

Table 22. OC performance comparison by varying load shedding

The response of all 164 possible disturbances to the scheme with the new shedding values shows a more oscillatory behavior compared to the base case. This is mainly due to the reduction in the overall amount of load shed. Note that, compared to the base case, the system remains below the frequency limit for a longer period in certain incidents. However, in all cases except one, it is below 48 Hz for less than 2s. In the only case where this threshold is violated, it is by 0.089s, resulting in a 4.5% excess over the maximum allowed time limit.

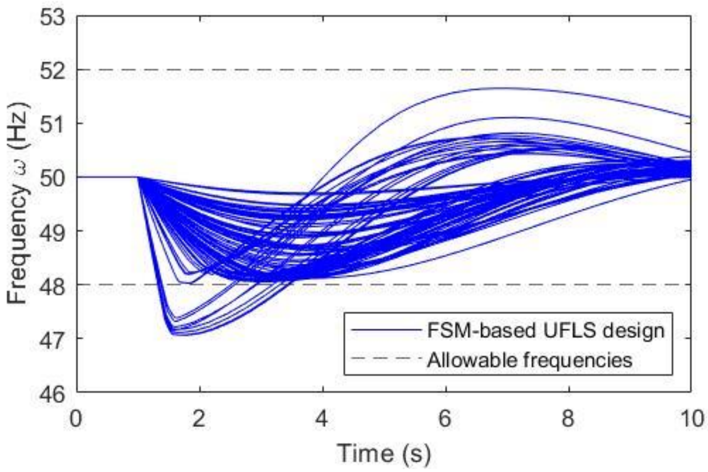

Figure 21. FSM-based UFLS scheme including step size: Overall system response

As previously mentioned, and as illustrated in Table 23, with this new scheme, the amount of shed load is reduced by compromising and increasing frequency deviations.

	UFLS performance		
Case	Total shed (MW)	Nº Relays	ΣΔωmin (Hz)
Base Case	210.70	120	207.59
Step size design	203.88	143	217.32

Table 23. Comparison of UFLS scheme performance including step size

It is important to note that this design is unrealistic, as it was developed by releasing the step design threshold but did not include specific criteria that these steps had to meet.

Chapter 5. CONCLUSIONS

The main objective of this project has been the optimal design of a UFLS scheme based on the frequency stability margin (FSM). UFLS schemes are a last-resort tool to guarantee frequency stability, a major concern for small isolated power systems that is expected to grow with the increasing penetration of RES.

While current UFLS schemes have successfully addressed some of the challenges related to load shedding, this study aimed to further improve the performance of conventional static and semi-adaptative schemes by including the FSM. To achieve this, a two-step design approach, striving for efficiency and robustness, has been adapted to FSM-based UFLS scheme and applied to small isolated power systems.

To guarantee the UFLS scheme's efficiency, the adjustment of the parameters has been achieved by solving an optimization problem to minimize load shedding. This was carried out using heuristic algorithms, in particular simulated annealing. To ensure robustness, representative scenarios were selected using a clustering method. To evaluate the feasibility of the FSM-based UFLS scheme, it has been designed and implemented for both the La Palma and the Gran Canaria power systems.

Moreover, the two proposed schemes have been compared with the existing UFLS scheme and its optimized version, respectively. For the La Palma power system, both the optimized and FSM-based schemes showed enhanced performance. However, the FSM-based scheme provided the most effective frequency response. The FSM-based model successfully reduced the load to be shed and showed less severe maximum and minimum frequency peaks. It also demonstrated the ability to differentiate between critical contingencies and those where load-shedding could be delayed or avoided, effectively delaying activation to allow natural recovery during minor contingencies while accelerating the response in severe ones. This approach minimized load shedding and reduced extreme frequency deviations.

In contrast, for the Gran Canaria power system, while the FSM-based scheme provided an adequate dynamic response, it struggled to maintain frequency above the desired threshold during steady-state conditions in some scenarios. To address this, a 49 Hz – 5s constraint was implemented, which improved frequency control under critical conditions. However, the conventional optimized UFLS scheme for Gran Canaria demonstrated a superior ability to arrest sustained low frequencies in the steady state, as it integrates both UF and Rate of Change of Frequency (RoCoF) relays. This dual-relay approach enabled the conventional optimized scheme to manage load shedding more effectively, thereby stabilizing operational frequencies at lower frequency deviation values.

The proposed method for designing robust and efficient FSM-based UFLS schemes relies on certain assumptions about design conditions. Consequently, the effects of changing these conditions have been thoroughly examined by tuning the UFLS schemes for the La Palma power system based on variations in one of the design conditions. The following results highlight the impact of these design condition variations:

- Increasing RES penetration in the La Palma power system with the proposed UFLS scheme leads to higher RoCoF values and greater frequency deviations. With higher RES levels, load shedding and operational errors rise, primarily due to lower frequencies and excessive load disconnections that result in overshoots. Two optimized FSM-based schemes are developed for RES integration levels of up to 14% and 39% above the base case. While the first scheme maintains frequency stability without errors, the second experiences one overshoot and several instances of frequency dropping below 48 Hz for more than 2 seconds, leading to extended stabilization times and oscillations. These results underscore that, to ensure both stability and efficiency, RES should contribute to primary frequency control so that a safe reduction in thermal generation can be achieved.
- Incorporating an energy storage system (ESS) into the UFLS scheme significantly reduces load shedding by approximately 55%, enhancing system stability and reliability. The primary improvement is achieved through the addition of storage itself, with optimization providing only minor gains. Although ESS reduces the need

for frequent load-shedding activations, it results in slightly higher frequency deviations due to decreased load disconnection levels. Overall, integrating ESS improves the efficiency, flexibility, and security of the UFLS scheme, maintaining system integrity with reduced load disconnections.

- Varying the objective function by incorporating frequency-weighted factors enhances system stability by reducing frequency deviations, although it slightly increases the total amount of shed load. Designs that prioritize both load shedding and frequency stability show a balanced improvement, reducing frequency deviations while maintaining a higher minimum frequency than the base case. More conservative configurations, which place greater emphasis on frequency stabilization, achieve the lowest frequency deviations but require higher load shedding. Additionally, the approach that penalizes the objective function based on the number of online generators in each scenario results in a moderate increase in load shedding. Overall, these findings underscore the trade-offs between frequency stability and load management in optimizing UFLS schemes.
- By including step sizes as a decision variable, the new design leads to a reduction in the amount of load shed, from 46.7% in the base case to 41.61%. However, this reduction in load disconnection slows frequency recovery and results in lower minimum frequency values. Consequently, the frequency response exhibits a more oscillatory behavior compared to the base case, with extended periods below frequency limits in certain disturbances. Although the scheme achieves a more flexible response by modifying step sizes, it lacks specific criteria for meeting realistic operational thresholds, limiting its practical applicability. This analysis suggests that while releasing load constraints and adjusting step sizes may improve flexibility in UFLS design, it requires further refinement to balance frequency stability and reliability.

In conclusion, an efficient and robust method for the design of UFLS schemes based on frequency stability margin has been developed and successfully implemented in real power systems. Further, the comparison with conventional schemes indicated that the incorporation of UF relays could improve the ability to arrest sustained frequency deviations in the steady state, specifically in larger power systems. Finally, the analysis of varying design conditions offered valuable insights into the performance and adaptability of the proposed method, highlighting its potential for application across diverse power system operating contexts.

Chapter 6. BIBLIOGRAPHY

[1] IEA, "Electrification," 11 July 2023. [Online]. Available: https://www.iea.org/energy-system/electricity/electrification.

[2] United Nations, "The Paris Agreement".

[3] Eurostat, "CO2 emissions from EU territorial energy use: -2.8%," *Eurostat*, 2023.

[4] European Commission, "European Green Deal: EU agrees stronger legislation to accelerate the rollout of renewable energy," Brussels, 2023.

[5] R. Roca, "Red Eléctrica vuelve a parar la industria durante tres horas por falta de suministro eléctrico," *El periódico de la energía*, 12 July 2024.

[6] D. Zhao, L. Yin, Z. Xin, Bao and Wei, "Comprehensive assessment method for inertia and frequency stability of high proportional renewable energy system," *2022 IEEE 10th Joint International Information Technology and Artificial Intelligence Conference (ITAIC),* pp. 1769-1774, 2022.

[7] REE, *Estudios de prospectiva del sistema y necesidades para su operabilidad*, 2020.

[8] I. Egido, S. Lukas and L. Rouco, "Energy storage systems for frequency stability enhancement in small-isolated power systems," *Renewable Energy and Power Quality Journal*, April 2015.

[9] I. Egido, F. Fernández-Bernal, P. Centeno and L. Rouco, "Maximum Frequency Deviation Calculation in Small Isolated Power Systems," *IEEE Transactions on Power Systems*, vol. 24, no. 4, pp. 1731-1738, November 2009.

[10] REE, "Criterios generales de protección de los sistemas eléctricos," 2005.

[11] REE, "El sistema eléctrico Canario," 2016.

[12] Gobierno de Canarias, "Anuario Energético de Canarias 2022," 2024.

[13] Instituto Tecnológico de Canarias, "Estrategia de la generación gestionable de Canarias," Dirección General de Energía del Gobierno de Canarias., Laa Palmas de Gran Canaria, 2022.

[14] ABC, "Apagón general en La Gomera: más de 22.000 personas sin suministro eléctrico a causa de un incendio," *ABC,* July 2023.

[15] V. Guillermo, "Tenerife sufre su segundo apagón total en menos de un año," *El País,* 2020.

[16] R. Corujo, P. Santos and R. Ascanio, "Operation of small isolated power system with large non-controllable RES penetration – System Operator's experience in El Hierro Island," *Renewable Energy and Power Quality Journal,* no. 17, 2019.

[17] J. Rodriguez, "Estudio sobre las interconexiones de los sistemas eléctricos de las Islas Canarias.," 2011.

[18] REE, "Red Eléctrica inicia las obras del nuevo enlace eléctrico submarino entre Tenerife y La Gomera," March 2023.

[19] Parlamento de Canarias, "Comunicaciones del Gobierno En trámite 11L/CG-0002 Declaración de Emergencia Energética en la Comunidad Autónoma de Canarias," in *Boletín Oficial del Parlamento de Canarias*, 2023.

[20] Gobierno de Canarias, "Plan de Transición Energética de Canarias," Las Palmas de Gran Canaria, 2023.

[21] Energías Renovables, "Canarias marca nuevo horizonte: 37% de energías renovables para 2030," *Energías Renovables,* 16 December 2022.

[22] G. Magby, G. Shabib, A. Elbaser and Y. Mitani, "Renewable power systems dynamic security using a new coordination of frequency control strategy based on virtual synchronous generator and digital frequency protection," *International Journal of Electrical Power & Energy Systems,* vol. 109, pp. 351-368, 2019.

[23] P. Pourghasem, H. Seyedi and K. Zare, "A new optimal under-voltage load shedding scheme for voltage collapse prevention in a multi-microgrid system," *Electric Power Systems Research,* vol. 203, 2022.

[24] L. Sigrist, L. Rouco and F. M. Echavarren, "A review of the state of the art of UFLS schemes for isolated power systems," *Electrical Power and Energy Systems,* vol. 99, pp. 525-539, 2018.

[25] D. Yang, G. Cai, Y. Jiang and C. Liu, "Centralized Adaptive Under Frequency Load Shedding Schemes for Smart Grid Using Synchronous Phase Measurement Uni," *Journal of Electrical Engineering and Technology*, vol. 8, no. 3, pp. 446-452, 2013.

[26] M. Zhang, "Modeling and Verification of Advanced Under-Frequency Load Shedding Schemes," Master of Science Thesis, Delft (Netherlands), 2016.

[27] L. Sigrist, L. Rouco and F. M. Echavarren, "A review of the state of the art of UFLS schemes for isolated power systems," *Electrical Power and Energy Systems*, vol. 99, pp. 525-539, July 2018.

[28] M. N. Acosta, C. Adiyabazar, F. Gonzalez-Longatt, M. A. Andrade, J. L. Rueda Torres, E. Vazquez and J. M. R. Santos, "Optimal under-frequency load shedding setting at Altai-Uliastai regional power system, Mongolia," *Energies*, vol. 13, no. 20, pp. 1-18, 2020.

[29] L. Jenkins, "Optimal load shedding algorithm for power system emergency control," in *1983 Proceedings of the International Conference on Systems, Man and Cybernetics*, Bombay and New Delhi, India, 1983.

[30] Y. Halevi and D. Kottick, "Optimization of load shedding system," *IEEE Transactions on Energy Conversion*, vol. 8, no. 2, pp. 207 - 213, 1993.

[31] A. Denis Lee Hau, "A General-Order System Frequency Response Model Incorporating Load Shedding: Analytic Modeling and Applications," *IEEE Transactions on Power Systems*, vol. 21, no. 2, pp. 709 - 717, 2006.

[32] J. Lopes, W. wong Chan and L. Proenca, "Genetic algorithms in the definition of optimal load shedding strategies," *PowerTech Budapest 99. Budapest, Hungary, IEEE.*, 1999.

[33] L. Sigrist, I. Egido and L. Rouco, "A Method for the Design of UFLS Schemes of Small Isolated Power Systems," *IEEE Transactions on Power Systems*, vol. 27, no. 2, pp. 951-958, May 2012.

[34] L. Sigrist and L. Rouco, "Design of UFLS Schemes Taking Into Account Load Variation," *2014 Power Systems Computation Conference*, pp. 1-7, 2014.

[35] H. H. Alhelou, M. E. Hamedani Golshan, T. C. Njenda and N. D. Hatziargyriou, "An Overview of UFLS in Conventional, Modern, and Future Smart Power Systems: Challenges and Opportunities," *Electric Power Systems Research*, vol. 179, 2020.

[36] MINETAD, "Resolución de 1 de febrero de 2018, de la Secretaría de Estado de Energía, por la que se aprueba el procedimiento de operación 12.2 de los sistemas eléctricos no peninsulares.," Boletín Oficial del Estado, 2018.

[37] L. Sigrist, *Design of UFLS schemes of small isolated power systems*, 2010.

[38] U. J. Ibe and V. C. Oguejiofor, "Underfrequency in generating units: effects and mitigations," *International Journal of Research and Publication,* vol. 5, 2024.

[39] L. Sigrist, I. Egido and L. Rouco, ""A Method for the Design of UFLS Schemes of Small Isolated Power Systems," *IEEE Transactions on Power Systems,* vol. 27, no. 2, pp. 951-958, May 2012.

[40] M. Vadillo Díaz de Aguilar, "System protection of island power systems under large shares of RES," Madrid, 2022.

[41] U. Rudez and R. Mihalic, "RoCoF-based Improvement of Conventional Under-Frequency Load Shedding," *2019 IEEE Milan PowerTech,* pp. 1-5, 2019.

[42] L. Sigrist, I. Egido, E. Sánchez-Úbeda and L. Rouco, "Representative Operating and Contingency Scenarios for the Design of UFLS Schemes," *IEEE Transactions on power systems,* vol. 25, pp. 906-913, 2010.

[43] M. Rodriguez, C. Comin, D. Casanova, O. Bruno, D. Amancio and L. Costa, "Clustering algorithms: A comparative approach," *PLoS ONE,* 2019.

[44] A. Kuraria, N. Jharbade and M. Soni, "Centroid Selection Process Using WCSS and Elbow Method for K-Mean Clustering Algorithm in Data Mining," *International Journal of Scientific Research in Science, Engineering and Technology,* pp. 190-195, 2018.

[45] M. Vadillo, L. Sigrist and U. Rudez, "Design an comparison of UFLS schemes of isolated power systems based on frequency stability margin," *2023 IEEE Belgrade PowerTech,* pp. 1-6, 2023.

[46] El periódico de la energía, "La Unión Europea elige a La Palma para ser 100% renovable en 2030," *El periódico de la energía,* 11 November 2023.

[47] AEE, "Ecoener construirá dos parques eólicos en la isla canaria de La Palma," 2020.

[48] M. Rajabdorri, L. Sigrist, E. Lobato, M. d. C. Prats and F. Echavarren, "Viability of providing spinning reserves by RES in Spanish islandpower systems," *IET Renewable Power Generation,* vol. 15, 2021.

[49] D. Page, "El mercado de la electricidad marca precios negativos por primera vez en la historia," *El Periódico de España*, 2024.

[50] S. Paola, L. O. Á. Sigrist and E. Lobato, "Optimal coordinated design of under-frequency load shedding and energy storage systems," *Electric Power Systems Research*, vol. 211, 2022.

[51] United Nations, “The 17 goals,” 2015. [Online]. Available: https://sdgs.un.org/goals.

[52] S. Kirkpatrick, D. Gelatt and M. P. Venchi, "Optimization by Simulated Annealing," *Science*, vol. 220, no. 4598, pp. 671-677, 1983.

[53] V. Cerny, "A Thermodynamical Approach to the Travelling Salesman Problem: An Efficient Simulation Algorithm," *Journal of Optimization Theory and Applications*, vol. 45, pp. 41-51, 1985.

[54] M. Mitchel, J. Lopes, J. Fidalgo and J. McCalley, "Using a neural network to predict the dynamic frequency response of a power system to an under-frequency load shedding scenario," *Power Engineering Society Summer Meeting, 2000. IEEE*, pp. 346-351, 2000.

APPENDIX I.

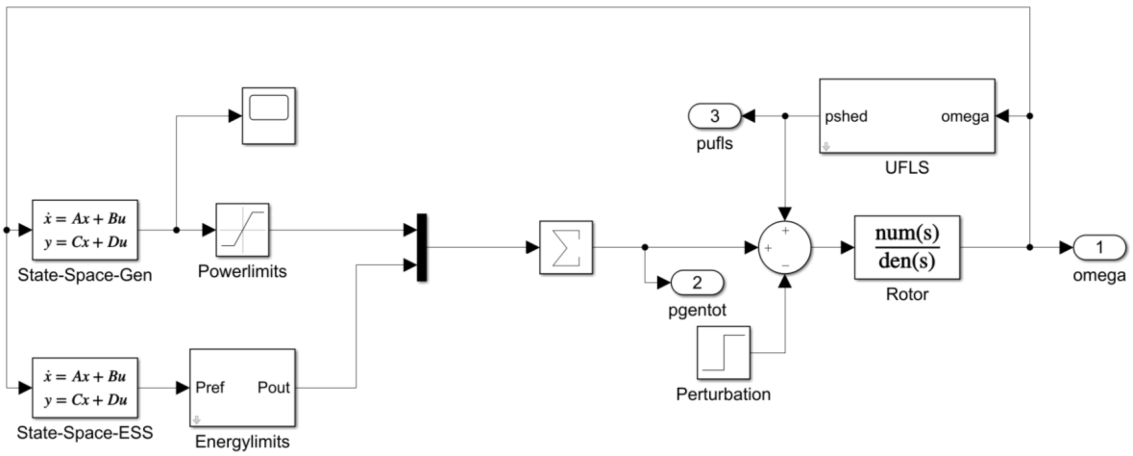

Figure 22. Block diagram: Electrical power system

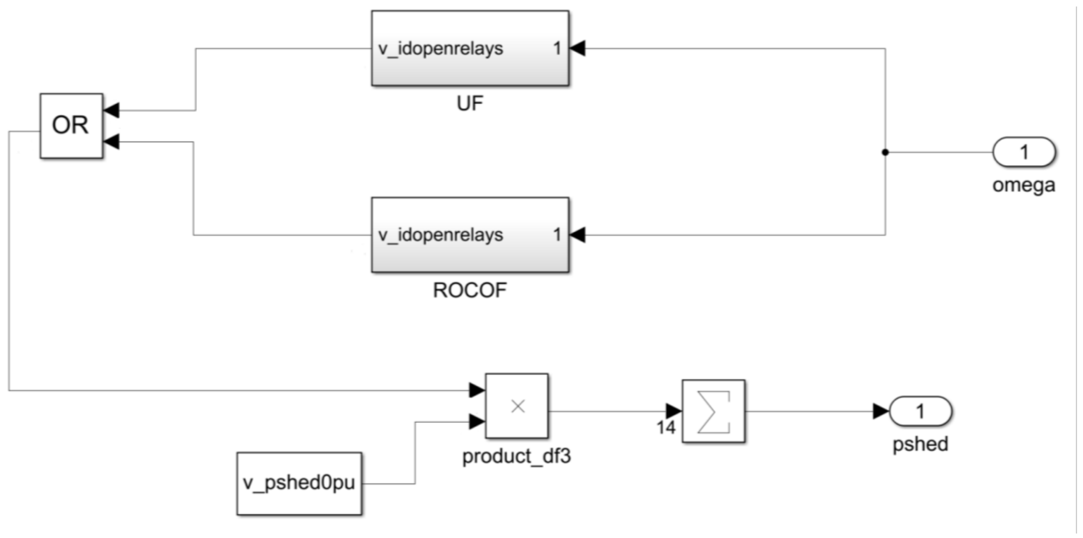

Figure 23. Block diagram: Conventional UFLS scheme

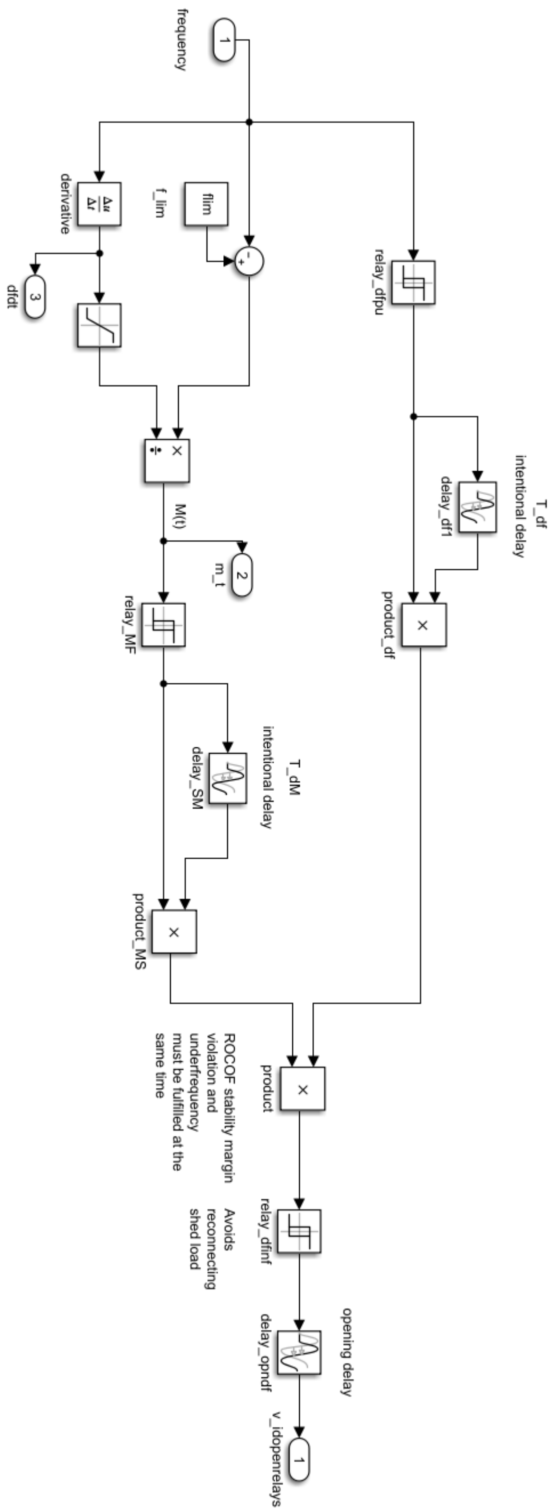

Figure 24. Block diagram: FSM-based UFLS scheme

APPENDIX II.

Allignment with SDGs

This project addresses the pressing challenges of integrating RES into small isolated power systems. By enhancing the stability and efficiency of these systems, it aligns with several SDGs.

The primary focus of this project contributes directly to SDG 7 (Affordable and Clean Energy). This goal aims to ensure access to affordable, reliable, sustainable, and modern energy for all by significantly increasing the share of renewable energy in the global energy mix and doubling the global rate of improvement in energy efficiency by 2030 [51]. The modification of the UFLS scheme in this project facilitates the penetration and effective utilization of RES, thereby contributing to the attainment of SDG 7.

In alignment with SDG 12 (Responsible Consumption and Production), this project strives to achieve the efficient use and sustainable management of natural resources. The proposed UFLS scheme seeks to enhance the effective and sustainable management of energy resources, thereby promoting sustainable consumption and production patterns. By improving how energy resources are managed, the project contributes to a more sustainable and responsible approach to energy use.

Furthermore, the research contributes to SDG 9 (Industry, Innovation, and Infrastructure). By utilizing advanced techniques such as data mining and heuristic algorithms to optimize UFLS schemes, the project enhances the resilience and efficiency of power infrastructures. This emphasis on innovation in energy management fosters the development of more robust and reliable infrastructure, contributing to sustainable industrial growth and technological advancement.

The project is also closely linked to SDG 13 (Climate Action), which calls for urgent action to combat climate change and its impacts [51]. By implementing a novel UFLS scheme, the project accelerates and supports the creation of a more extensive RES infrastructure in small isolated power systems. This reduces reliance on unsustainable, fossil fuel-based energy sources, which are highly polluting.

Additionally, the project promotes SDG 11 (Sustainable Cities and Communities) by ensuring stable and sustainable access to electricity in isolated and potentially underserved communities. This enhancement in energy security is vital for the development and well-being of these communities.

Finally, the project supports the achievement of other SDGs to a lesser extent. For example, it contributes to SDG 3 (Good Health and Well-being) by reducing pollution and improving air quality, and SDG 8 (Decent Work and Economic Growth) by fostering job creation in the renewable energy sector.